
Electronic Theses and Dissertations, 2004-2019

2016

Anthropogenic Organic Chemical Removal from a Surficial Groundwater and Mass Transfer Modeling in a Nanofiltration Membrane Process

Samantha Black
University of Central Florida



Part of the [Environmental Engineering Commons](#)

Find similar works at: <https://stars.library.ucf.edu/etd>

University of Central Florida Libraries <http://library.ucf.edu>

This Doctoral Dissertation (Open Access) is brought to you for free and open access by STARS. It has been accepted for inclusion in Electronic Theses and Dissertations, 2004-2019 by an authorized administrator of STARS. For more information, please contact STARS@ucf.edu.

STARS Citation

Black, Samantha, "Anthropogenic Organic Chemical Removal from a Surficial Groundwater and Mass Transfer Modeling in a Nanofiltration Membrane Process" (2016). *Electronic Theses and Dissertations, 2004-2019*. 5090.

<https://stars.library.ucf.edu/etd/5090>

ANTHROPOGENIC ORGANIC CHEMICAL REMOVAL FROM A SURFICIAL
GROUNDWATER AND MASS TRANSFER MODELING IN A NANOFILTRATION
MEMBRANE PROCESS

by

SAMANTHA J. BLACK
B.S. University of Central Florida, 2012
M.S. University of Central Florida, 2013

A dissertation submitted in partial fulfillment of the requirements
for the degree of Doctor of Philosophy
in the Department of Civil, Environmental, and Construction Engineering
in the College of Engineering and Computer Science
at the University of Central Florida
Orlando, Florida

Summer Term
2016

Major Professor: Steven J. Duranceau

© 2016 Samantha J. Black

ABSTRACT

This dissertation reports on research related to trace organic compounds (TrOCs) in surficial groundwater supplies and their subsequent removal from nanofiltration (NF) membranes. The research was conducted along coastal South Florida in cooperation with the Town of Jupiter Water Utilities, Jupiter, FL (Town). The focus of the research was to determine the extent of reclaimed water impacts on surficial groundwater supplies and subsequent effects on the Town's NF water treatment plant.

Routine monitoring of fourteen TrOCs in reclaimed water and at the water treatment facility revealed varying degrees of TrOC detection in the environment. Certain TrOCs, including caffeine and DEET, were detected in a majority of the water sampling locations evaluated in this work. However, subsequent dilution with highly-treated reverse osmosis (RO) permeate from alternative supplies resulted in TrOCs below detection limits in potable water at the point-of-entry (POE).

Pilot testing was employed to determine the extent of TrOC removal by NF. Prior to evaluating TrOC removal, hydraulic transients within the pilot process were first examined to determine the required length of time the pilot needed to reach steady-state. The transient response of a center-port NF membrane process was evaluated using a step-input dose of a sodium chloride solution. The pilot was configured as a two-stage, split-feed, center-exit, 7:2 pressure vessel array process, where the feed water is fed to both ends of six element pressure vessels, and permeate and concentrate streams are collected after only three membrane elements. The transient response was described as a log-logistic system with a

maximum delay time of 285 seconds for an 85% water recovery and 267 gallon per minute feed flowrate.

Eleven TrOC pilot unit experiments were conducted with feed concentrations ranging from 0.52 to 4,500 $\mu\text{g/L}$. TrOC rejection was well-correlated with compound molecular volume and polarizability, with coefficient of determination (R^2) values of 0.94. To enhance this correlation, an extensive literature review was conducted and independent literature sources were correlated with rejection. Literature citations reporting the removal effectiveness of an additional sixty-one TrOCs by loose NF membranes (a total of 95 data points) were found to be well-correlated with molecular volume and polarizability, with R^2 values of 0.72 and 0.71, respectively.

Of the TrOC's detected during this research, the anthropogenic solute caffeine was selected to be modeled using the homogeneous solution diffusion model (HSDM) and the HSDM with film theory (HSDM-FT). Mass transfer coefficients, K_w (water) K_s (caffeine), and k_b (caffeine back-transport) were determined experimentally, and K_s was also determined using the Sherwood correlation method. Findings indicate that caffeine transport through the NF pilot could be explained using experimentally determined K_s values without incorporating film theory, since the HSDM resulted in a better correlation between predicted and actual caffeine permeate concentrations compared to the HSDM-FT and the HSDM using K_s obtained using Sherwood applications. Predicted versus actual caffeine content was linearly compared, revealing R^2 values on the order of 0.99, 0.96, and 0.99 for the HSDM without FT, HSDM-FT, and HSDM using a K_s value obtained using the

Sherwood correlation method. However, the use of the HSDM-FT and the Sherwood number resulted in the over-prediction of caffeine concentrations in permeate streams by 27 percent and 104 percent, respectively.

ACKNOWLEDGMENTS

This work would not have been possible without the support provided by a number of individuals. Thank you to Dr. Steven Duranceau for providing the opportunity to conduct this research, and for contributing his time, knowledge, and invaluable experience. Thank you to Dr. Woo Hyoung Lee, Dr. Anwar Sadmani, and Dr. Cherie Yestrebsky for serving as committee members and donating their expertise to review this document. Additional thanks are offered to past and present UCF research students who directly assisted in this work: Maria Arenas, Paul Biscardi, Martin Coleman, Cassidy Conover, Carlyn Higgins, Samantha Myers, Andrea Netcher, Jonathan Ousley, Benjamin Yoakum, David Yonge. Special thanks are offered to Dr. Carolina Franco for her effort in obtaining a portion of the results reported in this work.

Thanks are in order for the municipalities and companies that assisted the UCF research team in this effort. Thanks are offered to the support provided by the Town of Jupiter Water Utilities Department (Jupiter, FL), including David Brown, Amanda Barnes, Paul Jurczak, and Tony Fogel. Special thanks are offered to Town staff who directly assisted in this work, Rebecca Wilder and Mark Cantor, who greatly aided the research efforts. Additional thanks are offered to the Town's consultants John E. Potts (Kimley-Horn & Associates; West Palm Beach, FL) and Ian Watson (RosTek Associates; Tampa, FL) for sharing their invaluable knowledge and experience.

TABLE OF CONTENTS

LIST OF FIGURES	xii
LIST OF TABLES	xiv
LIST OF ABBREVIATIONS.....	xvii
CHAPTER 1: GENERAL INTRODUCTION	1
CHAPTER 2: DETECTION OF ANTHROPOGENIC ORGANIC CHEMICALS IN RECLAIMED WATER, RECHARGE BASIN WATER, SURFICIAL GROUNDWATER, AND DRINKING WATER IN NORTHWEST PALM BEACH COUNTY, FLORIDA.....	2
Abstract.....	2
Introduction.....	3
Site Description.....	7
Screening Evaluation	9
Methods.....	11
Trace Organic Compounds and Descriptions	11
Sample Collection, Transport, and Analysis.....	11
Results and Discussion	13
Irrigation Quality Water.....	14
Recharge Basin	16

Surficial Groundwater.....	17
Nanofiltration Permeate and Point-of Entry	20
Conclusions.....	20
Acknowledgments.....	21
References.....	22
Web References	25
CHAPTER 3: MASS TRANSFER AND TRANSIENT RESPONSE TIME OF A SPLIT-FEED NANOFILTRATION PILOT UNIT.....	26
Abstract.....	26
Introduction.....	27
Background.....	28
Full-Scale Nanofiltration Plant	28
Split-Feed Pilot Unit	30
Homogeneous Solution Diffusion Model.....	31
Materials and Methods.....	33
Results and Discussion	36
Pilot Response.....	36
Predictive Modeling.....	42
Homogeneous Solution Diffusion Model.....	48

Conclusions.....	49
Acknowledgments.....	50
References.....	51
CHAPTER 4: THE INFLUENCE OF SOLUTE POLARIZABILITY AND MOLECULAR VOLUME ON THE REJECTION OF TRACE ORGANICS IN LOOSE NANOFILTRATION MEMBRANE PROCESSES	53
Abstract.....	53
Introduction.....	54
Materials and Methods.....	57
Pilot Plant Description	57
Water Quality Description	60
Selected Trace Organic Compounds.....	61
Experimental Set Up.....	63
Analytical Methods.....	64
Results and Discussion	66
Trace Organic Compound Rejection Results.....	66
Solute Rejection Mechanisms.....	68
Examining Polarizability with Independent Sources.....	72
Conclusions.....	76

Acknowledgments.....	78
References.....	79
CHAPTER 5: CAFFEINE REMOVAL AND MASS TRANSFER IN A NANOFILTRATION MEMBRANE PROCESS.....	83
Abstract.....	83
Introduction.....	84
Theory.....	86
Materials and Methods.....	90
Site Description.....	90
Caffeine Characterization	94
Experimental Procedure.....	95
Sample Preparation and Analytical Methods.....	96
Results and Discussion	97
Model Parameter Determination.....	97
Caffeine Prediction and Model Validation	101
Conclusions.....	105
Acknowledgments.....	106
References.....	107
CHAPTER 6: GENERAL CONCLUSION	111

APPENDIX A: QUALITY ASSURANCE AND QUALITY CONTROL.....	113
APPENDIX B: SHERWOOD CORRELATION CALCULATIONS	118
APPENDIX C: TRACE ORGANIC COMPOUND CONCENTRATIONS AND MASS BALANCES.....	122
APPENDIX D: DESALINATION AND WATER TREATMENT COPYRIGHT PERMISSION LETTER.....	130
APPENDIX E: DESALINATION AND WATER TREATMENT ACCEPTANCE LETTER	132

LIST OF FIGURES

Figure 2-1: Surficial Wells in Relation to the Water and Wastewater Treatment Plants ...	8
Figure 3-1: Simplified Schematic of the Split-Feed Nanofiltration Process	30
Figure 3-2: First Stage Permeate Conductivity at 85% and 80% Recoveries.....	40
Figure 3-3: Second Stage Permeate Conductivity at 85% and 80% Recoveries	40
Figure 3-4: Total Pilot Permeate Conductivity at 85% and 80% Recoveries.....	41
Figure 3-5: Pilot Response at 85% Recovery	42
Figure 3-6: Minitab [®] Figure Describing First Stage Permeate Conductivity versus Time	44
Figure 3-7: Model (experiment 2) versus Actual Data (experiment 2)	46
Figure 3-8: Model (experiment 2) versus Actual Data (experiment 3)	46
Figure 3-9: Predicted versus Actual Permeate Sodium and Chloride Concentrations	49
Figure 4-1: Simplified Schematic of the Full-Scale Nanofiltration Process.....	58
Figure 4-2: TrOC Rejection from the First Stage, Second Stage, and Total Pilot System	67
Figure 4-3: Rejection vs TrOC Polarizability ($R^2=0.94$)	70
Figure 4-4: Rejection vs TrOC Molecular Volume ($R^2=0.94$)	70
Figure 4-5: Rejection vs TrOC Log K_{ow} ($R^2=0.87$)	71
Figure 4-6: Rejection vs TrOC Log D ($R^2=0.43$)	71
Figure 4-7: Rejection vs TrOC Molecular Weight ($R^2=0.30$)	71
Figure 4-8: Rejection vs TrOC Polarizability ($R^2=0.71$)	75
Figure 4-9: Rejection vs TrOC Molecular Volume ($R^2=0.72$)	75
Figure 4-10: Rejection vs TrOC Log K_{ow} ($R^2=0.14$)	76

Figure 4-11: Rejection vs TrOC Molecular Weight ($R^2=0.67$)	76
Figure 5-1: Membrane Schematic.....	87
Figure 5-2: Simplified schematic of NF pretreatment and flow configuration	91
Figure 5-3: Total pilot system water flux as a function of net applied pressure.....	98
Figure 5-4: Total pilot system solute flux as a function of change in caffeine concentration	100
Figure 5-5: Predicted versus actual caffeine concentration from first stage, second stage, and total pilot system permeate using the HSDM at low and high feed concentrations. Results are plotted on a log-scale due to the wide range of concentrations.	102
Figure 5-6: Predicted versus actual caffeine concentration from first stage, second stage, and total pilot system permeate using the HSDM and HSDM-FT at low feed concentrations.	102
Figure 5-7: Predicted versus actual caffeine concentration from first stage, second stage, and total pilot system permeate using the HSDM and HSDM-FT at high feed concentrations.	103
Figure 5-8: Predicted versus actual caffeine concentration in permeate from left and right sides of first and second stages of pilot system using the HSDM with the mass transfer coefficients calculated using Sherwood relationships.	104
Figure 5-9: Predicted caffeine concentration versus actual caffeine concentration in permeate using results found in the literature.	105

LIST OF TABLES

Table 2-1: Trace Organic Compound Servings	5
Table 2-2: Trace Organic Compound Preliminary Investigation Findings	10
Table 2-4: Sampling Event Summary.....	13
Table 2-5: IQ Composite and Grab Sample Results.....	15
Table 2-6: Recharge Basin Grab Sample Results	16
Table 2-7: Surficial Groundwater Well Grab Sample Results.....	18
Table 2-8: Raw Water Composite Sample Results.....	19
Table 3-1: Feed Solution Conductivities and Recoveries Operated during Three Experiments	35
Table 3-2: Summary of Data Collection Procedures	36
Table 3-3: Conductivity Measurements in Feed and Permeate Streams at Various Water Recoveries.....	38
Table 3-4: Response Time (seconds) during Experiments 1, 2, & 3 at 85% Recovery....	39
Table 3-5: Minitab® Model Statistics Summary.....	44
Table 3-6: Theta Values for Permeate Log-logistic Models at 85% Recovery	45
Table 3-7: Minitab ® Model and Statistics Summary and Theta Values	47
Table 3-8: Comparison between First-Order and Log-logistic Models.....	47
Table 3-9: Solute Flux (lb/sfd).....	48
Table 3-10: Mass Transfer Coefficients (ft/d)	48
Table 4-1: Membrane and Pilot Characteristics.....	59
Table 4-2: Nanofiltration Pilot Feed Water Quality	60

Table 4-3: Trace Organic Compound Uses and Physical and Chemical Characteristics .	62
Table 4-4: Target Feed Concentrations.....	64
Table 4-5: TrOC Detection Limits.....	65
Table 4-6: Number of Rejection Values Obtained	68
Table 4-7: Statistical Analysis for Correlations between TrOC Properties and Rejection	69
Table 4-8: Statistical Analysis for Correlations between TrOC Properties and Rejection	75
Table 5-1: NF pilot unit specifications and operating parameters	92
Table 5-2: NF pilot water quality in feed and permeate samples	94
Table 5-3: Caffeine properties	95
Table 5-4: Caffeine experiment summary	96
Table 5-5: Water flux and water mass transfer coefficients	98
Table 5-6: Caffeine mass transfer coefficients	100
Table A-1: RSD and Percent Recovery for Organic Carbon Analysis.....	115
Table A-2: RSD and Percent Recovery for Chloride.....	116
Table A-3: RSD and Percent Recovery for Sodium	117
Table C-1: Caffeine Concentrations from Pilot Experiments.....	125
Table C-2: Carbamazepine Concentrations from Pilot Experiments.....	126
Table C-3: DEET Concentrations from Pilot Experiments	126
Table C-4: Naproxen Concentrations from Pilot Experiments.....	127
Table C-5: Sulfamethoxazole Concentrations from Pilot Experiments.....	127
Table C-6: Mass Balance Calculations for Caffeine.....	128
Table C-7: Mass Balance Calculations for Carbamazepine	128

Table C-8: Mass Balance Calculations for DEET	128
Table C-9: Mass Balance Calculations for Naproxen.....	129
Table C-10: Mass Balance Calculations for Sulfamethoxazole	129

LIST OF ABBREVIATIONS

ΔP	change in pressure
$\Delta\pi$	osmotic pressure
φ	solvent association factor
M	solution viscosity
ρ	density
A	area
BDL	below detection limit
BPA	bisphenol A
CAF	caffeine
CBZ	carbamazepine
C_f, C_p, C_c	concentration in feed, permeate, and concentrate streams
C_m	concentrate at membrane surface
DEET	N,N-Diethyl-meta-toluamide
DF	degrees of freedom
d_h	hydraulic diameter
D_i	diffusivity of a species
DOC	dissolved organic carbon
EST	estrone
F_s	solute flux
F_w	water flux

GEM	gemfibrozil
gpm	gallon per minute
GW	groundwater
HPLC	high performance liquid chromatography
HSDM	homogeneous solution diffusion model
IQ	irrigation quality
k_b	solute back-transport mass transfer coefficient
K_s	solute mass transfer coefficient
K_w	water mass transfer coefficient
Log D	octanol-water partition coefficient at given pH
Log K_{ow}	octanol-water partition coefficient
LS	lime softening
MDL	method detection limit
MGD	million gallons per day
MSE	mean square error
MTC	mass transfer coefficient
MV	molecular volume
MW	molecular weight
MWCO	molecular weight cut off
NF	nanofiltration
NPU	nanofiltration pilot unit
NPX	naproxen

POE	point-of-entry
ppb	part per billion
PPCP	pharmaceuticals and personal care products
ppt	part per trillion
psi	pounds per square inch
Q_f, Q_p, Q_c	flow rate in feed, permeate, and concentrate streams
R	recovery
R_e	Reynolds number
RO	reverse osmosis
RSD	relative standard deviation
s	standard deviation
S_c	Schmidt number
SCADA	supervisory control and data acquisition
SDM	solution diffusion model
SDM-FT	solution diffusion model with film theory
S_h	Sherwood number
SMX	sulfamethoxazole
SOC	synthetic organic compound
SSE	sum of the square error
SUC	sucralose
TDS	total dissolved solids
TOC	total organic carbon

TrOC	trace organic compound
UCF	University of Central Florida
USEPA	United States Environmental Protection Agency
UV ₂₅₄	ultraviolet absorption at 254 nanometers
V _i	solute molar volume at normal boiling point
WTP	water treatment plant
WWTP	wastewater treatment plant

CHAPTER 1: GENERAL INTRODUCTION

Research related to trace organic compounds (TrOCs) has increased since the initial discovery of pesticides in water in the 1980's. TrOC contamination in groundwater supplies is often due to irrigation with reclaimed water. Although the precise adverse effects of TrOCs due to human consumption are still under investigation and TrOCs are not currently regulated, compound detection in drinking water supplies has caused concern in the public eye. For this reason, the Town of Jupiter (Town) tasked the University of Central Florida (UCF) with determining the extent of reclaimed water quality impacts (i.e. TrOC contamination) on their surficial groundwater wellfield, and subsequent impacts on their water treatment plant.

To accomplish this goal, a set of tasks was established:

1. Routinely monitor reclaimed water, surficial groundwater wells, and various water treatment plant sample ports throughout the facility for TrOCs,
2. Conduct experiments evaluating TrOC rejection by a nanofiltration (NF) pilot unit by spiking known amounts of TrOCs into pilot feed water and collecting and analyzing permeate and concentrate samples.

In conjunction with satisfying these objectives, a literature review was conducted to identify gaps in the existing TrOC/water treatment knowledge base. The ability to model an anthropogenic solute through a NF process would be desirable for a utility concerned with TrOCs in its water supplies; consequently, pilot experiments were carried out with this in mind.

CHAPTER 2: DETECTION OF ANTHROPOGENIC ORGANIC CHEMICALS IN RECLAIMED WATER, RECHARGE BASIN WATER, SURFICIAL GROUNDWATER, AND DRINKING WATER IN NORTHWEST PALM BEACH COUNTY, FLORIDA

Abstract

This chapter presents the results of an investigation that examined of sixteen trace organic compounds in a variety of water matrices within the environment. Samples collected from reclaimed water, a surface water recharge basin, three surficial groundwater wells, and the Town of Jupiter Water Utilities (Town's) water treatment plant (WTP) raw water, nanofiltration permeate, and point-of-entry locations were analyzed. Results indicate that the wastewater treatment plant was unable to remove a number of trace organic compounds, as they were frequently detected in reclaimed water used for irrigation. These compounds are discharged into the environment and were subsequently detected in surface water and groundwater supplies. Intermediate sampling of the recharge basin and surficial groundwater wells that supply the water treatment plant revealed that a majority of the sixteen compounds make their way into the WTP. Bisphenol A and caffeine were detected in nanofiltration permeate at 34 and 23 ng/L, respectively. Subsequent dilution with the Town's reverse osmosis permeate results in trace organics found below detection in a point-of-entry sample.

Keywords: pharmaceutical, endocrine disrupting compound, surficial groundwater, nanofiltration, reclaimed water, wastewater contaminant

Introduction

Trace organic compounds (TrOCs), defined to include pesticides, endocrine disrupting compounds (EDCs), pharmaceuticals and personal care products (PPCPs), have been detected in surface and groundwater (GW) that serve as potable water supplies (Heberer, 2002; Kolpin et al., 2002; Focazio et al., 2008; Lapworth et al., 2012; Mawhinney et al., 2012). Researchers have demonstrated that TrOCs can be found in concentrations ranging from parts per trillion (ppt; ng/L) to parts per billion (ppb; µg/L), and have been detected at concentrations greater than 1 µg/L in some surface water supplies (Vulliet et al., 2011; Watkinson et al., 2009); however, the precise effect of TrOCs at these low concentrations on human health remains unknown.

Although TrOCs are typically detected near the practical quantitation level of most modern analytical equipment, some researchers suspect that long-term consumption of trace constituents could result in adverse health effects (Jobling et al., 1996; Fawell & Ong, 2012). Alternatively, Stanford et al. (2010) conducted a comparative study evaluating exposure to estrogenic activity and TrOCs in drinking water, food, beverage and air, and concluded that drinking water represents a small fraction of TrOCs sources, suggesting that the trace levels of compounds detected in drinking water do not pose adverse human health effects. Table 2-1 lists some typical doses of pharmaceuticals, in addition to atrazine application rates, the caffeine content in coffee, and N,N-Diethyl-meta-toluamide (DEET) composition in insect repellents. Pharmaceutical doses range from 2 to 10 mg per dose for diazepam, and up to 800 mg per dose for sulfamethoxazole. Additionally, the caffeine

content in coffee ranges from 95 to 200 mg per 8 ounce beverage, corresponding to a concentration range of 400 to 844 mg/L. Furthermore, a 2.5 ounce canister of OFF![®] contains 25% DEET, or 18.5 mL, and one packet of Splenda[®] contains one gram of sucralose. These concentrations are of course significantly higher than what has been reported in the environment (Barnes et al., 2008; Focazio et al., 2008; Benotti et al., 2009; Loos et al., 2010; Fram & Belitz, 2011; Lapworth et al., 2012; Padhye et al., 2014); however, mounting evidence supports their widespread occurrence of TrOCs in the environment.

While the adverse effects of TrOCs in drinking water are not well known (Lapworth et al., 2012; Murray et al., 2010, Padhye et al., 2014), TrOCs in water supplies has caused concern regarding public perception (Macpherson et al., 2015). Furthermore, future regulations could include certain TrOCs, specifically hormonal pharmaceuticals, as many of them have been included in the United States Environmental Protection Agency's (USEPA's) Contaminant Candidate List 4 (USEPA, 2015). For these aforementioned reasons, some water utilities have examined or are initiating the examination of the occurrence of TrOCs in their water supply, whether that be surface or groundwater, in addition to TrOC removal via a pilot- or full-scale treatment process (Duranceau, 1990; Radjenovic et al., 2008; Padhye et al., 2013).

Table 2-1: Trace Organic Compound Servings

Compound	Primary Use	Typical Serving
Atrazine	Herbicide	Agricultural application rate = 1.6 - 2.5 lbs/acre, depending on season
Caffeine	Stimulant	95 - 200 mg in an 8 ounce brewed coffee
Carbamazepine	Anti-Epileptic Drug	Typical Dose = 100 - 200 mg, 2 times per day
DEET	Insect Repellent	Off! [®] insect repellent contains 25% DEET in 2.5 and 4 ounce canisters
Gemfibrozil	Lipid Regulator	Typical Dose = 600 mg, 2 times per day
Iopromide	X-Ray Contrast Medium	Typical Dose = 150 - 370 mg/mL, depending on reason for use
Meprobamate	Anti-Anxiety Drug	Typical Dose = 1.2 - 1.6 g/day in 3 to 4 doses
Naproxen	Anti-Inflammatory	Typical Dose = 250 - 750 mg, depending on reason for use
Sucralose	Artificial Sweetener	1 pack of Splenda [®] = 1 gram
Sulfamethoxazole	Antibiotic	Typical dose = 800 mg/12 hrs, 75 - 100 mg/day, depending on use
Trimethoprim	Antibiotic	Typical dose = 15 – 20 mg/6 hrs, 160 mg/12 hrs, depending on use

*See Web References

Although a majority of research has been conducted evaluating the occurrence of surface water sources, evaluating TrOC occurrence in groundwater has increased in recent years (Fu et al., 2013; Padhye et al., 2014; Sorensen et al., 2015; Gaffney et al., 2015; Petrie et al., 2015). Furthermore, the impact that reclaimed water used for irrigation can have on surficial groundwater wells should also be investigated, as researchers have detected TrOCs in groundwater as a result of wastewater discharge (Barnes et al., 2008; Estévez et al., 2012; Fawell & Ong, 2012; Mawhinney et al., 2012; Li et al., 2015; Wang et al., 2015). Others have declared wastewaters as the main sources of TrOCs in the environment (Lapworth et al., 2012; Focazio et al., 2008; Andreu et al., 2015; Petrie et al., 2015); consequently, surficial groundwater wells where reclaimed water is utilized could potentially contain detectable levels of TrOCs.

Researchers have suggested that certain TrOCs could serve as markers of wastewater impacts on groundwater sources. Specifically, researchers have demonstrated that sucralose could serve as an indicator compound for wastewater influence on other waters (Oppenheimer et al., 2011; Mawhinney et al., 2012). Additionally, Clara et al. (2004) evaluated the persistence of carbamazepine, an epileptic drug, in groundwater, and found it could serve as an indicator for anthropogenic influence in the environment, since it is not naturally found in the environment, but is discharged from wastewater facilities.

The primary purpose of this work was to evaluate the detection of TrOCs from wastewater effluent to a water treatment plants' point-of-entry (POE). Results reported herein include

sampling from irrigation quality water (IQ), a recharge basin, three surficial wells, raw water entering the WTP, NF permeate, and POE water.

Site Description

The Town utilizes a surficial groundwater source to supply their existing 14.5 million gallon per day (MGD) NF plant, constructed in 2010, which operates parallel to a 13.7 MGD reverse osmosis plant. The groundwater source utilizes 51 wells that have a combined production capacity of 26.2 MGD. Individual well capacities range from 200 to 800 gallons per minute (gpm) (0.29 to 1.2 MGD), where older wells produce less water than newer wells. Well age ranges from 9 to 42 years, and their average depth below the surface is 150 feet (46 meters).

Since 1983, WWTP effluent has been used as reclaimed water over a portion of the Town's surficial well locations. A portion of the Town's surficial wells are located under the influence of IQ water. It is suspected that IQ water contaminates surficial wells, as evidenced by increasing chloride concentrations in surficial wells, since the chloride concentration in the IQ water is around 133 mg/L, significantly higher than the Town's surficial water, which typically has a chloride concentration below 60 mg/L. Figure 2-1 depicts a map of the relationship between the WTP, WWTP, and the Town's surficial wells. The area where IQ water is used is depicted within the black box in the southeast portion of Figure 2-1. Surficial wells that have not increased in chloride concentrations are presented as black diamonds in Figure 2-1, and the wells that have experienced a significant increase in chloride are shown in gray circles.

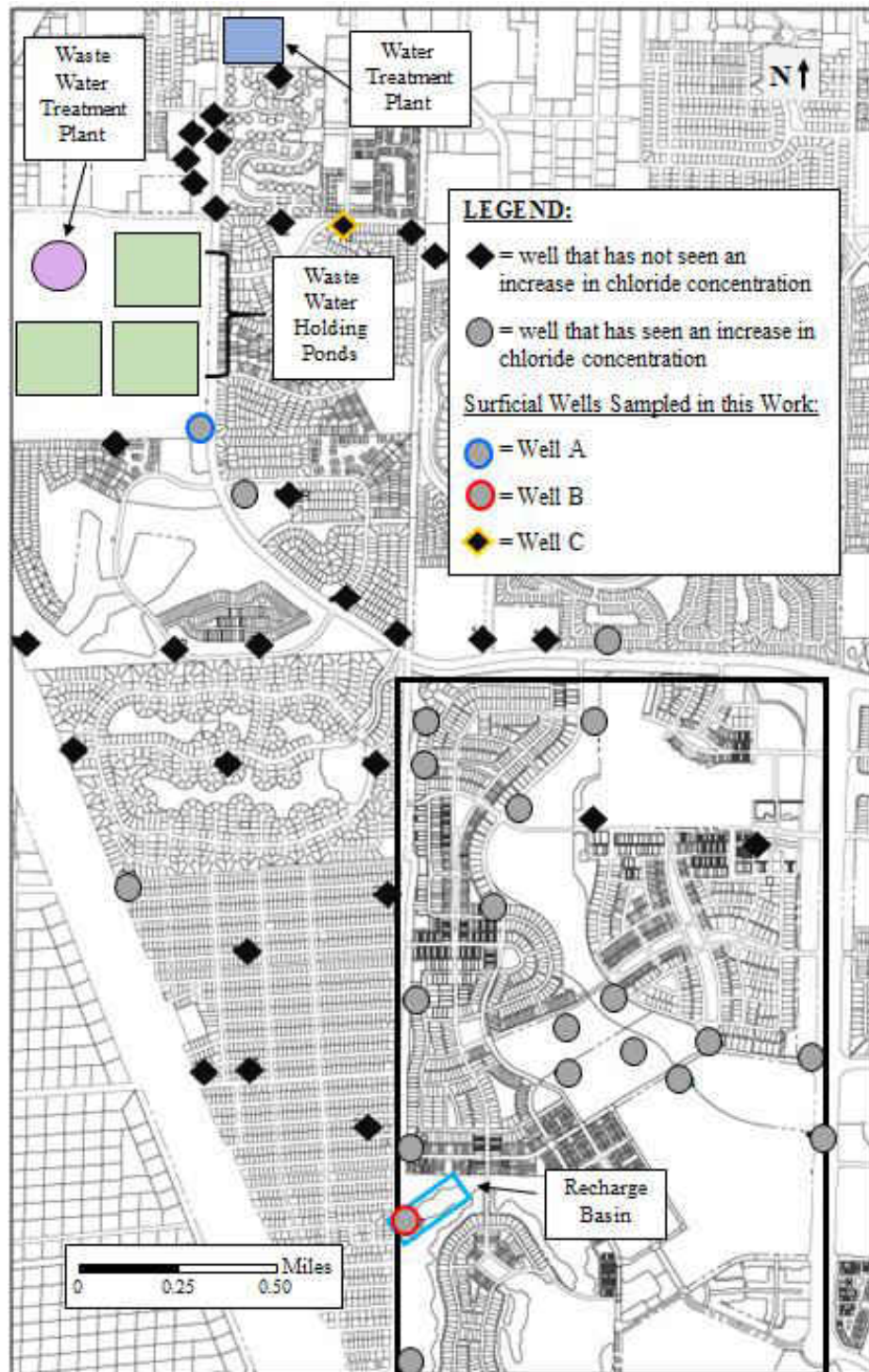


Figure 2-1: Surficial Wells in Relation to the Water and Wastewater Treatment Plants

Screening Evaluation

As a result of increasing chlorides, the Town desired to understand the possible relationship between IQ water and surficial groundwater wells. In 2008 and 2009, a preliminary investigation of IQ water, raw water entering the WTP, and permeate from a NF pilot unit was conducted, and a summary of the compounds detected in any of the three samples are presented in Table 2-2. TrOCs that were below detection in each of these samples are not shown in Table 2-2, but can be found elsewhere (Wilder et al., 2016). The three sampling events did not occur on the same day. IQ and NF pilot permeate samples were collected as grab samples, while the raw water was collected as a composite sample.

Of the 32 trace organic compounds analyzed, 17 were detected in IQ water. The compound with the highest concentration detected in the IQ water sample was iopromide, with a concentration of 590 ng/L, followed by meprobamate, with a concentration of 310 ng/L. Three compounds, bisphenol A, DEET, and sulfamethoxazole were detected in the Town's raw water, with concentrations of 66, 100, and 5.4 ng/L, respectively. Bisphenol A was the only compound detected in nanofiltration pilot permeate, with a concentration of 26 ng/L.

Table 2-2: Trace Organic Compound Preliminary Investigation Findings

Compound	Method Detection Limit (MDL) (ng/L)	Concentration (ng/L)		
		IQ Water	Raw Water	NF Pilot Permeate
Atrazine*	1.0	52	ND	ND
Bisphenol A*	10	150	66	26
Caffeine*	5.0	210	ND	ND
Carbamazepine*	1.0	180	ND	ND
DEET*	5.0	150	100	ND
Diazepam*	1.0	3.9	ND	ND
Estrone*	1.0	4.1	ND	ND
Gemfibrozil*	10	62	ND	ND
Iopromide*	10	590	ND	ND
Meprobamate*	5.0	310	ND	ND
Naproxen*	1.0	140	ND	ND
Oxybenzone	2.0	8.0	ND	ND
Sulfamethoxazole*	1.0	100	5.4	ND
Trimethoprim*	5.0	120	ND	ND
Pentoxifylline	1.0	5.8	ND	ND
Methadone	5.0	16	ND	ND
Salicylic Acid	10	55	ND	ND

“ND” indicates compound was below detection limit; *Analyzed in 2015-2016 analyses.

Methods

Trace Organic Compounds and Descriptions

Fourteen compounds were analyzed in this work, presented previously in Table 2-2 in addition to sucralose, an artificial sweetener. Of the fourteen compounds analyzed in this work, 7 are prescription drugs (carbamazepine, diazepam, gemfibrozil, meprobamate, naproxen, sulfamethoxazole, and trimethoprim), three (caffeine, estrone, and sucralose) are secreted by humans, two (oxybenzone and salicylic acid) are personal care products, one (atrazine) is a herbicide, one (bisphenol A) is a plastic derivative, and one (iopromide) is used as a contrast medium in radiology. The compounds listed in Table 2-3 do not naturally occur in the environment, and the primary method for entering the environment would be through incomplete removal by wastewater treatment, with the exception of atrazine, which is commonly applied directly to residential and commercial areas (i.e. golf courses, public parks,) as herbicide.

Sample Collection, Transport, and Analysis

Six sampling events were conducted related to TrOC occurrence in IQ water, surficial wells, raw water, and the Town's NF permeate and POE water. Table 2-4 presents sampling years, locations, and sample type (grab or composite). As previously mentioned, "IQ water" refers to reclaimed water used for irrigation. Well A denotes a well located near WWTP holding ponds, Well B refers to a well located under the influence of IQ water, and Well C represents a well not impacted by IQ water. The term "raw water" refers to surficial groundwater entering the water plant, prior to any treatment. NF permeate was collected

following the full-scale nanofiltration process, which proceeds sand filtration and cartridge filtration. The POE sample was collected prior to entering the Town's distribution system. Raw water and POE water were collected as composite samples, while recharge basin and surficial wells were collected as grab samples. IQ water and NF permeate were collected as both composite and grab samples, depending on the sampling event. To form composite samples, grab samples were collected at least four times over an eight-hour period, then combined to form the composite sample. Sample ports were opened and allowed to flush for at least two minutes in order to remove stagnant water out of the system.

After collection, samples were packed in a cooler with ice and shipped to one of two commercial laboratories. Prior to 2015, samples were shipped to ALS Environmental (1317 S. 13th Avenue, Kelso, WA 98626). In 2015, samples were shipped to Eurofins Eaton Analytical (EEA) (750 Royal Oaks Drive, Suite 100, Monrovia, California, 91016-3629) for analysis. Method reporting limits (MRLs) for TrOCs ranged from 1.9 to 480 ng/L were analyzed by ALS Environmental, and 5-100 ng/L when analyzed by EEA.

Samples shipped to ALS Environmental were analyzed using liquid chromatography/mass spectroscopy/mass spectroscopy (LC/MS/MS). When samples were shipped to EEA, two 40-mL glass amber vials containing 80 μ L of 32 g/L NaOmadine and 5 mg ascorbic acid were used as preservatives to collect each sample. Samples were analyzed using a fully automated on-line solid phase extraction, high performance liquid chromatography, mass spectrometry-mass spectrometry system (HPLC/MS/MS). A detailed description of EEA's laboratory methods can be found elsewhere (Oppenheimer et al., 2011).

Table 2-3: Sampling Event Summary

Event No., Month & Year, Sample Location, Sample Type*
1, October 2014 Recharge Basin (G)
2, January 2015 Raw Water, NF Permeate, POE (C)
3, March 2015 IQ Water (C) Well A, Well B (G)
4, July 2015 Raw Water, IQ Water, NF Permeate (C) Well A, Well B (G)
5, August 2015 Raw Water, IQ Water (C) IQ Water (G) Well A, Well B (G)
6, October 2015 Raw Water, IQ Water (C) Well A, Well B, Well C, NF Permeate (G)

*G = grab sample; C = composite sample

Results and Discussion

Results are categorized according to sample location. Results are presented starting from the samples collected farthest from the WTP, to those located at the water treatment facility. When a location was sampled more than once, average TrOC concentrations are reported. Only results with concentrations above the MDL were used to calculate the average TrOC concentrations. For this reason, frequency of detection is presented alongside the average TrOC results. When only one sample was collected for a given location (i.e. IQ grab sample, recharge basin, and Well C), TrOC concentrations for that single event are presented.

Irrigation Quality Water

Table 2-4 presents average IQ water composite and grab sampling results, in addition to the compound detection frequency in the composite samples. For composite sampling, TrOCs were analyzed during four sampling events (events 3 – 6). Bisphenol A and diazepam were not detected during any of the four composite sampling events, although some TrOCs, including carbamazepine, DEET, gemfibrozil, sucralose, and sulfamethoxazole, were detected during each of the four sampling events. Average composite sampling results of IQ samples range from 8.5 ng/L (estrone) to 22 µg/L (sucralose). Gemfibrozil and sulfamethoxazole were detected at relatively high levels during each of the sampling events, with concentrations of 738 and 1,115 ng/L, respectively.

Of the fourteen TrOCs analyzed in the IQ grab sample, three were below the MDL of 5 ng/L: diazepam, estrone, and iopromide. The lowest concentration in this sample was atrazine, with a concentration of 6.7 ng/L, followed by naproxen, with a concentration of 13 ng/L. The TrOCs with the highest concentration was sucralose, with a concentration of 29 µg/L. Bisphenol A, sulfamethoxazole, and gemfibrozil were also detected at relatively high concentrations ranging from 500 to 750 ng/L. Iopromide was not frequently detected – only one time in the composite sample. Bisphenol A was also frequently detected – only one time in the grab sample.

Table 2-4: IQ Composite and Grab Sample Results

Compound	Composite Sampling		Grab Sampling
	Average Conc. (ng/L)*	Detection Frequency	Conc. (ng/L)
Atrazine	14	3/4	6.7
Bisphenol A	ND	0/4	650
Caffeine	75	3/4	60
Carbamazepine	61	4/4	53
DEET	85	4/4	200
Diazepam	ND	0/4	ND
Estrone	8.5	2/4	ND
Gemfibrozil	738	4/4	750
Iopromide	380	1/4	ND
Meprobamate	36.3	3/4	44
Naproxen	59	1/4	13
Sucralose	22,000	4/4	29,000
Sulfamethoxazole	1,115	4/4	500
Trimethoprim	28	2/4	32

*Average represents the average concentrations of samples detected, those below MDL are excluded from calculation; "ND" indicates compound was below detection limit

Recharge Basin

Table 2-5 presents results of a single grab sample collected from a recharge basin during sampling event 1. In this event, samples were shipped to a commercial lab that analyzed for 23 TrOCs, due to differing analytical techniques. In the recharge basin sample, nine out of 23 TrOCs were detected above MRLs which ranged from 1.9-480 ng/L depending on the compound. Bisphenol A, estrone, naproxen and trimethoprim were not detected in the recharge basin, but were detected in other locations during other sampling events. Sucralose was not analyzed for samples collected from the recharge basin. Atrazine had the lowest concentration of 6.8 ng/L, and the TrOC with the highest concentration was sulfamethoxazole (440 ng/L). The remainder of the TrOCs detected in the recharge basin grab sample ranged from 110 to 260 ng/L.

Table 2-5: Recharge Basin Grab Sample Results

Compound	Concentration (ng/L)
Atrazine	6.8
Carbamazepine	130
Caffeine	170
DEET	150
Gemfibrozil	230
Meprobamate	260
Oxybenzone	110
Sulfamethoxazole	440
Salicylic Acid	240

Surficial Groundwater

Table 2-6 presents the average results and detection frequency of four grab samples collected from Well A (located southeast of the WWTP holding ponds) and Well B (under the influenced of reclaimed water used for irrigation), in addition to results obtained from one grab sample collected from Well C (not impacted by IQ water).

It appears that TrOC results of Well A were relatively consistent, meaning compounds were either detected during the four events, or not detected during any. Among the TrOCs analyzed, five of them (bisphenol A, caffeine, diazepam, estrone, and trimethoprim) were below detection for each sampling event. Alternatively, five TrOCs (carbamazepine, DEET, gemfibrozil, meprobamate, and sucralose) were detected in each of the four sampling events.

In Well B, fewer TrOCs were detected when compared to Well A results. Additionally, the TrOCs detected were at relatively low concentrations, the lowest detection being carbamazepine and gemfibrozil with 6.9 and 5.8 ng/L, respectively. The highest average concentration detected was sucralose (1,640 ng/L). Similar to the results obtained from Well A, many compounds are consistently detected in all of the samples or none of the samples, and only gemfibrozil, iopromide and sulfamethoxazole are detected in some samples.

Three TrOCs were detected in the Well C grab sample, including DEET, iopromide, and sucralose, with concentrations of 18, 37, and 270 ng/L, respectively. The remaining eleven TrOCs were below detection limits. In comparison to Well A and B results, the

concentration of sucralose is relatively low, as expected, since this well is not expected to be impacted by reclaimed water. Well C results indicate the persistence and ability of certain TrOCs to travel in soil to groundwater. While DEET was not detected in samples collected from a well impacted by irrigation (Well B), it was frequently detected in a well that could experience contamination due to traveling within soil (Well A).

Table 2-6: Surficial Groundwater Well Grab Sample Results

Compound	Well A		Well B		Well C
	Average Conc. (ng/L)*	Detection Frequency	Average Conc. (ng/L)*	Detection Frequency	Conc. (ng/L)
Atrazine	7.4	1/4	ND	0/4	ND
Bisphenol A	ND	0/4	49	4/4	ND
Caffeine	ND	0/4	ND	0/4	ND
Carbamazepine	31	4/4	7	4/4	ND
DEET	57	4/4	ND	0/4	18
Diazepam	ND	0/4	ND	0/4	ND
Estrone	ND	0/4	ND	0/4	ND
Gemfibrozil	270	4/4	6	3/4	ND
Iopromide	26	1/4	42	1/4	37
Meprobamate	30	4/4	ND	0/4	ND
Naproxen	13	1/4	ND	0/4	ND
Sucralose	2,025	4/4	1,640	4/4	270
Sulfamethoxazole	40	1/4	12	1/4	ND
Trimethoprim	ND	0/4	ND	0/4	ND

*Average represents the average concentrations of samples detected, those below detection limits are excluded from calculation

Table 2-7 presents samples collected from the utilities' raw water sampling port. Raw water samples were collected four times and TrOCs presented in Table 2-6 were analyzed during each sampling event. The raw water sampling port is located upon entering the water treatment facility, but prior to any pretreatment processes.

The highest average concentration in the raw water samples was sulfamethoxazole (1,500 ng/L), followed by sucralose (627 ng/L). Five TrOCs were not detected in any of the samples collected from the raw water sampling port, including atrazine, diazepam, meprobamate, naproxen, and trimethoprim. Of the TrOCs detected, those with the lowest concentrations were estrone (5 ng/L) and carbamazepine (7.7 ng/L). Gemfibrozil and sucralose were detected the most frequently, present in three out of four samples. Additionally, caffeine and carbamazepine were detected in two out of four samples.

Table 2-7: Raw Water Composite Sample Results

Compound	Average Conc. (ng/L)*	Detection Frequency
Atrazine	ND	0/4
Bisphenol A	66	1/4
Caffeine	215	2/4
Carbamazepine	7.7	2/4
DEET	15	1/4
Diazepam	ND	0/4
Estrone	5.0	1/4
Gemfibrozil	62	3/4
Iopromide	30	1/4
Meprobamate	ND	0/4
Naproxen	ND	0/4
Sucralose	627	3/4
Sulfamethoxazole	1,500	1/4
Trimethoprim	ND	0/4

*Average represents the average concentrations of samples detected, those below detection limits are excluded from calculation

Nanofiltration Permeate and Point-of Entry

NF permeate was collected three times, twice as a composite sample and once as a grab sample. In the two composite samples, two TrOCs were detected: bisphenol A and caffeine, with average concentrations of 34 and 23 ng/L. The other twelve TrOCs analyzed in these samples were below detection limits, and none of the fourteen TrOCs were detected in the NF permeate grab sample.

One composite sample was collected from the Town's POE, and TrOCs were below detection limits. This was expected, since the POE is comprised of 51% RO permeate and 49% NF permeate, and has been chlorinated and chloraminated. It is likely that the low and infrequently detected TrOCs found in NF permeate would be heavily diluted by RO permeate, which is not expected to contain trace organic compounds due to its superior removal capabilities, in addition to its pristine water source, the deep Floridan aquifer.

Conclusions

Although the adverse impact of trace organic compounds on humans are not completely understood, their presence in certain water supplies remains a concern for water purveyors. Results reported herein have further validated the suggestion that WWTP effluent has a large influence on surficial groundwater. Results indicate incomplete TrOC removal by a wastewater treatment plant based on their frequent detection in reclaimed water. These TrOCs are subsequently detected in a groundwater supply impacted by the aforementioned reclaimed water by percolation into a surficial aquifer. Although nine organic compounds were detected in the raw water entering the water treatment facility, only two have been

detected in full-scale NF permeate, and none were detected in POE water. This indicates adequate compound removal by the nanofiltration plant and further dilution by reverse osmosis permeate treating water from the deep Floridan aquifer. This work has added to the growing knowledge base regarding trace organic compounds in the aquatic environment, specifically surficial groundwater that supplies a drinking water treatment facility.

Acknowledgments

The work reported herein was funded by UCF project agreement number 16208114. The authors acknowledge the Town of Jupiter Utilities staff, including David Brown, Amanda Barnes, Paul Jurczak, and Rebecca Wilder, for their assistance and support, without whom this work would not have possible. The authors also acknowledge the consultation and advice of Ian Watson (RosTek Associates Inc.) and John Potts (Kimley-Horn & Associates, Inc.). Additional thanks are offered to the UCF graduate and undergraduate students who assisted in this work.

References

- Andreu, V., Gimeno-Garcia, E., Pascual, J.A., Vazquez-Roig, P., & Pico, Y. (2015). Presence of pharmaceuticals and heavy metals in the waters of a Mediterranean coastal wetland: Potential interactions and the influence of the environment. *Science of the Total Environment*,
- Barnes, K.K., Kolpin, D.W., Furlong, E.T., Zaugg, S.D., Meyer, M.T., & Barber, L.B. (2008). A national reconnaissance of pharmaceuticals and other organic wastewater contaminants in the United States – I) Groundwater. *Science of the Total Environment*, 402, 192-200.
- Benotti, M.J., Trenholm, R.A., Vanderford, B.J., Holady, J.C., Stanford, B.D., & Snyder, S.A. (2009). Pharmaceuticals and Endocrine Disrupting Compounds in U.S. Drinking Water. *Environmental Science and Technology*, 43 (3), 597-603.
- Clara, M., Strenn, B., & Kreuzinger, N. (2004). Carbamazepine as a possible anthropogenic marker in the aquatic environment: investigations on the behavior of Carbamazepine in wastewater treatment and during groundwater infiltration. *Water Research*, 38, 947-954.
- Duranceau, S.J., (1990). *Modeling of Mass Transfer and Synthetic Organic Compound Removal in a Membrane Softening Process*. (Doctoral Dissertation).
- Estévez, E., del Carmen Cabrera, M., Molina-Díaz, A., Robles-Molina, J., & del Pino Palacios-Díaz, M. (2012). Screening of emerging contaminants and priority substances (2008/105/EC) in reclaimed water for irrigation and groundwater in a volcanic aquifer (Gran Canaria, Canary Islands, Spain). *Science of the Total Environment*, 433 (1), 538-546.
- Fawell, J. & Ong, C.N. (2012). Emerging Contaminants and the Implications for Drinking Water. *International Journal of Water Resources Development*, 28 (2), 247-263.
- Focazio, M.J., Kolpin, D.W., Barnes, K.K., Furlong, E.T., Meter, M.T., Zaugg, S.D., Barber, L.B., & Thurman, M.E. (2008). A national reconnaissance for pharmaceuticals and other organic wastewater contaminants in the United States – II. Untreated drinking water sources. *Science of the Total Environment*, 402 (2-3), 201-216.
- Fram, M.S., & Belitz, K. (2011). Occurrence and concentrations of pharmaceutical compounds in groundwater used for public drinking-water supply in California. *Science of the Total Environment*, 409 (18), 3409-3417.
- Fu, H.-Z., Wang, M.-H., & Ho, Y.-S. (2013). Mapping of drinking water research: A bibliometric analysis of research output during 1992-2011. *Science of the Total Environment*, 443 (15), 757-765.

- Gaffney, V., Almeida, C.M.M., Rodrigues, A., Ferriera, E., Benoliel, M.J., & Cardoso, V.V. (2015). Occurrence of pharmaceuticals in a water supply system and related human health risk assessment. *Water Research*, 72, 199-208.
- Heberer, T. (2002). Occurrence, fate, and removal of pharmaceutical residues in the aquatic environment: a review of recent research data. *Toxicol. Lett.*, 131 (1-2), 5-17.
- Kolpin, D.W., Furlong, E.T., Meter, M.T., Thurman, E.M., Zaugg, S.D., Barber, L.B., & Buxton, H.T. (2002). Pharmaceuticals, hormones, and other organic wastewater contaminants in US streams, 1999-2000: a national reconnaissance. *Environmental Science & Technology*, 36 (6), 1202-1211.
- Jobling, S., Sheahan, D., Osborne, J.A., Matthiessen, P., & Sumpter, J.P. (1996). Inhibition of testicular growth in rainbow trout (*Oncorhynchus mykiss*) exposed to estrogenic alkylphenolic chemicals. *Environ Toxicol Chem*, 15 (2), 194-202.
- Lapworth, D.J., Baran, N., Stuart, M.E., & Ward, R.S. (2012). Emerging organic contaminants in groundwater: A review of sources, fate and occurrence. *Environmental Pollution*, 163, 287-303.
- Li, Z., Xiang, X., Li, M., Ma, Y., Wang, J., & Liu, X. (2015). Occurrence and risk assessment of pharmaceuticals and personal care products and endocrine disrupting chemicals in reclaimed water and receiving groundwater in China. *Ecotoxicology and Environmental Safety*, 119, 74-80.
- Loos, R., Locoro, G., Comero, S., Contini, S., Schwesig, D., Werres, F., Balsaa, P., Gans, O., Weiss, S., Blaha, L., Bolchi, M., & Gawlik, B.M. (2010). Pan-European survey on the occurrence of selected polar organic persistent pollutants in groundwater. *Water Research*, 44 (14), 4115-4126.
- Macpherson, L., Callaway, E., Snyder, S.S., Venette, S., Sellnow, T., & Slovic, P. (2015). *Core Messages for Chromium, Medicines and Personal Care Products, NDMA, and VOCs*. Denver, CO: Water Research Foundation.
- Mawhinney, D.B., Young, R.B., Vanderford, B.J., Borch, T., & Snyder, S.A. (2011). Artificial Sweetener Sucralose in U.S. Drinking Water Systems. *Environ. Sci. Technol.*, 45 (20), 8716-8722.
- Murray, K.E., Thomas, S.M., & Bodour, A.A. (2010). Prioritizing research for trace pollutants and emerging contaminants in the freshwater environment. *Environmental Pollution*, 158, 3462-3471.
- Oppenheimer, J., Eaton, A., Badruzzaman, M., Haghani, A.W., Jacangelo, J.G. (2011). Occurrence and suitability of sucralose as an indicator compound of wastewater loading to surface waters in urbanized regions. *Water Research*, 45 (13), 4019-4027.

- Padhye, L.P., Yao, H., Kung'u, F.T., & Huang, C.-H. (2014). Year-long evaluation on the occurrence and fate of pharmaceuticals, personal care products, and endocrine disrupting chemicals in an urban drinking water treatment plant. *Water Research*, *51*, 266-276.
- Petrie, B., Barden, R., & Kasprzyk-Hordern, B. (2015). A review on emerging contaminants in wastewaters and the environment: Current knowledge, understudied areas and recommendations for future monitoring. *Water Research*, *72*, 3-27.
- Petrovic, M., Eljarrat, E., Lopez de Alda, M.J., & Barcelo, D. (2004). Endocrine disrupting compounds and other emerging contaminants in the environment: A survey on new monitoring strategies and occurrence data. *Anal Bioanal Chem*, *378*, 549-562.
- Radjenovic, J., Petrovic, M., Ventura, F., & Barcelo, D. (2008). Rejection of pharmaceuticals in nanofiltration and reverse osmosis membrane drinking water treatment. *Water Research*, *42* (14), 3601-3610.
- Sorensen, J.P.R., Lapworth, D.J., Nkhuwa, D.C.W., Stuart, M.E., Goody, D.C., Bell, R.A., Chirwa, M., Kabika, J., Liemisa, M., Chibesa, M., & Pedley, S. (2015). *Water Research*, *72*, 51-63.
- Stanford, B.D., Snyder, S.A., Trenholm, R.A., Holady, J.C., & Vanderford, B.J. (2010). Estrogenic activity of US drinking waters: A relative exposure comparison. *Journal AWWA*, *102* (11), 55-65.
- United States Environmental Protection Agency (USEPA). (2015). Summary of Nominations for the Fourth Contaminant Candidate List. Office of Water, EPA 815-R-15-001.
- Vulliet, E., Cren-Olive, C., Grenier-Loustalot, M.-F. (2011). Occurrence of pharmaceuticals and hormones in drinking water treated from surface water. *Environ Chem Lett*, *9*, 103-114.
- Watkinson, A.J., Murby, E.J., Kolpin, D.W., & Costanzo, S.D. (2009). The occurrence of antibiotics in an urban watershed: From wastewater to drinking water. *Science of the Total Environment*, *407* (8), 2711-2723.
- Wang, S., Wenyong, W., Liu, F., Yin, S., Bao, Z., Liu, H. (2015). Spatial distribution and migration of nonylphenol in groundwater following long-term wastewater irrigation. *Journal of Contaminant Hydrology*, *177-178*, 85-92.
- Wilder, R., Duranceau, S.J., Jeffery, S., Brown, D., & Arrington, A. (2016). Contaminants of Emerging Concern: Occurrence in Shallow Groundwater and Removal by Nanofiltration. *Proceedings from the American Membrane Technology Association Conference*.

Web References

- Drugs.com (October 28, 2015). Carbamazepine Uses, Dosage, & Side Effects. <http://www.drugs.com/carbamazepine.html>. Date Accessed December 17, 2015.
- Drugs.com (December 1, 2015). Meprobamate (Profession Patient Advice). <http://www.drugs.com/ppa/meprobamate.html>. Date Accessed December 17, 2015.
- Heartland Food Products Group, LLC. Conversion Charts. SPLENDA®. <https://www.splenda.com/cooking-baking/conversion-charts>. Date Accessed December 17, 2015.
- Mayo Foundation for Medical Education and Research. (May 13, 2014). Caffeine content for coffee, tea, soda and more. <http://www.mayoclinic.org/healthy-lifestyle/nutrition-and-healthy-eating/in-depth/caffeine/art-20049372>. Date Accessed December 17, 2015.
- Mayo Foundation for Medical Education and Research (September 1, 2015). Sulfamethoxazole/Trimethoprim (Oral Route) Proper Use. <http://www.mayoclinic.org/drugs-supplements/sulfamethoxazole-trimethoprim-oral-route/proper-use/drg-20071899>. Date Accessed December 17, 2015.
- Mayo Foundation for Medical Education and Research. (December 1, 2015). Naproxen (Oral Route) Proper Use. <http://www.mayoclinic.org/drugs-supplements/naproxen-oral-route/proper-use/DRG-20069820>. Date Accessed December 17, 2015.
- Mayo Foundation for Medical Education and Research (December 1, 2015). Gemfibrozil (Oral Route) Proper Use. <http://www.mayoclinic.org/drugs-supplements/gemfibrozil-oral-route/proper-use/drg-20064018>. Date Accessed December 17, 2015.
- OFF!® <http://www.off.com/en-us/products/pages/off-deep-woods.aspx>. Date Accessed December 17, 2015.
- Syngenta Crop Protection, Inc. Using Atrazine and Protecting Water Quality. http://www.atrazine.com/atrazine/images/using_atrazine_protecting_water.pdf. Date Accessed December 17, 2015.

CHAPTER 3: MASS TRANSFER AND TRANSIENT RESPONSE TIME OF A SPLIT-FEED NANOFILTRATION PILOT UNIT

The following information has been published in the peer-reviewed journal *Desalination and Water Treatment*:

Jeffery-Black, S., & Duranceau, S.J. (2016). Mass Transfer and Transient Response Time of a Split-Feed Nanofiltration Pilot Unit. *Desalination & Water Treatment*. Doi: 10.1080/19443994.2016.1155498.

Abstract

The transient response of a center-port nanofiltration membrane process was evaluated using a step-input dose of a sodium chloride solution. The pilot was configured as a two-stage, split-feed, center-port, 7:2 pressure vessel array process, where the feed water is fed to both ends of six element pressure vessels, and permeate and concentrate streams are collected after only three membrane elements. The transient response was described as a log-logistic system with a maximum delay time of 285 seconds for an 85% water recovery and 267 gallon per minute feed flowrate. The log-logistic model was shown to be >98% accurate in predicting the transient response of the permeate streams. When compared with a first-order nonlinear regression model, there was no difference in the predictability of transient response when using the log-logistic model in first-stage and second-stage membrane processes. However, the log-logistic model was found to be more predictive in describing third-stage transient response by a factor of 236 over a first-order method.

Furthermore, the homogeneous solution diffusion model was shown to effectively predict the permeate concentration for any transient permeate perturbation.

Key words: Nanofiltration, mass transfer, split-feed, transient response, pilot plant, homogeneous solution diffusion model, log-logistic, nonlinear regression

Introduction

Nanofiltration (NF) is often employed as a water softening technology due to its ability to provide superior multivalent ion removal, including calcium, magnesium and sulfate, in addition to enhanced natural and synthetic organics removal (Conlon & McClellan, 1989; Blau et al., 1992; USEPA, 1996; Duranceau & Taylor, 1992). Since NF is considered a more “loose” form of reverse osmosis, it offers many advantages, including a lower operating pressure, resulting in lower energy costs and a higher water flux (Hilal et al., 2004; Mohammad, et al., 2015).

Prior to constructing a full-scale treatment process, water utilities typically operate pilot units to gauge how a certain technology will react to a given water source. Pilot testing is often conducted to confirm process performance, optimize operating parameters, or verify process economics (Wilf, 2011). Pilot testing can also be used to conduct innovative research where results may be difficult to predict without piloting. Prior research has shown that the time required to determine the effect of a feed water concentration change can be estimated by monitoring the transient response to steady-state operations (Duranceau, 2009). Furthermore, when investigating how effectively a membrane removes feed water

constituents, knowing the time required for permeate and concentrate streams to be affected by feed water changes is critical when developing sampling protocols (Duranceau, 2009).

Tracer studies could help in estimating times required to observe changes in unit operations, as they are used to study time transients that occur in treatment processes, typically intended to evaluate contact time for disinfectants (Teefy, 1996). However, evaluations intended to study the transient response of a permeate concentration change to a feed water change are less common. Previous transient response evaluations were based on simple first-order empirical models for prediction of perturbations to water quality changes. In this work, a log-logistic approach was used to determine the permeate response to a step input of salinity ahead of a two-stage, split-feed, center-port nanofiltration process.

Background

Full-Scale Nanofiltration Plant

This research was conducted at the Town of Jupiter (Town) Water Treatment Plant (WTP), located along the southeast coast of Florida. In 2010, the Town constructed a 14.5 million gallon per day (MGD) nanofiltration plant to replace its aging lime softening (LS) facility and provide enhanced organics and hardness removal.

The Town's full-scale NF plant operates at an overall 85% recovery with first- and second-stage recoveries of 67% and 47%, respectively. The NF plant consists of five trains, each with capacities of 2,013 gallons per minute (gpm), and operates with a water flux of 14.9 gal/sfd. Stage 1 and stage 2 combine to form the total system permeate, which is comprised

80% from stage 1 permeate, and 20% from stage 2 permeate. A single train houses 486 membrane elements: 378 in stage 1 and 108 in stage 2, forming a 63:18 array, a ratio of 3.5:1. Membrane elements (NF270; DOW Filmtec) are 8" in diameter and have an area of 400 square feet, and a minimum magnesium sulfate rejection of 97.0 percent.

The Town's NF plant is unique in that it is a split-feed configuration – feed water enters and permeate exits each 6-element pressure vessel on both ends, and concentrate is collected in the center, after only three elements. For this reason, to distinguish between the multiple permeate streams, permeate is referred to as being collected from the left, right, or combined permeate streams hereinafter. Interstage concentrate (referred to as second stage feed) is routed to the second stage, which follows the same flow regime as the first stage. This configuration has provided decreased energy loss as a result of a lower osmotic pressure difference across the membrane surface. Figure 3-1 illustrates the split-feed flow path and configuration, in addition to the associated nanofiltration pretreatment process.

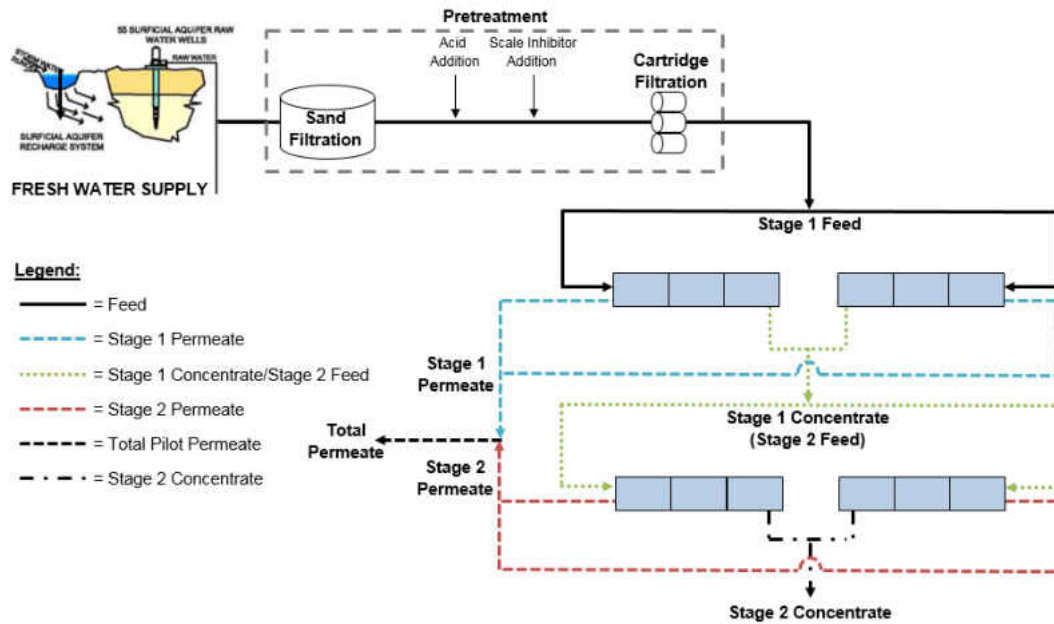


Figure 3-1: Simplified Schematic of the Split-Feed Nanofiltration Process

Split-Feed Pilot Unit

The split-feed pilot unit was commissioned in December of 2014, and designed to replicate the existing full-scale system operated by the Town. Feed water is routed directly to the pilot after the full-scale pretreatment process, which includes sand filtration, sulfuric acid and scale inhibitor addition, and cartridge filtration. The pilot operates a feed flow at 260 gpm, with an 85% recovery, and a 7:2 array. The pilot houses a total of 54 membrane elements in 9 pressure vessels, with 42 elements in the first stage, and 12 elements in the second stage. The pilot unit uses the same membrane elements as the full-scale plant (NF270; Dow Filmtec). The calculated water flux of the pilot unit is 15.1 gal/sfd, equivalent to that of the full-scale plant.

Homogeneous Solution Diffusion Model

The main purpose of NF modeling is to be as realistic as possible when describing the membrane process, allowing better model predictions when adjusting model parameters (Mohammad et al., 2015). A majority of nanofiltration modeling research utilized only very dilute and idealized solutions, containing few ions. Models have been derived to predict the response of traditionally configured nanofiltration pilots, frequently using the Nernst-Planck equation (or modified versions of the Nernst-Planck equation), the homogeneous solution diffusion model (HSDM) or nonlinear regression (Duranceau, 2009; Wesolowska, Koter, & Bodzek, 2004; Roy Sharqawy, & Lienhard, 2015; Duranceau, 1990; Wijmans & Baker, 1995; Chaabane et al., 2007; Schlogl, 1966; Dresner, 1972; Ahmad & Ooi, 2006; Bowen & Mukhtar, 1996; Garba et al., 1990).

The solution-diffusion model is based on the fundamental acceptance that water flux is proportional to a gradient in chemical potential (Wijmans & Baker, 1995). In this model, constituents dissolve through the membrane down a concentration gradient, and a separation is achieved based on the amount of the constituent that dissolved in the membrane and the rate the material diffuses through the membrane (Duranceau, 2009; Wijmans & Baker, 1995). Equations 3-1 and 3-2 present the water flux (F_w) and solute flux (F_s) in a membrane process, respectively. While the water flux is highly dependent on pressure, the solute flux is not (Wijmans & Baker, 1995).

$$F_w = K_w(\Delta P - \Delta\pi) = \frac{Q_p}{A} \quad (3-1)$$

$$F_s = K_s(C_m - C_p) = K_s \left[\left(\frac{C_f - C_c}{2} \right) - C_p \right] = \frac{Q_p C_p}{A} \quad (3-2)$$

Where,

F_w = water flux (gpd/ft²)

K_w = water mass transfer coefficient (day⁻¹)

ΔP = transmembrane pressure differential (psi)

$\Delta \pi$ = transmembrane osmotic pressure differential (psi)

Q_p = permeate flow rate (gpd)

A = membrane area (ft²)

F_s = solute flux (lb/ft²/d)

K_s = solute mass transfer coefficient (ft/d)

C_m = concentration at membrane surface (lb/ft³)

C_p = permeate concentration (lb/ft³)

C_f = feed concentration (lb/ft³)

C_c = concentrate concentration (lb/ft³)

Both water flux and solute flux are dependent on water recovery, defined as the permeate flow rate divided by the feed flow rate, and is presented in Equation 3-3.

$$R = 100 \times \frac{Q_p}{Q_f} \quad (3-3)$$

Once the water and solute mass transfer coefficients are obtained, either from the membrane manufacturer (for K_w) or experimentally (for K_s), Equations 3-1 through 3-3 in conjunction with standard mass balance equations, can be rearranged to form Equation 3-4, which is used to predict permeate concentration.

$$C_p = \frac{K_s C_f}{K_w (\Delta P - \Delta \pi) \left(\frac{2-2R}{2-R} \right) + K_s} \quad (3-4)$$

The development of models that predict the transient response for a permeate stream has been reported elsewhere (Duranceau, 2009). Equation 3-5 was developed to predict permeate concentration in a staged system where concentrate is used as feed water for succeeding stages at time infinity.

$$C_{p,system} = \frac{C_{f,i} \sum_{i=1}^n A_i K_{w,i} \Delta P_i Z_i \prod_{j=2}^i X_{j-1}}{\sum_{i=1}^n A_i K_{w,i} \Delta P_i} \quad (3-5)$$

Materials and Methods

Three experiments were conducted from June to September, 2015 to evaluate the pilot's response to NaCl addition to the feed water. Experimental methods similar to those used by (Duranceau, 2009) were adopted, and are summarized herein. For brevity, only the methods used for experiment 3 will be discussed in detail, although the same procedures were applied to the two preceding experiments conducted in this work.

Experiment 3 was conducted on September 11, 2015. Prior to starting the experiment, pilot operating parameters (including recovery, flow rate, and pressure) and initial conductivity measurements from feed, permeate, and concentrate streams were recorded. The conductivity of the pilot feed water, which is mainly composed of multivalent ions, measured 826 $\mu\text{S}/\text{cm}$. The conductivity in the system permeate measured 507 $\mu\text{S}/\text{cm}$, resulting in an estimated rejection of 37.7%, which was expected given the relatively loose NF membrane (NF270). A NaCl feed solution was created with a conductivity of 65 mS/cm, by adding NaCl to a bucket containing pretreated feed water. A positive displacement pump (Prominent[®]) was used to continuously add the salt solution to the pilot feed water stream. Prior to starting the experiments, flow tests were conducted using feed water without NaCl addition until a desired flow rate of 0.72 L/min was achieved. Since the pilot operates with a feed flow of 260 gpm (984 L/min), it was estimated that the feed water conductivity would increase to 874 $\mu\text{S}/\text{cm}$. Assuming a rejection of 37.7%, this would result in an estimated permeate conductivity of 544 $\mu\text{S}/\text{cm}$, enough to cause a noticeable change in permeate and concentrate conductivity. A summary of feed solution conductivities and recoveries operated is presented in Table 3-1. Experiment 3 is split into two sections, 3a and 3b, to distinguish between two different feed solution conductivities, although they were conducted on the same day.

Table 3-1: Feed Solution Conductivities and Recoveries Operated during Three Experiments

Experiment No.	Conductivity in Feed Solution (mS/cm)	Recoveries Operated (%)
1	115	80, 85
2	125	75, 80
3a	64	80, 85
3b	101	85

Immediately after the continuous addition of the saline feed test solution to the pilot's feed water began, water samples were collected every 15 seconds for a period of 9 minutes – well after the time estimated that the pilot required to reach steady-state based on previous screening evaluations. Samples were collected from stage 1, stage 2, and total permeate sample ports, including left and right sides of the pressure vessels, where applicable. In addition, conductivity measurements for feed, first- and second-stage permeate, total system permeate, interstage concentrate (stage 2 feed), and final concentrate obtained by supervisory control and data acquisition (SCADA) were recorded by video, then later transcribed into Microsoft Excel[®] for subsequent analyses. Samples were also collected intermittently from feed, interstage concentrate (stage 2 feed), and final concentrate sampling ports to validate SCADA readings throughout the experiment. Table 3-2 presents a summary of how and when permeate conductivity measurements were obtained.

After the completion of the experiment, the conductivity of the samples was measured and recorded. To start a new experiment, the pilot water recovery was adjusted to the desired

setpoint and allowed at least 30 minutes to reach steady-state. The same methods were followed during the previous experiments, although the feed solutions did not always have the same conductivities, as described previously in Table 3-1, consequently resulting in various conductivity changes in the feed, permeate, and concentrate streams.

Table 3-2: Summary of Data Collection Procedures

Sample Stream	Manually Collected	SCADA
Feed	Intermittently	Every 5 seconds
Stage 1 Permeate Left	Every 15 seconds	Never
Stage 1 Permeate Right	Every 15 seconds	Never
Stage 1 Permeate Combined	Every 15 seconds	Every 5 seconds
Interstage Concentrate (Stage 2 Feed)	Intermittently	Every 5 seconds
Stage 2 Permeate Left	Every 15 seconds	Never
Stage 2 Permeate Right	Every 15 seconds	Never
Stage 2 Permeate Combined	Every 15 seconds	Every 5 seconds
Total System Permeate	Every 15 seconds	Every 5 seconds
Final Concentrate	Intermittently	Every 5 seconds

Results and Discussion

Pilot Response

In this work, pilot response refers to the required length of time the pilot needed to reach steady state after NaCl was added to the feed water, and how the pilot reacted when feed

water chemistry changed. Table 3-3 presents a summary of conductivity measurements, increases, and salt rejection during experiments. The initial feed conductivity in experiments 1, 2, and 3 ranged from 810 to 836 $\mu\text{S}/\text{cm}$. After the addition of the NaCl solution was initiated, the feed conductivity increased anywhere in the range of 6.1 to 12%. Initial permeate conductivity measurements ranged from 483 $\mu\text{S}/\text{cm}$ in the lower recovery experiments to 510 $\mu\text{S}/\text{cm}$ in the experiments conducted at a higher water recovery, as expected. At a certain time after NaCl addition began, the permeate stream reached a steady conductivity value, ranging from 534 to 586 $\mu\text{S}/\text{cm}$, with lower values observed in lower water recoveries, and higher values measured in higher water recoveries, as would be expected. This resulted in an increased total system permeate conductivity increase ranging from 8.6 to 16%.

Table 3-3: Conductivity Measurements in Feed and Permeate Streams at Various Water Recoveries

Exp. No.	Recovery (%)	Initial Feed Conductivity (μS/cm)	Steady-State Feed Conductivity (μS/cm)	Increase in Feed Conductivity (%)	Initial Total Permeate Conductivity (μS/cm)	Steady-State Total Permeate Conductivity (μS/cm)	Increase in Total Permeate Conductivity (%)	Initial Salt Rejection (%)	Steady-State Salt Rejection (%)
1	80	836	889	6.3	483	534	11	42	40
	85	836	889	6.3	510	554	8.6	39	38
2	75	810	862	6.4	501	547	9.2	38	37
	80	837	888	6.1	483	534	11	42	40
	85	836	889	6.3	510	554	8.6	39	38
3a	75	825	888	7.6	494	549	11	40	38
	80	825	880	6.7	494	545	10	40	38
	85	825	885	7.3	510	559	9.6	38	37
3b	85	824	907	10.1	507	586	16	38	35

*3a and 3b were conducted on the same day, but with different NaCl concentrations in the feed solution

Table 3-4 presents the response times of the first stage-, second stage-, and total system permeate streams. The first stage permeate stream reached a steady conductivity value after 165 (2 minutes, 45 seconds) to 195 seconds (3 minutes, 15 seconds), while second stage and total system permeate reached a steady conductivity value after 255 seconds (4 minutes, 15 seconds) to 285 seconds (4 minutes, 45 seconds).

Table 3-4: Response Time (seconds) during Experiments 1, 2, & 3 at 85% Recovery

Permeate Stream	Experiment 1	Experiment 2	Experiment 3
1st Stage	180	195	165
2nd Stage & Total System	285	255	255

In figures illustrating conductivity as a function of time (Figures 3-2 through 3-6), there appears to be a lag from when NaCl is first in contact with the permeate stream to when the stream achieves steady-state with respect to NaCl concentration. For example, in Figure 3-2, during the time between 50 and 165 seconds the conductivity gradually increases, indicating NaCl diffusion. It is suspected that this gradual increase is caused from axial dispersion within the pilot pipes and appurtenances.

Figures 3-2, through 3-4 illustrate first stage, second stage, and total system permeate conductivities at 85% and 80% water recoveries during experiment 3a, respectively. As would be expected, the permeate streams have a higher conductivity throughout the experiment conducted at 85%, compared to the experiment conducted at 80% recovery. It appears that changing the recovery does not significantly affect the response time of the

permeate, or how long it takes for the permeate stream to be affected by changes in feed water chemistry. However, changing the recovery does impact the conductivity measured in the permeate streams.

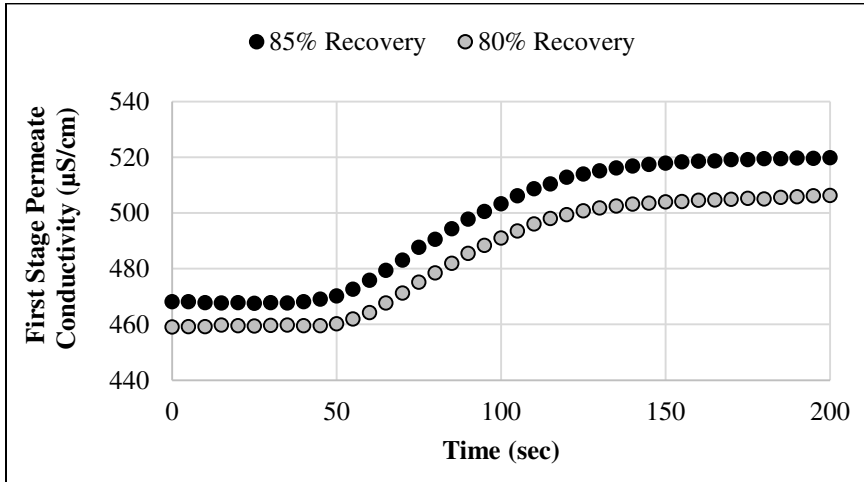


Figure 3-2: First Stage Permeate Conductivity at 85% and 80% Recoveries

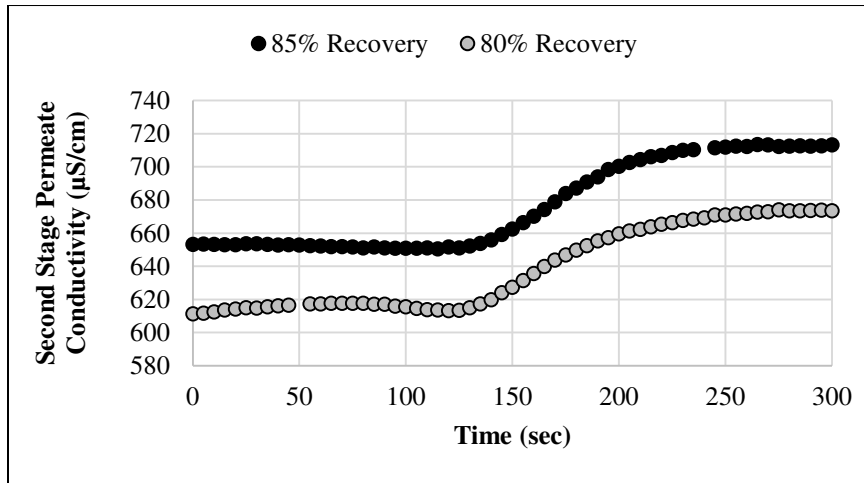


Figure 3-3: Second Stage Permeate Conductivity at 85% and 80% Recoveries

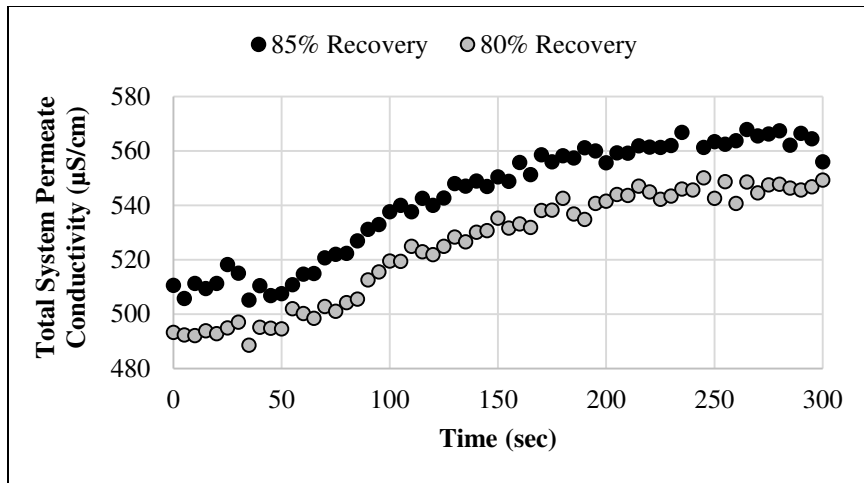


Figure 3-4: Total Pilot Permeate Conductivity at 85% and 80% Recoveries

Figure 3-5 depicts a graphical summary of experiment 3a. In this figure, stage 1 permeate conductivity is illustrated in dark gray, stage 2 permeate conductivity measurements are depicted in black, and total permeate conductivity is shown using light gray symbols. It is important to note that stage 1 and total system permeate conductivities are plotted on the right axis to allow for easier comparison with stage 2 conductivity. Based on these results, it appears that manually collected data and data obtained from the SCADA output agree closely with one another. In Figure 3-5, it is easier to compare how various permeate streams respond to NaCl addition to the feed water. First stage permeate conductivity begins to increase first, followed by total permeate conductivity. However, total conductivity does not stabilize until second stage permeate conductivity since total permeate is comprised of both first and second stage permeate.

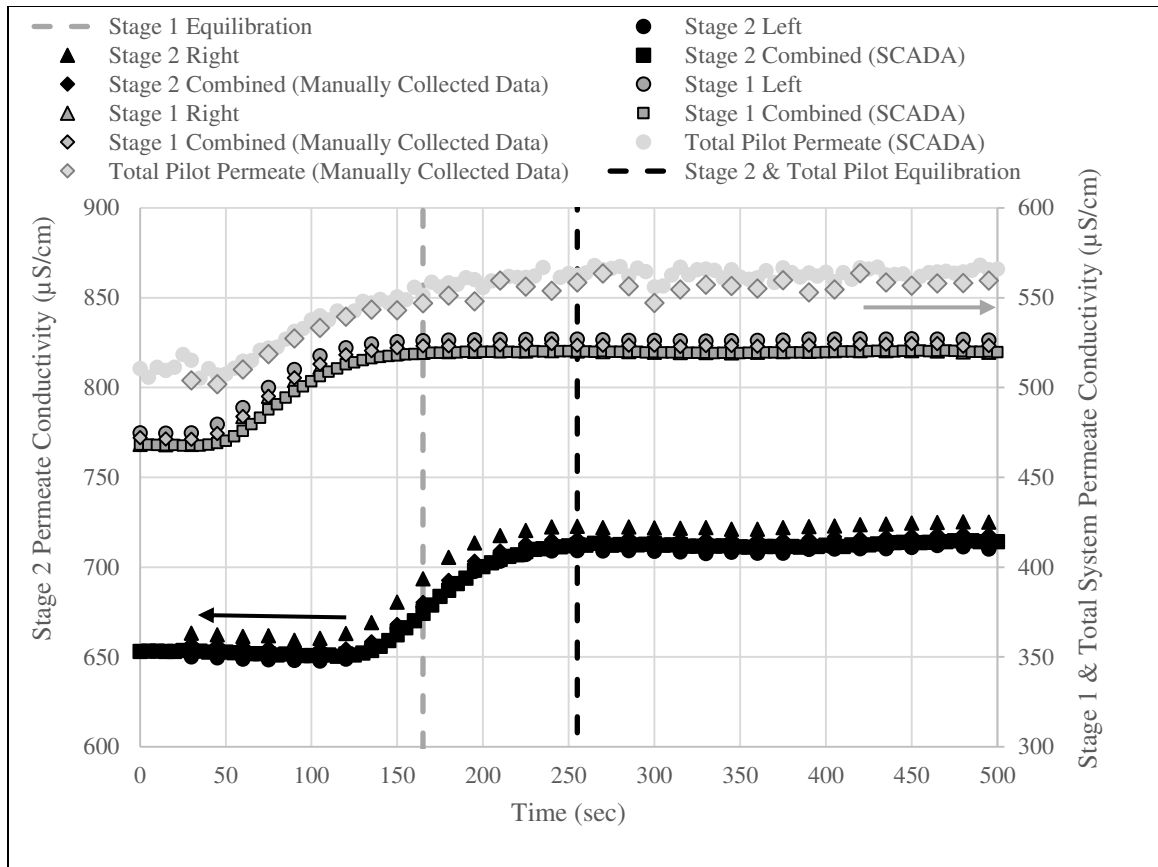


Figure 3-5: Pilot Response at 85% Recovery

Predictive Modeling

Logistic nonlinear regression equations are utilized to describe sigmoidal growth curves (Garba et al., 1990). In this work, an adaptation of the logistic model, the log-logistic model, was utilized to determine the response of permeate streams after NaCl addition, and it is presented in Equation 3-6. This model is frequently used in bioassay work to determine dose-response curves and has also been used to model water demand data (Streibig & Kudsk, 1993; Surendran & Tota-Maharaj, 2015).

$$\text{Predicted Concentration at time, } t: \theta_1 + \frac{\theta_2 - \theta_1}{[1 + \exp(\theta_4 \ln \frac{t}{\theta_3})]} \quad (3-6)$$

θ_1 = parameter describing upper boundary of conductivity measurements

θ_2 = parameter describing lower boundary of conductivity measurements

θ_3 = parameter describing time (sec) needed to reach conductivity halfway between upper and lower boundaries

θ_4 = parameter describing slope of increase in conductivity

t = time (sec)

An example of how Equation 3-6 was used in this research is demonstrated using Figure 3-6, which depicts the Minitab[®] output model for the first stage permeate stream at 85% recovery. In Figure 3-6, data from experiment 3a were used and are plotted in blue dots, while the red line represents the model. Table 3-5 and Table 3-6 present the Minitab[®] model statistics and the theta values obtained, respectively. The models summarized in Tables 3-5 and 3-6 were generated from first stage-, second stage-, and total pilot permeate response during experiments 2 and 3. In general, as the sum of the square error (SSE) and thus the mean square error (MSE) become lower, a model is more acceptable. The model generated and illustrated in Figure 3-6 has an SSE and MSE of 9.89 and 0.230, respectively. Of the six models summarized in Table 3-5, the model presented in Figure 3-6 (first stage permeate response, experiment 3a) provides the most accurate representation of transient response time.

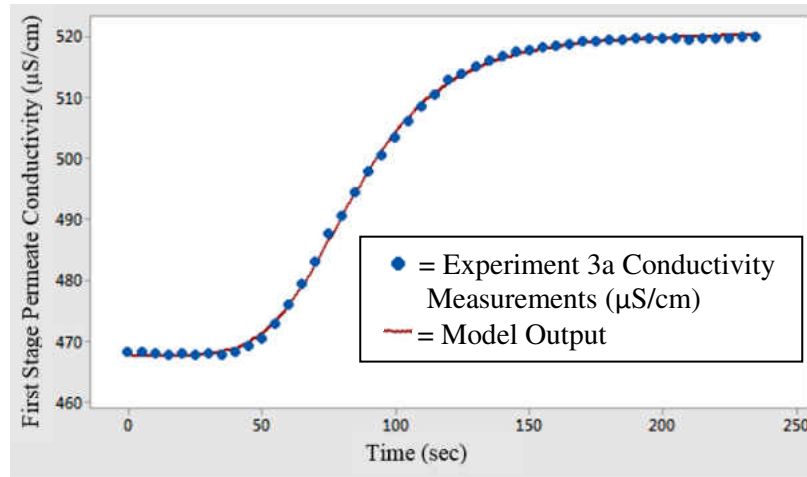


Figure 3-6: Minitab® Figure Describing First Stage Permeate Conductivity versus Time

Table 3-5: Minitab® Model Statistics Summary

Statistic	Experiment 2, 85% Recovery			Experiment 3, 85% Recovery		
	First Stage	Second Stage	Total System	First Stage	Second Stage	Total System
Iterations	10	8	8	7	8	12
SSE	13.8	10.4	131.3	9.89	60.3	437
DF	12	22	22	43	52	52
MSE	1.15	0.473	5.97	0.230	1.16	8.40
s	1.07	0.687	2.44	0.480	1.08	2.90
Model End Time (sec)	240	255	255	235	285	285

*SSE = sum of square error; DF = degrees of freedom; MSE = mean square error; s = standard deviation

Table 3-6: Theta Values for Permeate Log-logistic Models at 85% Recovery

Parameter	Experiment 2, 85% Recovery			Experiment 3, 85% Recovery		
	First Stage	Second Stage	Total System	First Stage	Second Stage	Total Permeate
θ_1	509	694	552	521	713	567
θ_2	461	634	499	467	652	509
θ_3	111	206	137	84.6	175	110
θ_4	4.74	5.63	3.82	4.89	10.4	3.32

Figures 3-7 and 3-8 illustrate how accurately the modeled data represent actual total system permeate response. In Figures 3-7 and 3-8, the vertical axis represents the modeled data from experiment 2, while the horizontal axes represent raw data from experiments 2 and 3, respectively. Figures 3-7 and 3-8 only include data during the time in which conductivity is increasing, 45 to 285 seconds. In Figure 3-7, the R^2 value of 0.985 indicates the predicted conductivity measurements predicts 98.5% of the actual conductivity data. Figure 3-8 illustrates experiment 2 predicted data versus experiment 3 actual data, and the R^2 value was calculated as 0.981, indicating the modeled data predicts 98.1% of experiment 3 data.

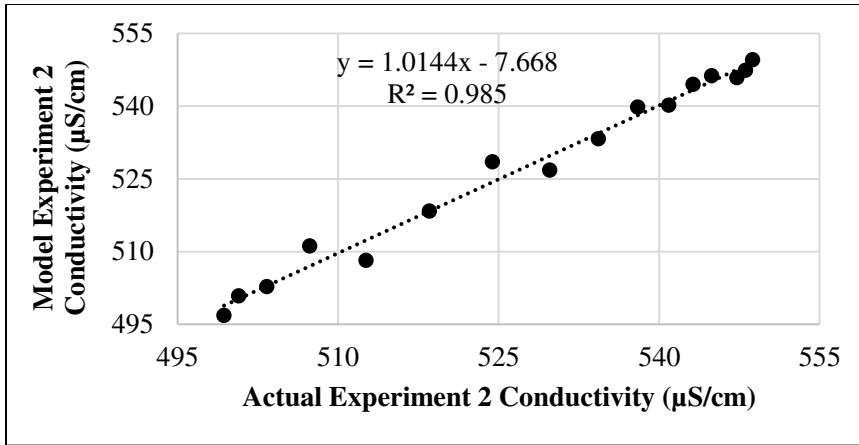


Figure 3-7: Model (experiment 2) versus Actual Data (experiment 2)

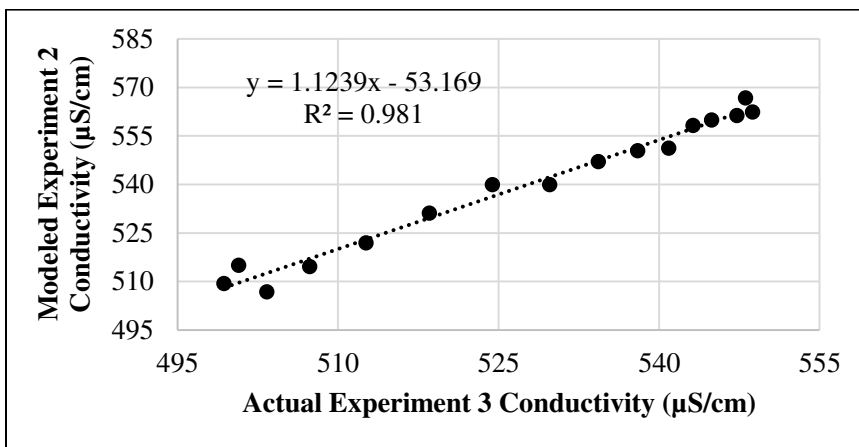


Figure 3-8: Model (experiment 2) versus Actual Data (experiment 3)

To compare the log-logistic model with a first-order nonlinear regression model presented in Equation 3-5, chloride data obtained from early transient response work using a three-stage nanofiltration pilot process were used (Duranceau, 2009). Statistical results and theta values generated using the log-logistic equation (Equation 3-4) Minitab® are presented in Table 3-7.

Table 3-8 provides a comparison between statistical SSE values from first-order and log-logistic models. First-order SSE values were obtained directly from (Duranceau, 2009). SSE values are used to describe the error of the model, meaning the larger the SSE, the more error the model produces; consequently, a lower SSE value indicates a better-fit model. Comparing values in Table 3-8, it appears that the first-order models are a better fit for stage 1 and stage 2 permeate streams, although the log-logistic model is still acceptable based on Table 3-7 statistics. In regards to stage 3 response time, the log-logistic model is a significantly better fit, where the first-order model provides an SSE of 161.8, and the log-logistic model provides an SSE of 0.6873.

Table 3-7: Minitab ® Model and Statistics Summary and Theta Values

Statistic/ Parameter	First Stage	Second Stage	Third Stage
Iterations	13	24	11
DF	13	13	13
MSE	0.136	0.821	0.0530
s	0.369	0.906	0.230
θ_1	13.9	22.4	21.6
θ_2	4.08	4.87	6.90
θ_3	1.59	2.28	2.04
θ_4	7.98	4.10	5.98

Table 3-8: Comparison between First-Order and Log-logistic Models

Statistic	First Stage		Second Stage		Third Stage	
	First-order	Log-logistic	First-order	Log-logistic	First-order	Log-logistic
SSE	1.4	1.8	10.9	10.8	161.8	0.6873

*First-order SSE values obtained from Duranceau (1990)

Homogeneous Solution Diffusion Model

The homogeneous solution diffusion model, presented previously in Equations 3-1 through 3-4, can be used to predict permeate concentrations, given water and solute mass transfer coefficients (MTCs), transmembrane pressure, and osmotic pressure differential values. In this work, the HSDM was used to predict the concentration of sodium and chloride in the permeate streams. Solute flux and mass transfer coefficients for various constituents evaluated in pilot sampling are presented in Tables 3-9 and 3-10, respectively. These values were calculated based on pilot start-up data obtained prior to the transient response experiments. Solute flux in the total system permeate stream (lb/sfd) ranges from 0.0005 for sulfate to 0.048 for total dissolved solids (TDS). MTCs (ft/day) range from 0.0150 for sulfate to 10.4 for chloride.

Table 3-9: Solute Flux (lb/sfd)

Stage/System	Solute Flux (lb/sfd)			
	chloride	sodium	TDS	sulfate
1st Stage	0.0070	0.0026	0.045	0.0004
2nd Stage	0.0081	0.0034	0.063	0.0006
Total System	0.0072	0.0027	0.048	0.0005

Table 3-10: Mass Transfer Coefficients (ft/d)

Constituent	Mass Transfer Coefficients (ft/d)
chloride	10.4
sodium	2.14
TDS	0.872
sulfate	0.0150

The values presented in Tables 3-9 and 3-10 were used in Equation 3-4 to predict permeate sodium and chloride concentrations prior to NaCl addition, and after permeate streams reached steady-state upon NaCl addition. Figure 3-9 depicts the predicted versus actual sodium and chloride concentrations obtained from first stage-, second stage-, and total system permeate streams during multiple experiments conducted at an 85% recovery. Data obtained using the predictive diffusion model presented in Equation 3-4 are able to predict 98.1% of sodium and chloride permeate concentrations accurately.

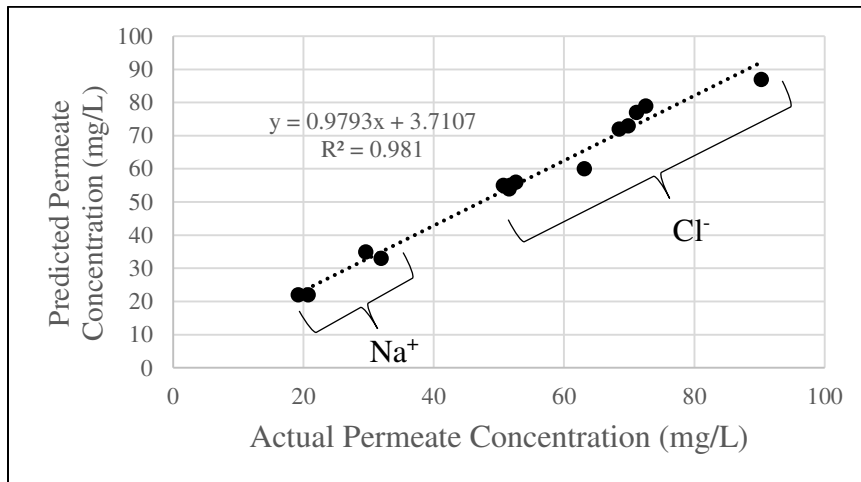


Figure 3-9: Predicted versus Actual Permeate Sodium and Chloride Concentrations

Conclusions

The purpose of this research was to monitor time transients that occurred in the permeate concentration of a two-stage, split-feed, center-port membrane process after a change in the feed water content was induced. The time required for first stage-, second stage-, and total system permeate streams to observe an affect in feed water changes was delineated and modeled using a log-logistic nonlinear regression equation. Total system permeate

required between 255 and 285 seconds to reach steady-state, as demonstrated during three repetitive experiments. Using a safety factor of three, it was determined that the system should be allowed to operate for at least 14 minutes and 15 seconds prior to sampling each process stream for chemical analysis.

When compared with a first-order nonlinear regression model, there was no difference in the predictability of transient response when using the log-logistic model in first-stage and second-stage membrane processes. However, the log-logistic model was found to be more predictive in describing a previously studied third-stage transient response by a factor of 236 over a first-order method. Furthermore, the homogeneous solution diffusion model was shown to effectively predict the permeate concentration for any transient permeate perturbation.

Acknowledgments

The work reported herein was funded by University of Central Florida (UCF) agreement number 16208114. Any opinions, findings, and conclusions expressed in this material are those of the authors and do not necessarily reflect the view of UCF (Orlando, FL) or its Research Foundation. The authors acknowledge the Town of Jupiter Utilities staff, including David Brown, Amanda Barnes, Paul Jurczak, and Rebecca Wilder, for their assistance and support, without whom this work would not have been possible. The consultation and advice of Ian Watson (RosTek Associates Inc.) and John Potts (Kimley-Horn & Associates, Inc.) were appreciated and hereby noted. The contributions of UCF students who assisted in field and laboratory work are deeply appreciated.

References

- Ahmad, A.L., & Ooi, B.S. (2006). Characterization of composite nanofiltration membrane using two-parameters model of Extended Nernst-Planck Equation. *Separation and Purification Technology*, 50, 300-309.
- Blau, T.J., Taylor, J.S., Morris, K.E., & Mulford, L.A. (1992). DBP Control by Nanofiltration: Cost and Performance. *J. AWWA*, 84 (12) 104-116.
- Bowen, W.R., & Mukhtar, H. (1996). Characterisation and prediction of separation performance of nanofiltration membranes. *Journal of Membrane Science*, 112, 263-274.
- Chaabane, T., Taha, S., Taleb Ahmed, M., Maachi, R., & Dorange, G. (2007). Coupled model of film theory and the Nernst-Planck equation in nanofiltration. *Desalination*, 206, 424-432.
- Conlon, W.J., & McClellan, S.A. (1989). Membrane Softening: A Treatment Process Comes of Age. *JAWWA*, 81 (11) 47-51.
- Dresner, L. (1972). Some remarks on the integration of the extended Nernst-Planck equation in the hyperfiltration of multicomponent solutions. *Desalination*, 10, 27-46.
- Duranceau, S.J. (1990). University of Central Florida. Doctoral Dissertation.
- Duranceau, S.J. (2009). Modeling the permeate transient response to perturbations from steady state in a nanofiltration process. *Desalination and Water Treatment* 1, 7-16.
- Duranceau, S.J., Taylor, J.S. (1992). SOC removal in a membrane softening process. *J. AWWA*, 84 (1) 68-78.
- Garba, Y., Taha, S., Gondrexon, N., & Dorange, G. (1990). Ion transport modelling through nanofiltration membranes. *Journal of Membrane Science*, 160, 187-200.
- Hilal, N., Al-Zoubi, H., Darwish, N.A., Mohammad, A.W., & Abu Arabi, M. (2004). A comprehensive review of nanofiltration membranes: Treatment, pretreatment, modelling, and atomic force microscopy. *Desalination*, 170, 281-308.
- Mohammad, A.W., Teow, Y.H., Ang, W.L., Chung, Y.T., Oatley-Radcliff, D.L., & Hilal, N. (2015). Nanofiltration membranes review: Recent advances and future prospects. *Desalination*, 356 226-254.
- Roy, Y., Sharqawy, M.H., & Lienhard V, J.H. (2015). Modeling of flat-sheet and spiral-wound nanofiltration configurations and its application in seawater nanofiltration. *Journal of Membrane Science*, 493, 360-372.

- Schlögl, R. (1996). Membrane permeate in system far from equilibrium. *Berichte der Bunsengesellschaft Physik. Chem.*, 70, 400-414.
- Seber, G.A.F., & Wild, C.J. (1989). Nonlinear Regression, John Wiley & Sons, Inc., United States.
- Streibig, J.C., Kudsk, P. (1993). Herbicide Bioassays, CRC Press, Boca Raton, FL.
- Surendran, S., & Tota-Maharaj, K. (2015). Log logistic distribution to model water demand data. *Procedia Engineering*, 119, 798-802.
- Teefy, S. (1996) Tracer Studies in Water Treatment Facilities: A Protocol and Case Studies. Denver, CO: Water Research Foundation.
- Wesolowska, K., Koter, S., & Bodzek, M. (2004). Modelling of nanofiltration in softening water. *Desalination* 163, 137-151.
- Wijmans, J.G., & Baker, R.W. (1995). The solution-diffusion model: a review. *Journal of Membrane Science*, 107, 1-21.
- United States Environmental Protection Agency (1996). ICR Manual for Bench- and Pilot-scale Treatment Studies. EPA 814/B-96-003, Washington D.C.
- Wilf, M. (2011) The Guidebook to Membrane Desalination Technology, Balaban Desalinations Publications, Hopkinton, MA.

CHAPTER 4: THE INFLUENCE OF SOLUTE POLARIZABILITY AND MOLECULAR VOLUME ON THE REJECTION OF TRACE ORGANICS IN LOOSE NANOFILTRATION MEMBRANE PROCESSES

The following information has been accepted for publication in the peer-reviewed journal

Desalination and Water Treatment:

Jeffery-Black, S., & Duranceau, S.J. (2016). The Influence of Solute Polarizability and Molecular Volume on the Rejection of Trace Organics in Loose Nanofiltration Membrane Processes. *Desalination and Water Treatment. In Press*.

Abstract

The removal of trace organic compounds of emerging concern (TrOC) from groundwater was evaluated using a split-feed, center exit, nanofiltration (NF) pilot process. Groundwater was dosed with varying amounts of bisphenol-A, caffeine, carbamazepine, N,N-diethyl-meta-toluamide, estrone, gemfibrozil, naproxen, sucralose, and sulfamethoxazole between 150 ng/L and 4.5 mg/L, and processed with NF membranes operating at a feed flow rate of 60,636 L/h (267 gpm), a flux rate of 25.6 L m⁻² h⁻¹ (15.1 gsf), and 85 percent water recovery. TrOC rejection by the NF process ranged from 68 percent for caffeine to below detection for gemfibrozil and sucralose. Correlations between rejection and various chemical and physical compound properties were investigated. It was found that TrOC rejection correlated well with polarizability (0.94 R²) and molecular volume (0.94 R²), and to a lesser extent hydrophobicity/hydrophilicity (0.87 R²). However, in this work, molecular weight and log D were not well-correlated with solute rejection.

Analysis of TrOC rejection data collected from five prior independent loose NF research studies representing 61 different TrOCs were found to correlate well with polarizability ($0.71 R^2$) and molecular volume ($0.72 R^2$), suggesting that polarizability and molecular volume are useful in estimating TrOC removal from fresh groundwater using loose NF membrane processes.

Keywords: pharmaceuticals, compound of emerging concern, pilot plant, polarizability, endocrine disrupting compound

Introduction

Trace organic compounds (TrOCs) continue to receive widespread attention due to their presence in wastewater treatment facilities and the aquatic environment. Research related to the removal of TrOCs in water treatment processes has been ongoing since the discovery of pesticides in water supplies in the 1980's (Duranceau et al., 1992). Understandably, the presence of pesticides and other TrOCs of emerging concern in drinking water are highly undesirable in the eyes of the consuming public. Membranes represent a technology that can cost-effectively deal with many of these emerging TrOCs. Although prior work has historically demonstrated the effectiveness of diffusion-controlled membrane technologies for pesticide removal (Chen et al., 2004; Duranceau et al., 1992; Hofman et al., 1997; Van der Bruggen et al., 1998; Van der Bruggen et al., 1999), these efforts did not include newly observed pharmaceuticals, health care products and plasticizer compounds. In more recent work, experiments are typically conducted using flat sheet or bench-scale membrane units in a laboratory, with few studies having examined TrOC removal using pilot- or full-scale

processes (Bellona & Drewes, 2007; Hofman et al., 2007; Radjenovic et al., 2008; Sadmani et al., 2014; Verliefde et al., 2009). While laboratory studies allowed the membrane industry to investigate TrOC behavior under controlled settings, including various feed water chemistries and operating conditions (i.e. flux, pressure, flow rate), this type of operation does not necessarily simulate a full-scale membrane treatment processes (Hofman et al., 2007; Radjenovic et al., 2008; Sadmani et al., 2014; Verliefde et al., 2009). Alternatively, while investigations using full-scale membrane processes provide utilities with actual data, these experiments are limited since feed water chemistry cannot be altered.

It is generally understood that TrOCs can be removed from a diffusion-controlled process by one of three primary removal mechanisms: size exclusion, electrostatic repulsion, and adsorption (Hofman et al., 2007; Radjenovic et al., 2008; Sadmani et al., 2014). These solute-membrane interactions are determined by TrOC properties, (molecular weight, molecular size (length and width), charge (determined using the acid dissociation constant and the solution pH), diffusion coefficient and hydrophobicity (expressed by the octanol-water partition coefficient, $\log K_{ow}$, and the octanol-water partition coefficient at any pH value, $\log D$)), membrane properties (molecular weight cutoff (MWCO), pore size, hydrophobicity (contact angle), surface charge (zeta-potential), surface morphology (roughness)), operating conditions (pressure, flux, and recovery), and solution chemistry (pH, temperature, conductivity, alkalinity, organic content) (Bellona et al., 2004; Comerton et al., 2008; Dang et al., 2014; Hajibabania et al., 2011; Gur-Reznik et al., 2011; Yangali-Quintanilla et al., 2009). This prior research indicated that the removal mechanism

responsible for TrOC rejection is largely dependent on whether or not a compound is hydrophobic or hydrophilic, as well as if the TrOC is ionic or neutrally charged. Others have shown that the organic and charged ionic content of the feed water can impact TrOC rejection by NF membranes (Comerton et al., 2008; Verliefe et al., 2009), which agrees with prior work performed studying pesticides (Duranceau et al., 1992; Van der Bruggen et al., 1999). However, correlations between the compound properties and rejection by the loose NF membranes studied were not statistically significant, indicating that loose NF did not reject lower molecular weight TrOCs due to the large MWCO of the NF membrane (Comerton et al., 2008).

Despite the significant amount of research performed as described herein, polarizability was one solute chemical property that has not been investigated when examining solute-membrane interactions. It appears that little to no research has investigated membrane solute rejection as a function of the TrOC's polarizability within any diffusion-controlled membrane process. Polarizability describes how easily electrons are able to move within a compound, and is related to the dipole moments within a molecule, and increases with molecular volume. While this parameter has been eluded to as an influence on compound adsorption to membranes (Van der Bruggen et al., 2002), as well as for its relationship with solvent and lipid bilayer interfaces (Vorobyov & Allen, 2010), this chemical property has not been extensively examined for its influence on TrOC removal.

The main objective of this work is to investigate solute-NF membrane interactions as determined by TrOC polarizability and molecular volume, and evaluate multiple

independent literature sources (95 data points) to investigate the relationship between TrOC properties and rejection. Several physical and chemical properties suspected to influence TrOC rejection were evaluated using a pilot unit housing NF270 membranes operating at full-scale plant conditions.

Materials and Methods

Pilot Plant Description

A nanofiltration pilot unit (NPU), owned by the Town of Jupiter (Town) water utility, was constructed and placed online in 2014 to investigate trace organic compound removal capabilities of their existing NF process, which utilizes NF270 (DOW) membranes. The NPU is located at the Town's water treatment facility in Jupiter, FL, and is operated by Town staff and University of Central Florida (UCF) researchers. TrOC experiments were conducted using feed water obtained after full-scale plant pretreatment, which includes sand filtration, cartridge filtration (5 micron), and scale inhibitor and sulfuric acid addition, which was then routed to the head of the 60,636 L/h (267 gpm) NPU. This pilot unit was designed and constructed to replicate the Town's existing full-scale, two-stage nanofiltration plant: both systems operate at 85% recovery, with a 7:2 configuration. Additionally, the water flux of the full-scale process is $25.3 \text{ L m}^{-2} \text{ h}^{-1}$ (14.9 gsf), while the flux of the pilot was experimentally determined as $25.6 \text{ L m}^{-2} \text{ h}^{-1}$ (15.1 gsf). The full-scale plant and the pilot operate at constant flux. Furthermore, both processes were designed as split-feed, center-exit configurations. After entering the full-scale NF train or NPU, feed water is split in two, and enters both sides of the 6-element pressure vessels. Water passes

through three membranes prior to exiting as permeate, at both ends of the vessels, or as concentrate, which is collected in the center of the vessels. A simplified schematic of this configuration is depicted in Figure 4-1, and pilot characteristics and typical operating parameters are presented in Table 4-1.

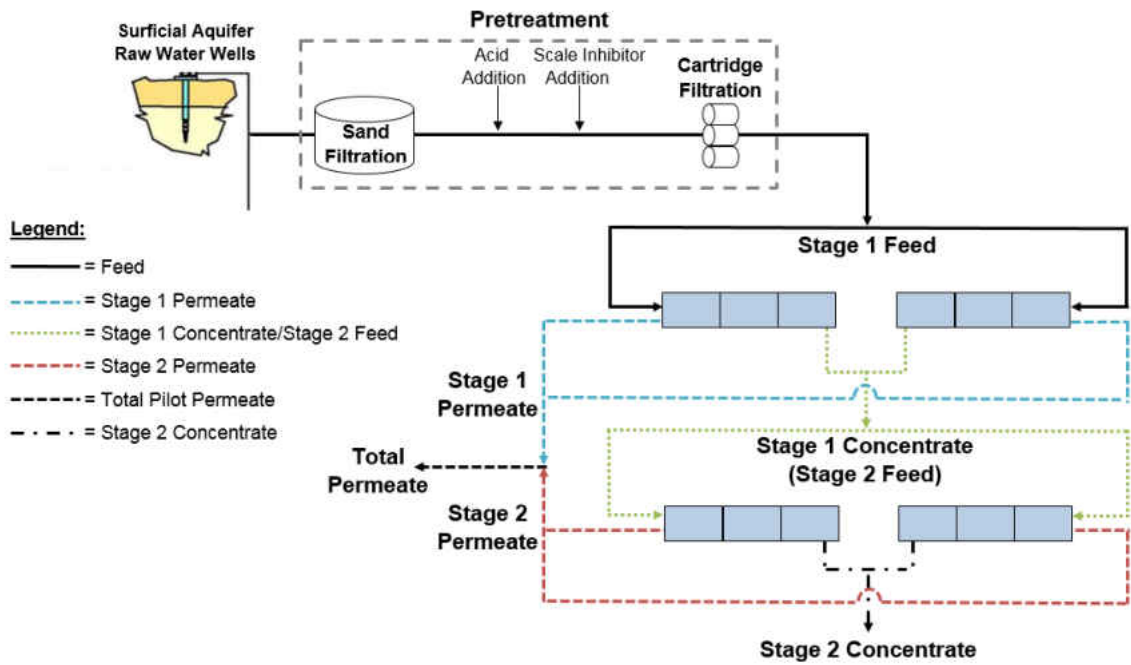


Figure 4-1: Simplified Schematic of the Full-Scale Nanofiltration Process

Table 4-1: Membrane and Pilot Characteristics

Item	Value	
Membrane Module	NF270 (DOW Filmtec)	
MgSO ₄ & CaCl ₂ Rejection (%) ^{a,†}	97* & 40-60**	
Pilot Recovery (%)	85	
Total Number of Membrane Elements	54	
Elements in Stage 1	42	
Elements in Stage 2	12	
Membranes per pressure vessel	6	
Array	7:2	
Membrane Surface Area (DOW Filmtec)	37.2 m ² /element	400 ft ² /element
Total Membrane Area in Pilot	2,007 m ²	21,600 ft ²
Feed Flow Rate	60,636 L/h	267 gpm
Total Permeate Flow Rate	51,552 L/h	227 gpm
Concentrate Flow Rate	9,084 L/h	40 gpm
Feed Pressure	3.93 bar	57 psi
Stage 1 Concentrate Pressure	3.72 bar	54 psi
Stage 1 Permeate Pressure	1.45 bar	21 psi
Stage 2 Concentrate Pressure	3.59 bar	52 psi
Stage 2 Permeate Pressure	1.45 bar	21 psi
Total Pilot Permeate Pressure	1.45 bar	21 psi
Water Flux	25.6 L m ⁻² h ⁻¹	15.1 gsf/d

[†]Test conditions: 70 psi (0.48 MPa), 77 °F (25 °C), 15% recovery; *2,000 MgSO₄; **500 mg/L CaCl₂; ^aBellona et al. (2012).

Water Quality Description

Water quality was obtained multiple times over a period of one year and results are presented as averages in Table 4-2. Feed water pH is maintained at 6.5 using sulfuric acid for scale control and degasification. Alkalinity is 240 mg/L as CaCO₃, conductivity of the feed water is typically 750 μS/cm, and the total dissolved solids concentration is 455 mg/L. Feed water consists primarily of multi-valent ions, specifically calcium, which has a concentration of 125 mg/L. Organic content, measured as dissolved organic carbon (DOC) and DOC's surrogate, ultraviolet absorption at 254 nm (UV₂₅₄), are typical for a surficial groundwater source in south Florida. The average DOC concentration in the feed water is 11 mg/L, while the average UV₂₅₄ measurement is 0.406 cm⁻¹.

Table 4-2: Nanofiltration Pilot Feed Water Quality

Water Quality Parameter	Average	Range	Units
pH	6.5	6.3-6.6	pH units
Temperature	25	22.4-25.7	°C
Alkalinity	240	200-292	mg/L as CaCO ₃
Conductivity	750	735-817	μS/cm
Total Dissolved Solids	455	424-492	mg/L
Dissolved Organic Carbon	10.8	10.6-11.0	mg/L
UV ₂₅₄	0.410	0.401-0.417	cm ⁻¹
Calcium	125	121-126	mg/L
Magnesium	4.9	4.5-5.5	mg/L
Sodium	23	19-24	mg/L

Selected Trace Organic Compounds

TrOCs evaluated in this work are presented in Table 4-3, along with basic chemical and physical properties. Dipole moments for TrOCs presented in Table 4-3 were obtained from Comerton et al. (2008), while other properties including polarizability were obtained from Chemicalize.org by ChemAxon (Budapest, Hungary), which utilizes calculation methods from Miller & Savchik (1979). TrOCs were selected based on occurrence in the Town's water supply (Wilder et al., 2016), the frequency of reported detection in other groundwater supplies, and the high volume of research related to these TrOCs in water treatment (Mawhinney et al., 2011; Li et al., 2015; Wang et al., 2015).

TrOCs presented in Table 4-3 have a range of uses and chemical and physical characteristics. Of the nine TrOCs examined in this research, four are pharmaceuticals, one is a plastic derivative, one is a stimulant, one is an insect repellent, one is an estrogen, and one is an artificial sweetener. Molecular weights ranged from 191 to 398 g/mole, while the MWCO of the membranes used in this work have been reported to range from 200 to 400 Da (Comerton et al., 2008; Garcia et al., 2013; Mohammad et al., 2015). Molecular volume and polarizability, range from 164 to 305 Å³ and 17.9 to 32.7 Å³, respectively. TrOC hydrophobicity/hydrophilicity is represented by log K_{ow} , which ranges from -0.55 to 4.4, and log D (at a pH of 6.5), which ranges from -0.60 to 4.4. Compound hydrophobicity increases with increasing log K_{ow} and log D. The dipole of TrOCs lies within the range of 1.0 to 4.9. TrOC pKa values range from <2.0 for DEET to 14.0 for caffeine.

Table 4-3: Trace Organic Compound Uses and Physical and Chemical Characteristics

Compound Name	Abbr.	Primary Use	MW (g/mol)	MV (Å³)	Log <i>K_{ow}</i>	Log D (pH 6.5)	Polarizability (Å³)	Dipole (Debye)	pKa
Bisphenol A	BPA	Plasticizer	228	221	4.0	4.0	26.6	1.7	10.3
Caffeine	CAF	Stimulant	194	164	-0.55	-0.60	17.9	1.0	N/A
Carbamazepine	CBZ	Anti-epileptic	236	210	2.8	2.6	27.0	1.7	2.3, 13.9
N,N-Diethyl-meta-toluamide	DEET	Insect Repellent	191	198	2.5	2.5	22.3	4.9	<2.0
Estrone	EST	Estrogen	270	263	4.3	4.4	30.8	2.0	10.3
Gemfibrozil	GEM	Lipid Regulator	250	255	4.4	2.1	27.9	3.6	4.43
Naproxen	NPX	Anti-inflammatory	230	213	3.0	0.68	26.4	1.2	4.2
Sucralose	SUC	Artificial Sweetener	398	305	-0.49	-0.40	32.7	4.6	3.5
Sulfamethoxazole	SMX	Antibiotic	253	205	0.79	0.36	24.2	2.1	1.8, 5.7

MW = molecular weight; MV = molecular volume; Dipole values obtained from Comerton et al. (2008); pKa values obtained from Sadmani et al. (2014) and Yangali-Quintanilla et al. (2011).

Experimental Set Up

At the commencement of each experiment, a predetermined weight or volume of TrOCs (purchased from Sigma-Aldrich) was measured and delivered to a 5-gallon bucket containing pretreated feed water. The 5-gallon bucket was thoroughly rinsed with pilot feedwater before and after each experiment was conducted. TrOC weights and volumes needed in the feed solution were determined according to calculations made based on pilot feed and TrOC feed solution pump flowrates. Upon addition to the feed solution bucket, TrOCs were completely dissolved and mixed using a stir plate and stir bar. After mixing, a 27 gallon per hour positive displacement pump was used to continuously inject the feed solution containing TrOCs to the feed stream of the pilot unit. Based on previous transient response work conducted on this pilot unit, TrOCs were continuously added to the feed stream for at least 15 minutes prior to sample collection (Jeffery-Black & Duranceau, 2016). Mass balance calculations were performed to ascertain if TrOC adsorbed to the membrane, process piping, or other appurtenances. It was determined that no measurable losses were observed in the data collected in this study. Table 4-4 presents the target TrOC feed concentrations for the eleven experiments conducted in this work. Of the eleven experiments, four (experiments 8 through 11) were designed to cover a wide range of caffeine concentrations in order to evaluate variable membrane loading rates; alternative TrOCs were not investigated in these instances.

Table 4-4: Target Feed Concentrations

Experiment No.	Target Feed Concentration ($\mu\text{g/L}$)
1	0.15
2	0.25
3	0.25
4	0.50
5	2.0
6	7.7
7	74
8	1,020
9	1,418
10	2,920
11	4,500

Analytical Methods

Nanogram-level Experiments

A portion of the water samples that were collected from the pilot were evaluated at method detection levels ranging between 5 and 100 nanograms per liter (ng/L). In this instance, two 40-mL glass amber vials were used to collect each sample. Vials contained 80 μL of 32 g/L sodium omadine (NaOmadine) and 5 mg ascorbic acid. Samples were analyzed using a fully automated on-line solid phase extraction, high performance liquid chromatography (HPLC), mass spectrometry-mass spectrometry (MS/MS) system. A detailed description of laboratory methods can be found elsewhere (Oppenheimer et al., 2011). Method detection limits (MDLs) for TrOCs evaluated in experiments 1 through 7 are presented in Table 4-5.

Table 4-5: TrOC Detection Limits

TrOC	MDL (ng/L)
BPA	10
CAF	5
CBZ	5
DEET	10
EST	5
GEM	5
NPX	10
SMX	5
SUC	100

Microgram-level Experiments

For the microgram-level caffeine analysis, stock solutions of caffeine were prepared in methanol and stored at -20 °C. Further dilutions were prepared in water:methanol mixtures (40:60 v/v) and were used as working standard solutions. Water samples were collected in silanized amber bottles, and were also prepared in water:methanol mixtures (40:60 v/v) upon returning to the laboratories and stored at -20 °C until analysis.

Samples were analyzed using HPLC. The HPLC experiments were performed using a Perkin-Elmer series 200 HPLC (Santa Clara, CA, USA) consisting of a series 200 binary pump, a series 200 UV-Vis detector with deuterium lamp set at a maximum wavelength of 273 nm, a series 200 autosampler, and a series 200 vacuum degasser. The analytical column used was a Zorbax (Agilent) SB-C18 packed column with a 4.6 x 150 mm dimensions. The mobile phase was water:methanol 40:60 (v/v) with a flow rate of 1 cm³/min. Sample run time was 10.0 minutes with a 10.0 µL injection volume and at isocratic conditions. The detection limit for caffeine was 200 µg/L for the microgram-level experiments.

Results and Discussion

Trace Organic Compound Rejection Results

Figure 4-2 presents average TrOC rejection and standard deviations for the first stage, second stage, and total pilot system. Rejection (R) of the TrOCs by the NF pilot were calculated using Equation 4-1, where C_f and C_p are concentrations measured in the feed and permeate samples, respectively. First stage rejection was calculated using stage 1 feed and stage 1 permeate, second stage rejection was calculated using stage 1 concentrate (stage 2 feed) and stage 2 permeate, and total pilot rejection was calculated using stage 1 feed and total pilot permeate.

$$R = \frac{C_f - C_p}{C_f} \times 100 \quad (4-1)$$

Bisphenol A and estrone were not detected in a majority of samples, including feed and concentrate, indicating adsorption to pilot pipes and appurtenances; consequently, these TrOCs are omitted from Figure 4-2. Adsorption was expected due to the hydrophobic nature of these compounds. GEM and SUC were below detection in permeate samples; consequently their rejection is assumed to be >99%, and results of these two TrOCs are also omitted from Figure 4-2. DEET and NPX were below their respective detection limits in a portion of permeate samples; therefore rejection data for DEET and NPX were based on values that could be measured. Error bars illustrate the standard deviation of rejection values for each TrOC reported. CBZ and NPX experienced total pilot system rejection of 91% and 92%, respectively. SMX had a rejection value of 83% from the total pilot system,

while DEET was rejected 84%. CAF was rejected the least, with a total pilot rejection of 68%. Although it appears that more rejection was observed in stage 2, this is due to the significantly high TrOC concentrations in the stage 1 concentrate, which provides water to the second stage of the pilot unit. It should be noted that TrOC concentrations in samples collected from stage 1 are lower than those observed in stage 2 permeate samples.

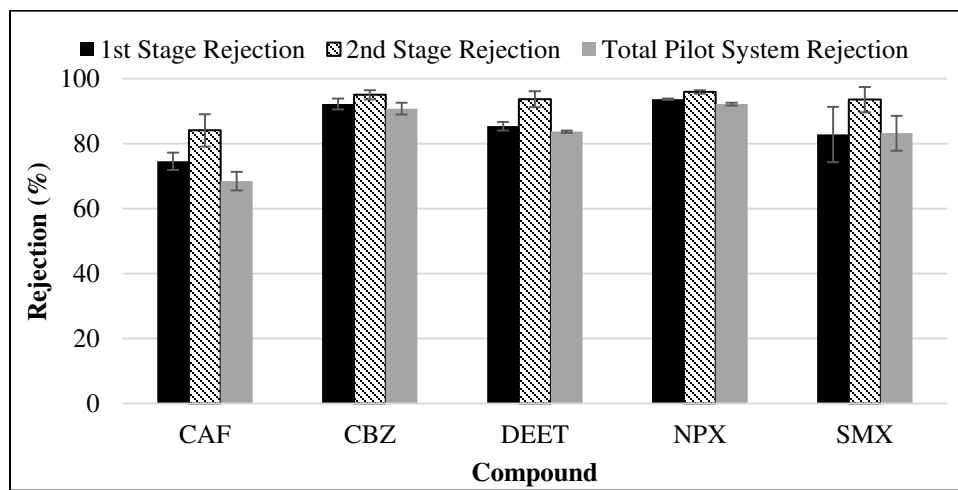


Figure 4-2: TrOC Rejection from the First Stage, Second Stage, and Total Pilot System

Table 4-6 presents the number of times that a specific TrOC was detected in permeate samples, as well as the number of experiments conducted for each TrOC. Due to the high cost associated with purchasing large amounts of certain TrOCs, not every TrOC could be incorporated into the experimentation, as indicated in Table 4-6.

Table 4-6: Number of Rejection Values Obtained

TrOC	Number of Permeate Detections / Number of Experiments Conducted		
	First Stage	Second Stage	Total Pilot
CAF	10/11	10/11	11/11
CBZ	5/5	5/5	5/5
DEET	2/2	2/2	2/2
NPX	2/5	4/5	2/5
SMX	5/5	5/5	5/5

*BPA and EST were not detected in the feed or permeate streams. GEM and SUC were not detected in the permeate.

Solute Rejection Mechanisms

In this research, the relationships between TrOC rejection and compound properties including polarizability, molecular volume, molecular weight, and hydrophobicity/hydrophilicity (represented by the octanol-water partition coefficients $\log K_{ow}$ and $\log D$), were evaluated for their influence on TrOC rejection. The acid dissociation constant was negatively correlated with TrOC rejection. Table 4-7 presents a summary of the statistical analysis conducted to determine if linear correlations between properties and rejection exist. The R^2 values describing the relationship between rejection and polarizability and molecular volume are both 0.94. Alternatively, the R^2 values describing the relationship between rejection and $\log K_{ow}$, $\log D$, and molecular weight are weak (0.87, 0.43, and 0.30 R^2 , respectively).

Critical F and t values were obtained using a 95% confidence interval. Based on their respective F-statistics, polarizability, molecular volume, and $\log K_{ow}$ are well-correlated with TrOC rejection since the F-statistic for each of these properties is significantly greater than the critical F value. Additionally, since the t-observed values for polarizability,

molecular volume, and $\log K_{ow}$ are greater than the critical t value, the slope generated by plotting rejection versus these parameters is useful in predicting TrOC removal. Alternatively, $\log D$ and molecular weight do not have F-statistic or t-observed values significantly greater than the critical F or t values; consequently this suggests that these parameters are not well-correlated with rejection (Mendenhall et al., 2006).

Table 4-7: Statistical Analysis for Correlations between TrOC Properties and Rejection

Property	R ²	F-statistic	Critical F Value	F-statistic > Critical F Value?	t-obs. value	Critical t value	t-observed > Critical t Value?
Polarizability	0.94	47.6	10.1	Yes	6.9	3.2	Yes
MV	0.94	51.4	10.1	Yes	7.2	3.2	Yes
Log K_{ow}	0.87	20.0	10.1	Yes	4.5	3.2	Yes
Log D	0.43	2.23	10.1	No	1.5	3.2	No
MW	0.30	1.31	10.1	No	1.2	3.2	No

Polarizability describes the ability of electrons to move throughout the molecule, and typically increases with molecular volume (Mohammad et al., 2015). It is well-known that more negatively charged TrOCs experience greater rejection rates in a polyamide membrane process due to the electrostatic interactions between the compound and the inherent negative charge of the membrane (Duranceau et al., 1992; Nghiem et al., 2006; Verleifde et al., 2008). It is reasonable to expect that TrOCs that exhibit higher polarizability should experience higher rejection rates due to the ability of the molecule's electrons to move more freely than compounds having lower polarizability values. This is because molecules possessing higher polarizability, due to free electron movement, could

create a condition where greater repulsive forces between the membrane and chemical would result in higher rejection rates.

Figures 4-3, 4-4, 4-5, 4-6 and 4-7 illustrate the relationship between TrOC rejection (across both pilot stages) and polarizability, molecular volume, Log K_{ow} , Log D, and molecular weight, respectively. TrOCs in Figures 4-3 through 4-7 include CAF, CBZ, DEET, NPX, and SMX as previously shown in Figure 4-2.

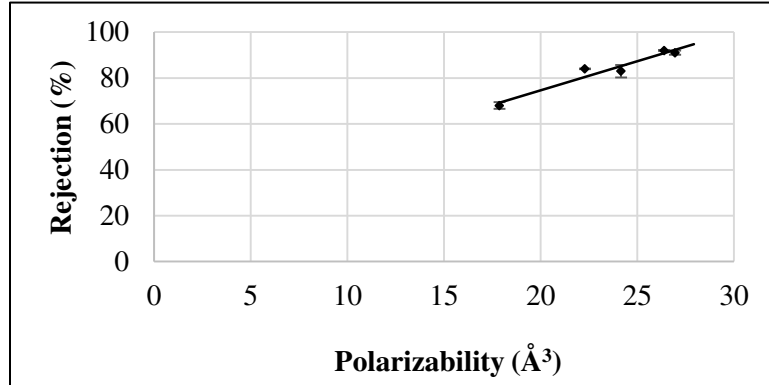


Figure 4-3: Rejection vs TrOC Polarizability ($R^2=0.94$)

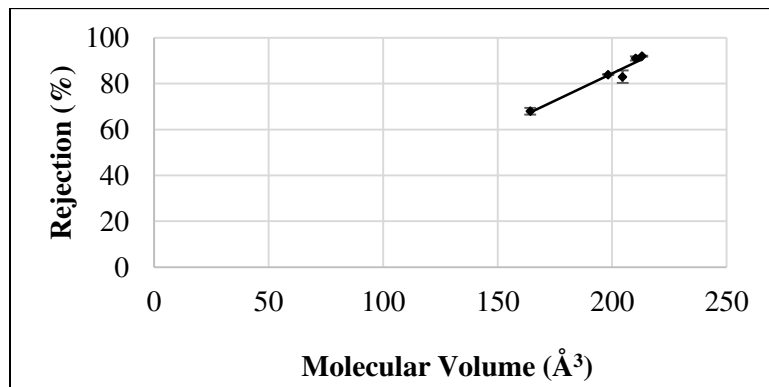


Figure 4-4: Rejection vs TrOC Molecular Volume ($R^2=0.94$)

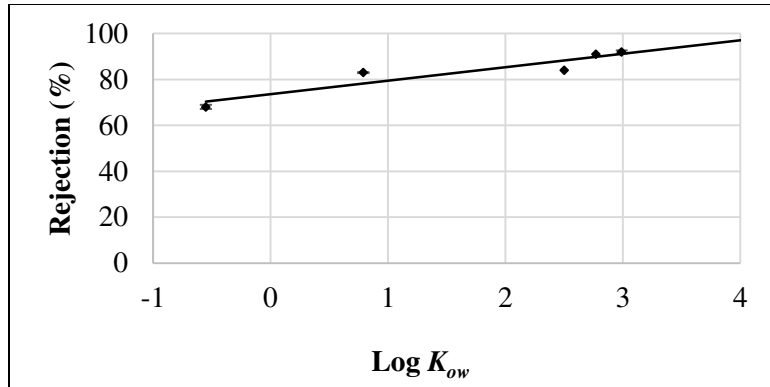


Figure 4-5: Rejection vs TrOC Log Kow ($R^2=0.87$)

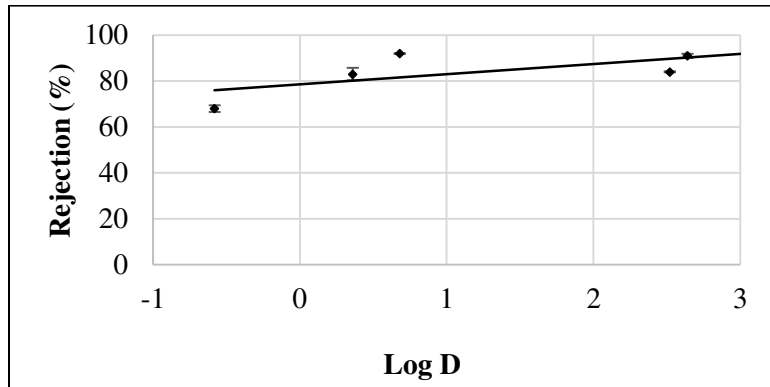


Figure 4-6: Rejection vs TrOC Log D ($R^2=0.43$)

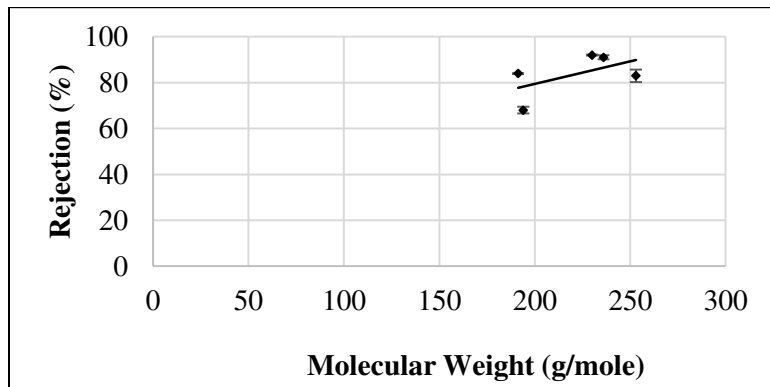


Figure 4-7: Rejection vs TrOC Molecular Weight ($R^2=0.30$)

Examining Polarizability with Independent Sources

The results obtained in pilot experiments were combined with results from other similar studies to investigate the relationship between rejection and TrOC properties. Literature was reviewed for studies that evaluated solute rejection data utilizing polyamide NF membranes with a relatively large MWCO (>250 Da), and 14 prior studies were identified for use in evaluating TrOC properties for further analysis. These prior studies were selected to correspond to the use of “loose” NF membranes possessing the higher MWCOs that included the NF270 (DOW), NF200 (DOW), and HL Desal (GE Osmonics).

Initially, the entire dataset was analyzed by plotting TrOC rejection as a function of polarizability. However, a weak correlation existed ($0.44 R^2$) using the entire dataset. Consequently, the data was further sorted by flux, membrane type, MWCO, and inclusive of an absolute rejection boundary. Of these fourteen independent sources, six sources were removed from the dataset due to the operation of experimental units with water flux rates not representative of actual practice, or those values outside the range of 17 and $34 \text{ L m}^{-2} \text{ h}^{-1}$ ($15 \pm 5 \text{ gsf}$). An additional three sources were removed because the flux rate or membrane type was unknown. Furthermore, TrOCs with polarizability values greater than 30 \AA^3 were excluded from the data set, since rejection approached >99%. As a result, five independent studies were selected for more detailed analysis.

The external evaluation, once sorted, resulted in the identification of 61 TrOC that provided 95 discrete data values (Bellona et al., 2012; Fujioka et al., 2014; Kosutic et al., 2007; Shahmansouri & Bellona, 2013; Yangali-Quintanilla et al., 2010). This information was

combined with the 5 TrOCs examined in the pilot plant experiments as described herein; the 5 TrOCs investigated in the pilot study were a match for 5 of the chemicals tested in several of the outside studies. This combined data set of 61 different TrOCs possessed polarizabilities ranging from 3.21 \AA^3 to 29.8 \AA^3 . Additionally, TrOCs in the combined dataset included compounds that exhibited a variety of chemistries, including chemicals that were ionic or neutrally charged, as well as chemicals exhibiting hydrophobic or hydrophilic properties ($\log K_{ow}$ values range from -4.53 to 5.28). Of these 61 different compounds, 25 were duplicates, while 10 represented triplicate data points. Findings suggested that as the water flux increased, the coefficient of determination describing the relationship between polarizability and rejection decreased. Consequently, by including only that data obtained from experiments using flux rates typically observed in full-scale nanofiltration treatment processes, it was found that polarizability exhibited a predictive means for determining rejection.

A statistical analysis was performed on the sorted dataset, and results are presented in Table 4-8. Figures 4-8, 4-9, 4-10, and 4-11 depict rejection as a function of polarizability, molecular volume, $\log K_{ow}$, and molecular weight, respectively. When rejection was plotted as a function of polarizability and molecular volume, the R^2 value was 0.71 and 0.72, respectively. It is suspected that this decrease in R^2 could be explained by the variability of experimental operations from the additional sources. Research has indicated that experiments utilizing bench-scale units may achieve different rejection under identical operating conditions compared to experiments conducted using a pilot unit or full-scale plant (Bellona & Drewes, 2007; Gur-Reznik et al., 2011; Radjenovic et al., 2008; Yangali-

Quintanilla et al., 2011). Furthermore, source water from the additional data had different chemical properties, including variable dissolved organic content as well as varying cation concentrations, which have also been shown to impact TrOC rejection (Comerton et al., 2008; Verliefde et al., 2009). The decreased R^2 could also be due to the possibility that hydrophobicity/hydrophilicity and molecular weight also influence rejection. Additionally, this correlation appears to apply when a water flux similar to that of a full-scale NF membrane plant is used, and might not hold true for laboratory-scale experiments operating under unrealistic operating conditions.

Because the F-statistic values describing the relationships between polarizability, molecular volume, $\log K_{ow}$ and molecular weight with rejection were larger than the critical F value, the hypothesis that there is no relationship between rejection and these properties can be rejected. However, the F-statistic for $\log K_{ow}$ is relatively small compared to the F-statistic values for polarizability, molecular volume, and molecular weight, indicating this parameter does not impact rejection to the same extent as does polarizability, molecular volume, and molecular weight. Furthermore, the t-observed values for these properties were greater than the critical t value, indicating the slope generated by plotting rejection as a function of these properties is useful when estimating rejection. Again, the critical t value calculated for $\log K_{ow}$ is relatively small compared to those obtained for polarizability, molecular volume, and molecular weight, further demonstrating the lack of relationship between $\log K_{ow}$ and TrOC rejection.

Table 4-8: Statistical Analysis for Correlations between TrOC Properties and Rejection

Property	R ²	F-statistic	Critical F Value	F-statistic > Critical F Value?	t-obs. value	Critical t value	t-observed > Critical t Value?
Polarizability	0.71	235	3.94	Yes	1.98	15.3	Yes
MV	0.72	252	3.94	Yes	1.98	15.9	Yes
Log <i>K_{ow}</i>	0.14	15.4	3.94	Yes	1.98	3.92	Yes
MW	0.67	197	3.94	Yes	1.98	14.0	Yes

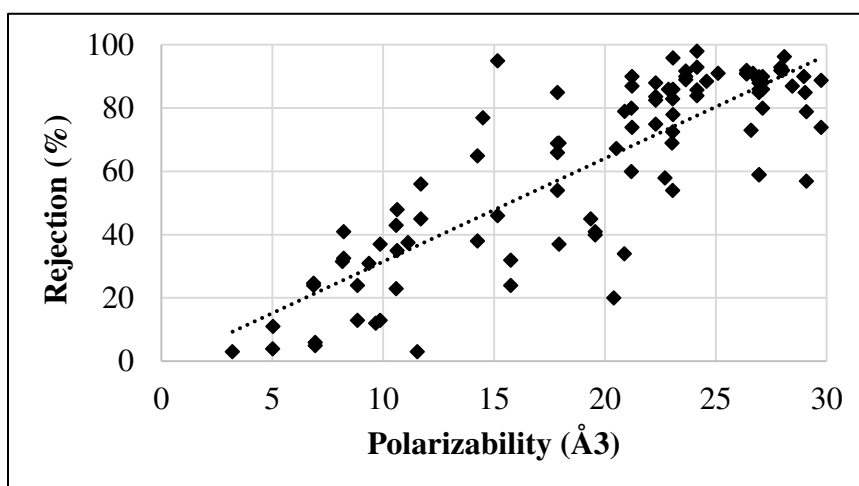


Figure 4-8: Rejection vs TrOC Polarizability (R²=0.71)

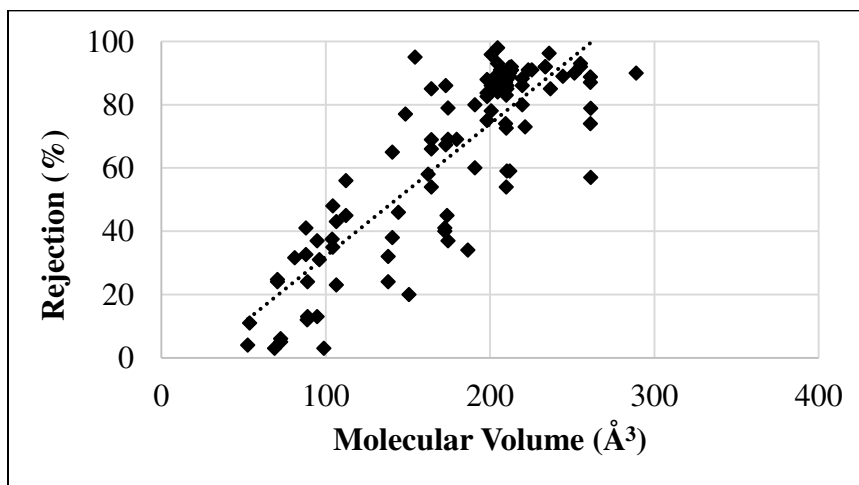


Figure 4-9: Rejection vs TrOC Molecular Volume (R²=0.72)

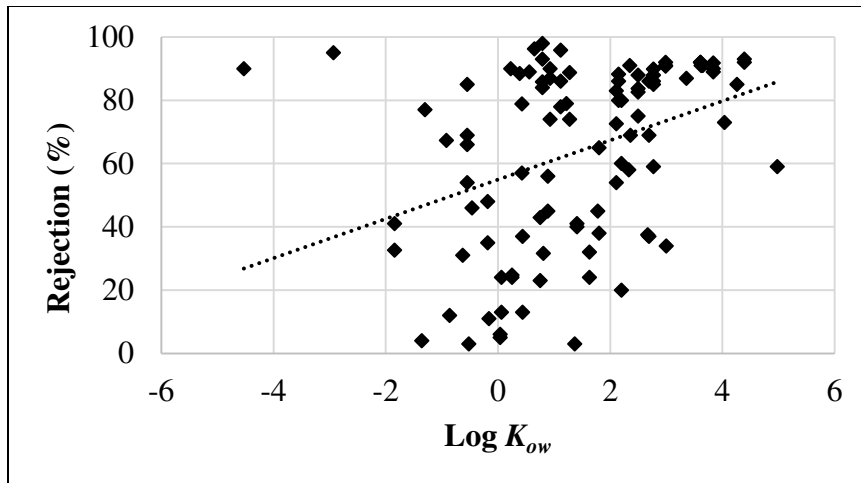


Figure 4-10: Rejection vs TrOC Log K_{ow} ($R^2=0.14$)

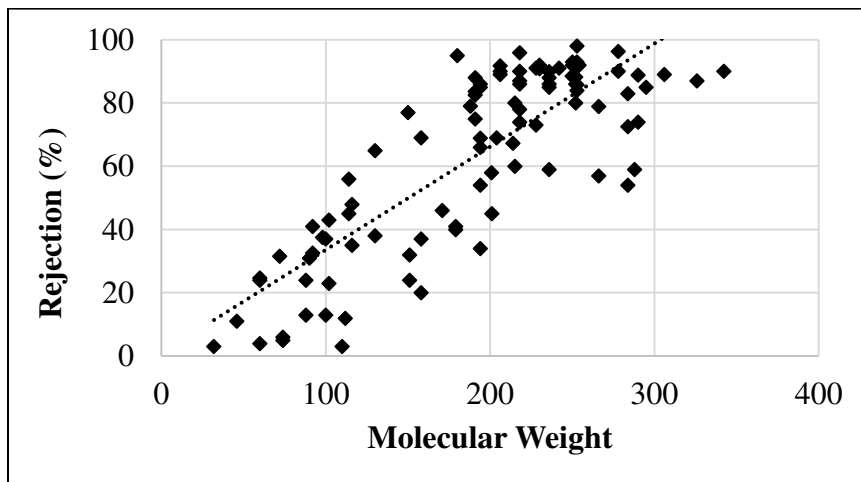


Figure 4-11: Rejection vs TrOC Molecular Weight ($R^2=0.67$)

Conclusions

The main objective of this work was to investigate solute-NF membrane interactions as determined by TrOC polarizability. The impact of several physical and chemical properties on TrOC rejection were evaluated using a pilot unit housing NF270 membranes operating at full-scale plant conditions, operating at a feed flow rate of 60,636 L/h (267 gpm), a flux

of $25.6 \text{ L m}^{-2} \text{ h}^{-1}$ (15.1 gsf), and 85 percent water recovery. Results indicate that TrOC polarizability and molecular volume were well-correlated with rejection ($0.94 R^2$).

Independent, analogous literature sources reporting on TrOC removal in “loose” NF processes were also used to investigate polarizability and molecular volume as rejection mechanisms, whereupon the R^2 value describing the relationship between these properties and rejection was shown to be 0.71 and 0.72, respectively. Additionally, after incorporating independent literature results, the molecular weight R^2 value was 0.67, indicating a correlation between this parameter and TrOC rejection. Alternatively, the R^2 value (0.14) describing the relationship between rejection and TrOC $\log K_{ow}$ values indicated there was no correlation between this property and rejection. TrOCs with polarizability values and molecular volumes greater than 30 and 290 \AA^3 , respectively, are expected to be rejected by loose NF membranes. Findings indicate that water flux plays an important role in whether or not polarizability can be used as an indicator for TrOC rejection by polyamide NF membranes. As the water flux increased, the R^2 representing the correlation between polarizability and rejection decreased. Hence it may be possible to use polarizability to qualitatively predict full-scale “loose” polyamide NF performance without the need to conduct expensive confirmation experiments.

Results of multiple experiments evaluating the rejection of TrOC’s dosed in fresh groundwater by a NF pilot unit were presented and discussed. Nine TrOCs were evaluated at varying feed concentrations ranging from 150 ng/L to 4.5 mg/L, and rejection of seven TrOCs ranged from 68 percent for caffeine to below detection in the permeate for

gemfibrozil and sucralose, while it was reasoned there was a high probability that estrone and bisphenol A were not detected in a majority of samples due to adsorption based on the work others (Bellona et al., 2004).

Acknowledgments

This work was funded by Jupiter Water Utilities (Jupiter, FL) and Kimley-Horn & Associates, Inc. (West Palm Beach, FL) via UCF project 16208114. The authors would like to acknowledge the Town of Jupiter Utilities staff, including David Brown, Amanda Barnes, Paul Jurczak, and Rebecca Wilder, for their assistance and support. The authors would also like to acknowledge engineering consultants who assisted on this project, including Ian Watson (RosTek Associates Inc.) and John E. Potts (Kimley-Horn & Associates, Inc.). Additional thanks are offered to Dr. Cherie Yestrebsky and Dr. Carolina Franco (UCF Chemistry Department) for their assistance in obtaining a portion of trace organic compound data, and for UCF CECE Department graduate and undergraduate students who assisted in the pilot experiments.

References

- Barnes, K.K., Kolpin, D.W., Furlong, E.T., Zaugg, S.D., Meyer, M.T., & Barber, L.B. (2008). A national reconnaissance of pharmaceuticals and other organic wastewater contaminants in the United States – I) Groundwater. *Science of the Total Environment*, 402, 192-200.
- Bellona, C., Drewes, J.E., Xu, P., & Amy, G. (2004). Factors affecting the rejection of organic solutes during NF/RO treatment – a literature review. *Water Research*, 38, 2795-2809.
- Bellona, C., & Drewes, J.E. (2007). Viability of a low-pressure nanofilter in treating recycled water for water reuse applications: A pilot-scale study. *Water Research*, 41, 3948-3958.
- Bellona, C., Heil, D., Yu, C., Fu, P., & Drewes, J.E. (2012). The pros and cons of using nanofiltration in lieu of reverse osmosis for indirect potable reuse applications. *Separation and Purification Technology*, 85, 69-76.
- Chen, S.S., Taylor, J.S., Mulford, L.A., & Norris, C.D. (2004). Influences of molecular weight, molecular size, flux, and recovery for aromatic pesticide removal by nanofiltration membranes. *Desalination*, 160, 103-111.
- Comerton, A.M., Andrews, R.C., Bagley, D.M., & Hao, C. (2008). The rejection of endocrine disrupting and pharmaceutically active compounds by NF and RO membranes as a function of compound and water matrix properties. *Journal of Membrane Science*, 313, 323-335.
- Dang, H.Q., Nghiem, L.D., & Price, W.E. (2014). Factors governing the rejection of trace organic contaminants by nanofiltration and reverse osmosis membranes. *Desal. Wat. Treat.*, 52, 589-599.
- Duranceau, S.J., Taylor, J.S., & Mulford, L.A. (1992). SOC removal in a membrane softening process. *Jour AWWA*, 84, 68-78.
- Estévez, E., del Carmen Cabrera, M., Molina-Díaz, A., Robles-Molina, J., & del Pino Palacioz-Díaz, M. (2008). Screening of emerging contaminants and priority substances (2008/105/EC) in reclaimed water for irrigation and groundwater in a volcanic aquifer (Gran Canaria, Canary Islands, Spain). *Science of the Total Environment*, 433, 538-546.
- Fawell, J., & Ong, J.N. (2012). Emerging Contaminants and the Implications for Drinking Water. *International Journal of Water Resources Development*, 28, 247-263.

- Fujioka, T., Khan, S.J., McDonald, J.A., & Nghiem, L.D. (2014). Nanofiltration of trace organic chemicals: A comparison between ceramic and polymeric membranes. *Separation and Purification Technology*, 136, 258-264.
- Garcia, N., Moreno, J., Cartmell, E., Rodriguez-Roda, I., & Judd, S. (2013). The application of microfiltration-reverse osmosis/nanofiltration to trace organics removal for municipal wastewater reuse. *Environmental Technology*, 34, 3183-3189.
- Gur-Reznik, S., Koren-Menashe, I., Heller-Grossman, L., Rufel, O., & Dosoretz, C.G. (2011). Influence of seasonal and operating conditions on the rejection of pharmaceutical active compounds by RO and NF membranes. *Desalination*, 277, 250-256.
- Hajibabania, S., Verliefde, A.R.D., McDonald, J.A., Khan, S.J., & Le-Clech, P. (2011). Fate of trace organic compounds during treatment by nanofiltration. *Journal of Membrane Science*, 373, 130-139.
- Hofman, J.A.M.H., Beerendonk, E.F., Folmer, H.C., & Kruithoff, J.C. (1997). Removal of pesticides and other micropollutants with cellulose acetate, polyamide and ultra-low pressure reverse osmosis membranes. *Desalination*, 113, 209-214.
- Hofman, J.A.M.H., Gijsbertsen, A.J., & Cornelissen, E. (2007). *Nanofiltration Retention Models for Organic Contaminants*. Denver, CO: American Water Works Association Research Foundation and Kiwa Water Research.
- Jeffery-Black, S., & Duranceau, S.J. (2016). Mass Transfer and Transient Response Time of a Split-Feed Nanofiltration Pilot Unit, Desalination and Water Treatment. *In Press*.
- Kosutic, K., Dolar, D., Asperger, D., & Kunst, B. (2007). Removal of antibiotics from a model wastewater by RO/NF membranes. *Separation and Purification Technology*, 53, 244-249.
- Li, Z., Xiang, X., Li, M., Ma, Y., Wang, J., & Liu, X. (2015). Occurrence and risk assessment of pharmaceuticals and personal care products and endocrine disrupting chemicals in reclaimed water and receiving groundwater in China. *Ecotoxicology and Environmental Safety*, 119, 74-80.
- Mawhinney, D.B., Young, R.B., Vanderford, B.J., Borch, T., & Snyder, S.A. (2011). Artificial Sweetener Sucralose in U.S. Drinking Water Systems. *Environmental Science and Technology*, 45, 8716-8722.
- Mendenhall, W., & Sincich, T. (2007). *Statistics for Engineering and the Sciences*. Upper Saddle River, N.J.: Pearson Prentice-Hall.

- Miller, K.J., & Savchik, J.A. (1979). A New Empirical Method to Calculate Average Molecular Polarizabilities. *Journal of the American Chemical Society*, *101*, 7206-7213.
- Mohammad, A.W., Teow, Y.H., Ang, W.L., Chung, Y.T., Oatley-Radcliffe, D.L., Hilal, N. (2015). Nanofiltration membranes review: Recent advances and future prospects. *Desalination*, *356*, 226-254.
- Nghiem, L.D., Schafer, A.I., & Elimelech, M. (2004). Removal of Natural Hormones by Nanofiltration Membranes: Measurement, Modeling, and Mechanisms. *Environmental Science and Technology*, *38*, 1888-1896.
- Nghiem, L.D., Schafer, A.I., & Elimelech, M. (2006). Role of electrostatic interactions in the retention of pharmaceutically active contaminants by a loose nanofiltration membrane. *Journal of Membrane Science*, *286*, 52-59.
- Oppenheimer, J., Eaton, A., Badruzzaman, M., Haghani, A.W., & Jacangelo, J.G. (2011). Occurrence and suitability of sucralose as an indicator compound of wastewater loading to surface waters in urbanized regions. *Water Research*, *45*, 4019-4027.
- Radjenovic, J., Petrovic, M., Ventura, F., & Barcelo, D. (2008). Rejection of pharmaceuticals in nanofiltration and reverse osmosis membrane drinking water treatment. *Water Research*, *42*, 3601-3610.
- Sadmani, A.H.M., Andrews, R.C., & Bagley, D.M. (2014). Nanofiltration of pharmaceutically active and endocrine disrupting compounds as a function of compound interactions with DOM fractions and cations in natural water. *Separation and Purification Technology*, *122*, 462-471.
- Shahmansouri, A., & Bellona, C. (2013). Application of quantitative structure-property relationships (QSPRs) to predict the rejection of organic solutes by nanofiltration. *Separation and Purification Technology*, *118*, 627-638.
- Van der Bruggen, B., Schaep, J., Maes, W., Wilms, D. & Vandecasteele, C. (1998). Nanofiltration as a treatment method for the removal of pesticides from groundwaters. *Desalination*, *117*, 139-147.
- Van der Bruggen, B., Schaep, J., Wilms, D., & Vandecasteele, C. (1999). Influence of molecular size, polarity and charge on the retention of organic molecules by nanofiltration. *Jour. Membrane Science*, *156*, 29-41.
- Van der Bruggen, B., Braeken, L., & Vandecasteele, C. (2002). Evaluation of parameters describing flux decline in nanofiltration of aqueous solutions containing organic compounds. *Desalination*, *147*, 281-288.
- Verliefde, A.R.D., Cornelissen, E.R., Heijman, S.G.J., Verberk, J.Q.J.C., Amy, G.L., Van der Bruggen, B., & van Dijk, J.C. (2008). The role of electrostatic interactions on

- the rejection of organic solutes in aqueous solutions with nanofiltration. *Journal of Membrane Science*, 322, 52-66.
- Verliefde, A.R.D., Cornelissen, E.R., Heijman, S.G.J., Verberk, J.Q.J.C., Amy, G.L., Van der Bruggen, B., & van Dijk, J.C. (2009). Construction and validation of a full-scale model for rejection of organic micropollutants by NF membranes. *Journal of Membrane Science*, 339, 10-20.
- Vorobyov, I., & Allen, T.W. (2010). The electrostatics of solvent and membrane interfaces and the role of electronic polarizability. *The Journal of Chemical Physics*, 132, 1-13.
- Wang, S., Wenyong, W., Liu, F., Yin, S., Bao, Z., & Liu, H. (2015). Spatial distribution and migration of nonylphenol in groundwater following long-term wastewater irrigation. *Journal of Contaminant Hydrology*, 177-178, 85-92.
- Wilder, R., Duranceau, S.J., Jeffery, S., Brown, D., & Arrington, A. (2016). Contaminants of Emerging Concern: Occurrence in Shallow Groundwater and Removal by Nanofiltration. Proceedings from the American Membrane Technology Association Conference.
- Yangali-Quintanilla, V., Sadmani, A., McConville, M., Kennedy, M., & Amy, G. (2009). Rejection of pharmaceutically active compounds and endocrine disrupting compounds by clean and fouled nanofiltration membranes. *Water Research*, 43, 2349-2362.
- Yangali-Quintanilla, V., Maeng, S.K., Fujioka, T., Kennedy, M., & Amy, G. (2010). Proposing nanofiltration as acceptable barrier for organic contaminants in water reuse. *Journal of Membrane Science*, 362, 334-345.
- Yangali-Quintanilla, V., Maeng, S.K., Fujioka, T., Kennedy, M., Li, Z., & Amy, G. (2011). Nanofiltration vs. reverse osmosis for the removal of emerging organic contaminants in water reuse. *Desal. Wat. Treat.*, 34, 50-56.

CHAPTER 5: CAFFEINE REMOVAL AND MASS TRANSFER IN A NANOFILTRATION MEMBRANE PROCESS

Abstract

The effectiveness of nanofiltration to remove a wide range of spiked caffeine (0.052 to 4,500 $\mu\text{g/L}$) from groundwater at the pilot-scale (60,636 L/h) has been demonstrated. Experiments were conducted using a pilot-scale unit, operating as a two-stage, split-feed, center-exit system, that relied on a well supply withdrawn from an average depth of 45 m that contained an average of 11 mg/L of dissolved organic carbon. The average caffeine removal efficiency across the pilot system was 68 percent, and removal did not vary by solute concentration for constant flux ($25.6 \text{ L m}^{-2} \text{ h}^{-1}$) and temperature (25°C) operating conditions. Mass transfer models evaluated in this work include the homogeneous solution diffusion model (HSDM) with and without film theory (FT), in addition to dimensional analysis, using the Sherwood number, and were shown to predict NF solute mass transfer. Predicted versus actual caffeine content was linearly compared, revealing correlation coefficients on the order of 0.99, 0.96, and 0.99 for the HSDM without FT, HSDM-FT, and the Sherwood number, respectively. However, the use of the HSDM-FT and the Sherwood number resulted in the over-prediction of caffeine concentrations in permeate streams by 27 percent and 104 percent, respectively.

Keywords: solution diffusion model, mass transfer coefficient, Sherwood number, dimensional analysis.

Introduction

Trace organic compounds (TrOCs), including endocrine disrupting compounds, pharmaceuticals, personal care products, and pesticides, are of growing concern due to their relatively recent detection in the aquatic environment. TrOCs typically make their way into the environment via wastewater effluent discharge to rivers and streams, in addition to wastewater reclamation for irrigation. Consequently, these compounds have been detected in drinking water sources with concentrations up to the parts per billion (ppb) level (Barnes et al., 2008; Focazio, et al., 2008; Kolpin et al., 2002; Wilder et al., 2016).

Research has shown that TrOCs can be effectively removed by certain membrane technologies, including nanofiltration (NF) and reverse osmosis (RO) processes (Bellona & Drewes, 2007; Duranceau, 1990; Radjenovic et al., 2008; Yangali-Quintanilla et al., 2011; Xu et al., 2005). The extent of TrOC removal is dependent on many factors, including solute properties (size, charge, hydrophobicity, geometry, etc.), membrane type (molecular weight cut off, pore size) and operation (flux, recovery), and feed water quality characteristics (pH, ionic strength, organic content) (Bellona et al., 2004; Comerton et al., 2009; Yangali-Quintanilla et al., 2009).

As public concern regarding TrOCs in water supplies increases and as more utilities consider indirect/direct potable reuse, the desire to investigate wastewater impacts on drinking water supplies increases (Benotti & Snyder, 2009). However, it is not feasible for many publicly owned water treatment facilities to routinely collect and analyze TrOC samples, as analytical techniques are challenging and compounds are often at trace

concentrations. To reduce monitoring costs, selecting one TrOC to monitor in water treatment processes may be beneficial. Consequently, the investigation of anthropogenic tracers, including caffeine, sucralose, and carbamazepine to evaluate wastewater impacts on drinking water supplies is often recommended, as these constituents are not naturally found in the environment (Boleda et al., 2010; Buerge et al., 2003; Clara et al., 2004; Hillebrand et al., 2012; Mawhinney et al., 2011; Oppenheimer et al., 2011). As a result of more and more utilities considering indirect/direct potable reuse and the increased attention that is being placed on TrOCs in the aquatic environment, the ability to predict TrOC concentrations in membrane permeate would be beneficial (Miller, 2006).

Diffusion-based models have been widely used to predict RO and NF performance (Hung et al., 2011; Zhao & Taylor, 2004; Zhao et al., 2005) in addition to trace organic compound modeling (Duranceau, 1990; Hidalgo et al., 2011; Hidalgo et al., 2012; Cerliefde et al., 2009). Duranceau (1990) studied the removal of six synthetic organic compounds (SOC) from a NF pilot, and used the homogeneous solution diffusion model (HSDM) to predict SOC removal. Hidalgo and colleagues (2012) used the solution diffusion model to predict atrazine in the permeate of four NF membranes, and Hidalgo and colleagues (2011) used the HSDM to predict aniline removal from reverse osmosis processes. Others have incorporated the use of the solution diffusion model modified by film theory (HSDM-FT) to account for concentration polarization effects (Zhao et al., 2005).

The purpose of this work was to predict the transport of an anthropogenic solute, caffeine, through a NF membrane process using two previously established diffusion-based models:

the HSDM and the HSDM-FT. This paper compares actual and predicted permeate stream caffeine concentrations for a two-stage NF pilot operating under full-scale plant conditions. Caffeine mass transfer coefficients were determined experimentally using linear regression and by using the Sherwood number correlation method, and these values were compared. The model was validated using results reported herein as well as use of outside independent literature sources.

Theory

Diffusion-based models have proven to be valid tools for describing transport in diffusion-controlled membrane processes (Duranceau, 1990; Hidalgo et al., 2012; Wijmans & Baker, 1995; Zhao et al., 2005). One of the more popular transport models, the HSDM assumes solutes permeate through membranes in three steps: (1) solutes partition into the polymeric membrane on the feed side, (2) solutes diffuse through the bulk portion of the membrane, and (3) solutes partition completely through the membrane and into the permeate stream (Wang et al., 2014). Incorporating film theory into the HSDM accounts for possible effects of concentration polarization (Zhao et al., 2005).

Equations 5-1 through 5-4 are commonly used in mass and flow balance calculations. Q_f , Q_p and Q_c are the feed, permeate, and concentrate flow rates, respectively, C_f , C_p and C_c are the feed, permeate, and concentrate concentrations, respectively, and R is the water recovery. These parameters are depicted graphically in a simplified membrane schematic, illustrated in Figure 5-1.

$$Q_f = Q_p + Q_c \quad (5-1)$$

$$Q_f C_f = Q_p C_p + Q_c C_c \quad (5-2)$$

$$R = \frac{Q_p}{Q_f} * 100 \quad (5-3)$$

$$Rejection = \frac{C_f - C_p}{C_f} * 100 \quad (5-4)$$

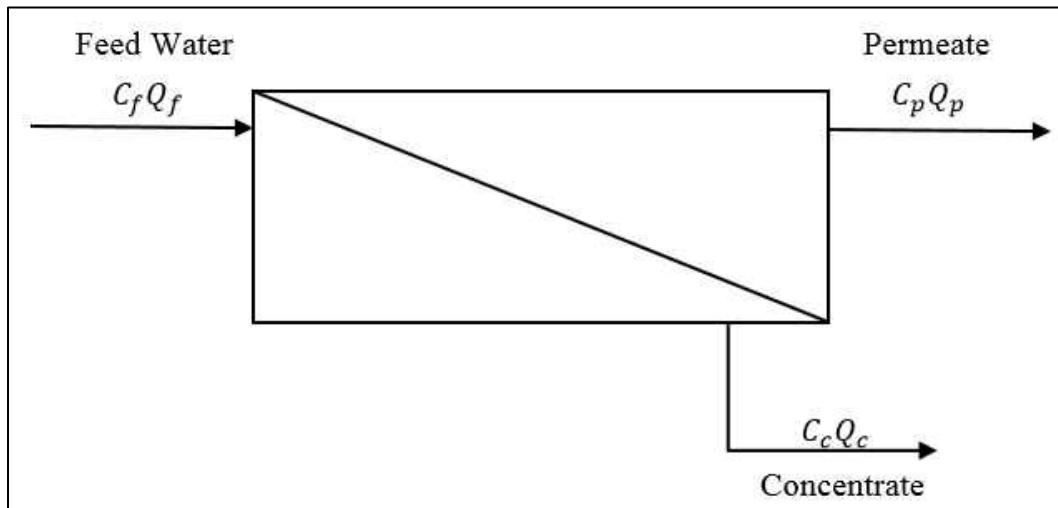


Figure 5-1: Membrane Schematic

Water flux, F_w , is the term used to describe the flow of water per unit of membrane area, and is calculated using Equation 5-5, where A is the membrane area. The osmotic pressure, $\Delta\pi$, is the pressure that must be overcome to push water from the feed to the permeate and concentrate sides of the membrane. The transmembrane pressure differential, ΔP , is the pressure drop across the membrane, determined by calculating the average pressure between the feed and concentrate sides of the membrane. Consequently, the net applied pressure can be calculated as the transmembrane pressure differential minus the osmotic

pressure differential (AWWA, 2007). K_w is the water mass transfer coefficient describing the water flux per unit of pressure, and is experimentally determined using Equation 5-5.

$$F_w = K_w(\Delta P - \Delta\pi) = \frac{Q_p}{A} \quad (5-5)$$

While water flux and water mass transfer coefficients are highly dependent on pressure, solute flux (F_s) and solute mass transfer coefficients (K_s) are controlled by diffusion (Zhao et al., 2005). The solute flux describes the throughput of a solute through a membrane process, and is calculated using Equation 5-6, where C_m is the concentration at the membrane surface, and is calculated using Equation 5-7.

The solute mass transfer coefficient is assumed to be constant for a specific solute, but can vary with water quality, operating conditions, and membrane properties (Zhao et al., 2005; Murthy & Gupta, 1997). The mass transfer coefficient for caffeine, K_s , can be determined experimentally by finding the slope between the solute flux and the change in solute concentration as demonstrated by Equation 5-6, or by applying a Sherwood number correlation method utilizing Equations 5-9 through 5-13.

$$F_s = K_s(C_m - C_p) = \frac{Q_p C_p}{A} \quad (5-6)$$

$$C_m = \frac{C_f + C_c}{2} \quad (5-7)$$

The solute back-transport mass transfer coefficient, k_b , is determined using Equation 5-8, and takes into account the concentration polarization effects describing the build-up of

solutes at the feed side of the membrane surface due to partial rejection of these solutes (Verliefde et al., 2009).

$$\frac{c_m - c_p}{c_f - c_p} = \exp\left(\frac{F_w}{k_b}\right) \quad (5-8)$$

The Sherwood number is calculated using Equation 5-9, assuming laminar flow conditions, where R_e is the Reynolds number, S_c is the Schmidt number, d_h is the hydraulic diameter (ft), L is the membrane channel length (ft), μ is the solution viscosity (kg/m/s), ρ is the density of water (kg/m³), D_i is the diffusivity of a species (m²/s), and V is the feed channel velocity (m/s). D_i is the Wilke-Chang correlation, calculated using Equation 5-12, where φ is solvent association factor (2.26 for water), MW is the solute molecular weight (g/mole), T is the water temperature (K), and V_i is the solute molar volume at normal boiling point (m³/kmol), calculated by adding the individual solute atomic volumes (Duranceau, 1990; Lee et al., 2004; Linton & Sherwood, 1950; Sherwood et al., 1967; Wilke & Chang, 1955).

$$S_h = 1.86 \left(R_e S_c \frac{d_h}{L} \right)^{0.33} \quad (5-9)$$

$$R_e = \frac{d_h V \rho}{\mu} \quad (5-10)$$

$$S_c = \frac{\mu}{\rho D_i} \quad (5-11)$$

$$D_i = \frac{(117.3 \times 10^{-15}) [(\varphi)(MW)]^{0.5} (T)}{\mu V_i^{0.6}} \quad (5-12)$$

Once the Sherwood parameters are known, K_s can be determined using Equation 5-13.

$$K_s = \frac{S_h D_i}{d_h} \quad (5-13)$$

Combining and rearranging Equations 5-1 through 5-7 results in Equation 5-14, which is used to predict permeate concentration based on the HSDM. Adding the solute back-transport mass transfer coefficient into Equation 5-14 results in the HSDM-FT, presented as Equation 5-15. To use Equations 5-14 and 5-15, water and solute mass transfer coefficients, assumed to be constant, must be determined (Chellam & Taylor, 2001; Murthy & Gupta, 1997; Zhao et al., 2005).

$$C_p = \frac{K_s C_f}{K_w (\Delta P - \Delta \pi) \left(\frac{2-2R}{2-R} \right) + K_s} \quad (5-14)$$

$$C_p = \frac{K_s C_f \exp\left(\frac{F_w}{k_b}\right)}{K_w (\Delta P - \Delta \pi) \left(\frac{2-2R}{2-R} \right) + K_s \exp\left(\frac{F_w}{k_b}\right)} \quad (5-15)$$

Materials and Methods

Site Description

This research was conducted using a 267-gallon per minute (gpm) NF pilot unit housing NF270 membranes (DOW Filmtec), owned and operated by the Town of Jupiter (Town) Water Utility. Jupiter is located along the southeast coast of Florida, and the water treatment facility serves approximately 80,000 customers over an area of 58 square miles. Their full-scale plant has a treatment capacity of 30 million gallons per day (MGD), utilizing reverse osmosis, NF, and anion exchange processes in parallel. The NF plant was constructed in 2010 and has a maximum production capacity of 14.5 MGD.

NF Pilot Unit

The pilot and full-scale processes are uniquely configured: feed water is split prior to entering both the left and right sides of the 6-element pressure vessels, then permeate is collected on both ends, while concentrate is collected in the center of the vessel, after only three membranes. A simplified schematic of the pretreatment system and unique membrane configuration is illustrated in Figure 5-2. This configuration has resulted in a lower pressure drop between stages, since the water path only flows through half of the number of membranes compared to a typical NF plant.

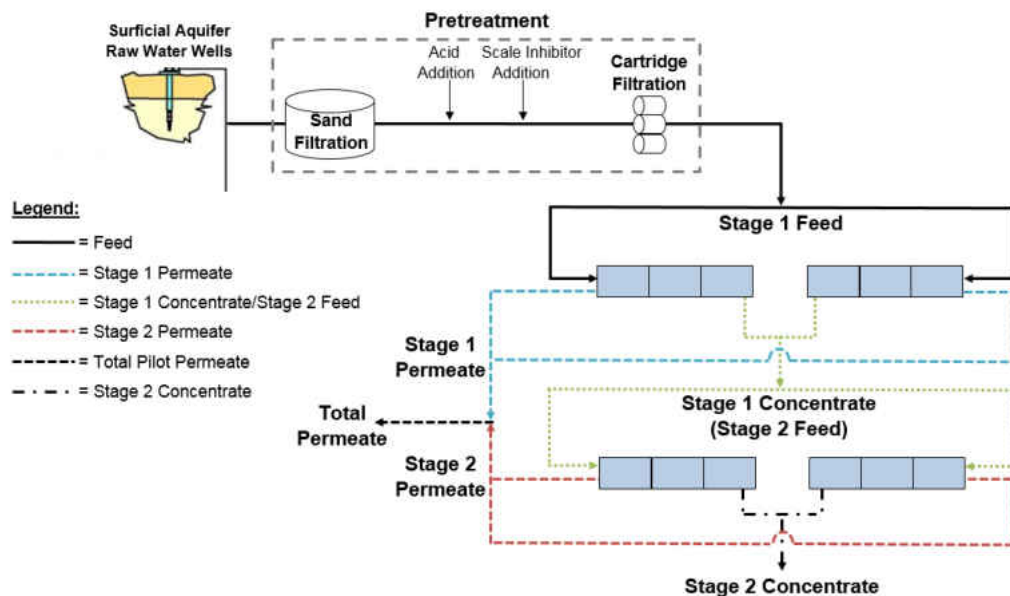


Figure 5-2: Simplified schematic of NF pretreatment and flow configuration

Pilot specifications and operating parameters are presented in Table 5-1. Membrane elements in the pilot unit are the same as those currently employed by the Town's full-scale NF plant. The membranes are 8" in diameter and have a surface area of 400 ft². There

are a total of 54 elements in the pilot, with 42 in the first stage and 12 in the second stage, and six elements per pressure vessel, forming a 7:2 array. This results in a total membrane area of 21,600 ft² in the pilot unit. The NF pilot operates with a feed flow rate of 267 gpm, resulting in a permeate flow rate of 226 gpm while operating at an 85% water recovery. The typical feed pressure of the pilot unit is 57 pounds per square inch (psi), while the permeate pressure is 21 psi.

Table 5-1: NF pilot unit specifications and operating parameters

Item	Value	
Membrane Module	NF270 (DOW Filmtec)	
Membrane pore diameter (nm) ^a	0.84	
MgSO ₄ & CaCl ₂ Rejection (%) ^b	97 & 40-60	
Pilot Recovery (%)	85	
Total Number of Membrane Elements	54	
Elements in Stage 1 & 2	42 & 12	
Membranes per pressure vessel	6	
Array	7:2	
Membrane Surface Area (DOW Filmtec)	37.2 m ² /element	400 ft ² /element
Total Membrane Area in Pilot	2,007 m ²	21,600 ft ²
Feed Velocity	0.043 m/s	0.14 ft/s
Feed Flow Rate	60,636 L/h	267 gpm
Permeate Flow Rate	51,552 L/h	227 gpm
Concentrate Flow Rate	9,084 L/h	40 gpm
Feed Pressure	3.93 bar	57 psi
Permeate Pressure	1.45 bar	21 psi
Water Flux	25.6 L m ⁻² h ⁻¹	15.1 gsfd

^aNghiem et al., 2004; ^bBellona et al., 2012.

Feed Water Quality

The Town's NF plant, and subsequently the Town's NF pilot unit, draws raw water from a fresh surficial groundwater source. Feed water is transferred to the head of the pilot following full-scale plant pretreatment, which includes sand filtration, cartridge filtration (5 μm), and sulfuric acid and scale inhibitor addition. Table 5-2 presents water quality in pilot feed water and total pilot system permeate, collected and analyzed by the University of Central Florida (UCF). Raw water entering the water treatment facility is usually around a pH of 7.1, although sulfuric acid is added as a pretreatment step to lower the pH to 6.5 for hydrogen sulfide and scale control. Conductivity in the feed water is typically 750 $\mu\text{S}/\text{cm}$, and the total dissolved solids (TDS) concentration in the feed water is around 455 mg/L. Due to the large molecular weight cut off (MWCO) of the NF270 membranes, there is no significant removal of monovalent anions and metals; consequently the typical conductivity and TDS in the pilot permeate are 500 $\mu\text{S}/\text{cm}$ and 250 mg/L, respectively. The organic content of the feed water is typical for a south Florida groundwater supply, with a dissolved organic carbon (DOC) concentration of 11 mg/L. The pilot unit removes a substantial portion of organics, with a permeate DOC concentration of <0.25 mg/L.

Table 5-2: NF pilot water quality in feed and permeate samples

Water Quality Parameter	Units	Feed Water	Total Pilot Permeate
pH	N/A	6.5	6.3
Temperature	°C	25	25
Conductivity	μS/cm	750	500
TDS	mg/L	455	250
Alkalinity	mg/L as CaCO ₃	240	172
Color*	Color Units (CU)	45	<5
UV ₂₅₄	cm ⁻¹	0.406	0.06
DOC*	mg/L	11	<0.25
Chloride	mg/L	50	50
Calcium	mg/L	125	66
Sodium	mg/L	23	19

*Method detection limits for color and DOC are 5 CU and 0.25 mg/L, respectively


Caffeine Characterization

Caffeine has frequently been detected in a surficial groundwater well that supplies the Town's water treatment facility and nearby irrigation water (Wilder et al., 2016), and does not naturally occur in the environment. Consequently, caffeine was selected as the TrOC to be modeled in this work.

Caffeine and high performance liquid chromatography (HPLC)-grade methanol were purchased from Sigma-Aldrich. Caffeine properties presented in Table 5-3 were obtained from Chemicalize.org. The molecular weight of caffeine is 194 g/mole, significantly less than the MWCO of NF270 membrane's used in this research. Therefore, the primary rejection mechanism would not be size exclusion. Additionally, caffeine is a neutral compound (Kimura et al., 2004); consequently, rejection due to electrostatic repulsion would not be plausible. Furthermore, caffeine has an octanol-water partition coefficient

(Low K_{ow}) of -0.55; therefore, caffeine adsorption to the membrane itself or pilot appurtenances was neither anticipated nor observed.

Table 5-3: Caffeine properties

Parameter	Value
Chemical Structure	
Classification	Stimulant
Chemical Formula	$C_8H_{10}N_4O_2$
Molecular Weight (g/mol)	194
Molecular Volume (\AA^3)	164
Polarizability (\AA^3)	17.9
Octanol-Water Partition Coefficient (Log K_{ow})	-0.55

Experimental Procedure

Experiments were conducted over a course of seven months to obtain enough data to calculate a solute mass transfer coefficient and create a model, while also obtaining enough data points to validate the model. Table 5-4 presents the feed caffeine concentrations of eleven experiments ranging from 0.052 $\mu\text{g/L}$ to 4,500 $\mu\text{g/L}$. Although caffeine is not found in water supplies with concentrations near the parts per million level, this wide range of data allowed a more accurate calculation of the caffeine mass transfer coefficient.

Table 5-4: Caffeine experiment summary

Experiment No.	Feed Concentration ($\mu\text{g/L}$)
1	0.052
2	0.18
3	0.24
4	0.55
5	2.0
6	7.7
7	74
8	1,020
9	1,418
10	2,920
11	4,500

Sample Preparation and Analytical Methods

Samples collected during experiments 1 through 7 were analyzed by a commercial laboratory. Two 40-mL glass amber vials containing 80 μL of 32 g/L sodium omadine (NaOmadine) and 5 mg ascorbic acid were used to collect each sample. Samples were analyzed using a fully automated on-line solid phase extraction, high performance liquid chromatography, mass spectrometry-mass spectrometry system. A detailed description of laboratory methods can be found elsewhere (Oppenheimer et al., 2011).

Samples collected during experiments 8 through 11 were analyzed by UCF's Civil, Environmental, and Construction (CECE) and Chemistry Departments. Stock solutions of caffeine were prepared in methanol and stored at $-20\text{ }^{\circ}\text{C}$. Further dilutions were prepared in water:methanol mixtures (40:60 v/v) and were used as working standard solutions. Samples were collected in silanized amber bottles, and were prepared in water:methanol

mixtures (40:60 v/v) upon returning to UCF laboratories and stored at -20 °C until analysis. Samples were analyzed using a Perkin-Elmer series 200 HPLC (Santa Clara, CA, USA) consisting of a series 200 binary pump, a series 200 UV-Vis detector with deuterium lamp set at a maximum wavelength of 273 nm, a series 200 autosampler, and a series 200 vacuum degasser. The analytical column used was a Zorbax (Agilent) SB-C18 packed column with a 4.6 x 150 mm dimensions. The mobile phase was water:methanol 40:60 (v/v) with a flow rate of 1 cm³/min. Sample run time was 10.0 minutes with a 10.0 μL injection volume and at isocratic conditions.

Results and Discussion

Model Parameter Determination

To predict caffeine transport using the HSDM and HSDM-FT, the water mass transfer coefficient, K_w , must be known, indicated by Equation 5-13. K_w was obtained experimentally by operating the pilot unit at various pressures and recording flux changes, then finding the slope of the line generated when water flux was plotted as a function of the net applied pressure, according to Equation 5-4. An example of this parameter determination method is represented in Figure 5-3 for the total pilot system, and this process was replicated for the first and second stage to determine their respective water mass transfer coefficients. A summary of water flux and mass transfer coefficients is presented in Table 5-5, and coefficient of determination values (R^2) are presented where applicable. The relationship between F_w and K_w , demonstrated in Equation 5-5, was used to predict the permeate concentration. The water mass transfer coefficient was 0.667 gsfd

for the total pilot system, and 0.587 and 0.679 gsfd for the first and second stages of the pilot unit, respectively.

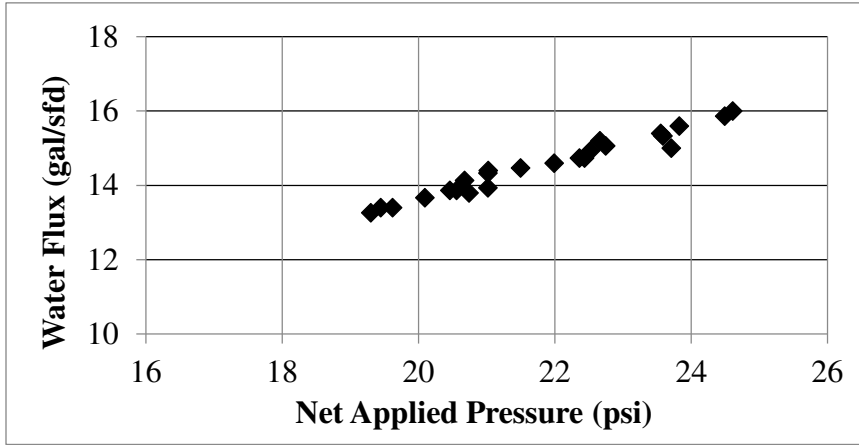


Figure 5-3: Total pilot system water flux as a function of net applied pressure

Table 5-5: Water flux and water mass transfer coefficients

Stage/System	Water flux (F_w)		Water mass transfer coefficient (K_w)		
	gsfd	Lmh	gsfd/psi	Lmh/bar	R^2
First Stage Combined	15.7	26.6	0.667	16.4	0.86
Second Stage Combined	12.9	21.9	0.587	14.5	0.79
Total Pilot System	15.1	26.6	0.679	16.7	0.83

To experimentally determine the caffeine mass transfer coefficient, K_s , experiments were conducted over a wide range of concentrations, as previously presented in Table 5-4. Average caffeine removal in the first stage, second stage, and total pilot system was 75%, 85%, and 68%, respectively, calculated using Equation 5-4. The concentration range of caffeine in the feed during the eleven experiments did not significantly impact rejection, as standard deviations for first stage, second stage, and total pilot system rejections were 2.6,

5.0, and 2.9, respectively. Similar findings have been demonstrated by others (Bodalo et al., 2010; Zhang et al., 2004).

K_S and k_b were both determined experimentally using linear regression, and K_S was also calculated using Sherwood relationships. To experimentally determine K_S , solute flux values were plotted as a function of the change in caffeine concentrations from the bulk side of the pilot to the total system permeate stream, and the slope of this line was calculated. This methodology was replicated for the first and second stages on the left and right sides of the pilot to determine their respective mass transfer coefficients. Furthermore, the same technique was applied to determine k_b values by using Equation 5-8. To create and validate a model, 70% of the data was used to create a model, while the remaining 30% of data is used for validation (Zhao et al., 2005). Due to the wide range of feed concentrations, Figure 5-4 is presented on a log-scale. The caffeine mass transfer coefficient was determined to be 0.21 ft/d for the total pilot system, while the first and second stage caffeine mass transfer coefficients were experimentally determined as 0.32 and 0.27 ft/d, respectively. The caffeine mass transfer coefficients for the first stage left and right sides were 0.31 and 0.27 ft/d, respectively, and 0.25 and 0.26 ft/d for the left and right sides of the second stage, respectively. A summary of experimentally determined caffeine mass transfer coefficients for the first and second stage, and total pilot system are presented in Table 5-6, as well as R^2 values, where applicable. When applying Sherwood relationships, the caffeine mass transfer coefficient was determined to be 2.36 ft/d (8.33×10^{-6} m/s) in the first stage and 2.44 ft/d (8.61×10^{-6} m/s) in the second stage.

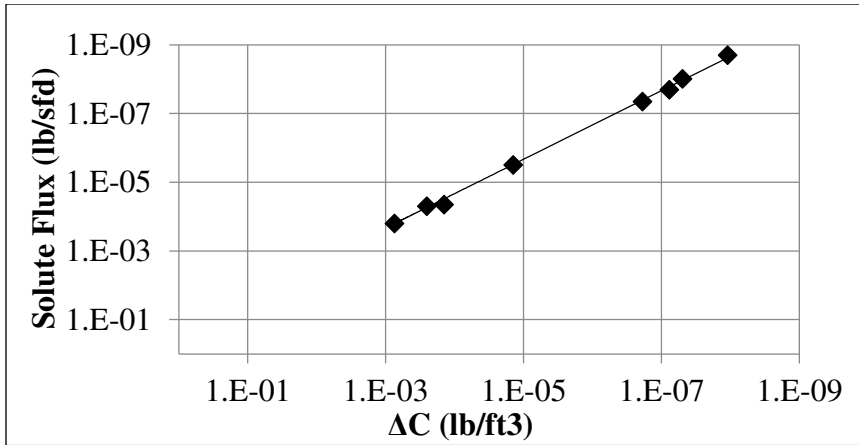


Figure 5-4: Total pilot system solute flux as a function of change in caffeine concentration

Table 5-6: Caffeine mass transfer coefficients

Stage/ System	Mass transfer coefficient (K_s)			$\exp\left(\frac{F_w}{k_b}\right)$		Back-transport mass transfer coefficient (k_b)	
	ft/d	m/s	R ²	Unitless	R ²	ft/d	m/s
First Stage Combined	0.32	1.1 x 10 ⁻⁶	1.0	2.44	1.0	2.35	8.3 x 10 ⁻⁶
First Stage Left	0.31	1.1 x 10 ⁻⁶	0.99	2.11	1.0	2.80	9.9 x 10 ⁻⁶
First Stage Right	0.27	9.6 x 10 ⁻⁷	0.99	2.06	1.0	2.87	1.0 x 10 ⁻⁵
Second Stage Combined	0.27	9.6 x 10 ⁻⁷	0.99	1.55	1.0	3.95	1.4 x 10 ⁻⁵
Second Stage Left	0.25	8.8 x 10 ⁻⁷	1.0	1.45	1.0	4.68	1.7 x 10 ⁻⁵
Second Stage Right	0.26	9.3 x 10 ⁻⁷	1.0	1.52	1.0	3.99	1.4 x 10 ⁻⁵
Total Pilot System	0.21	7.6 x 10 ⁻⁷	0.99	3.72	1.0	1.54	5.4 x 10 ⁻⁶

Caffeine Prediction and Model Validation

Flux and mass transfer coefficients presented in Tables 5-5 and 5-6 were used in the HSDM and HSDM-FT equations (Equations 5-14 and 5-15) to predict the caffeine concentration in the first stage, second stage, and total pilot system permeate, illustrated in Figures 5-5, 5-6, and 5-7.

Figure 5-5 illustrates predicted versus actual caffeine concentrations in pilot permeate from the total pilot system and from the left and right sides of stages 1 and 2 using the HSDM. Results are plotted on a log-scale due to the wide range of permeate concentrations, and represent a total of 16 data points. The solid 45° line represents a plot of predicted versus actual caffeine if there was no error in the model. Model verification was determined by conducting a paired *t*-test on predicted and actual caffeine data. Based on the paired *t*-test and the predicted versus actual caffeine concentrations demonstrated in Figure 5-5, it appears that experimentally derived caffeine mass transfer coefficients used in the HSDM are successful in predicting caffeine concentrations in the first stage, second stage, and total pilot system permeate. The average relative percent difference (RPD) of predicted and actual caffeine concentrations in the permeate streams was 12%.

Figures 5-6 and 5-7 represent predicted versus actual permeate concentration using the HSDM and HSDM-FT, at low and high feed concentrations, respectively. It appears that the HSDM-FT slightly over-predicts caffeine in the permeate streams, indicating concentration polarization does not significantly affect caffeine permeation through this NF pilot. When compared to the HSDM, the HSDM-FT is not as accurate in predicting the

caffeine concentration in permeate streams, as the RPD between predicted and actual caffeine concentrations was 27% and the paired *t*-test indicated a statistically significant difference between predicted and actual caffeine concentrations in permeate streams.

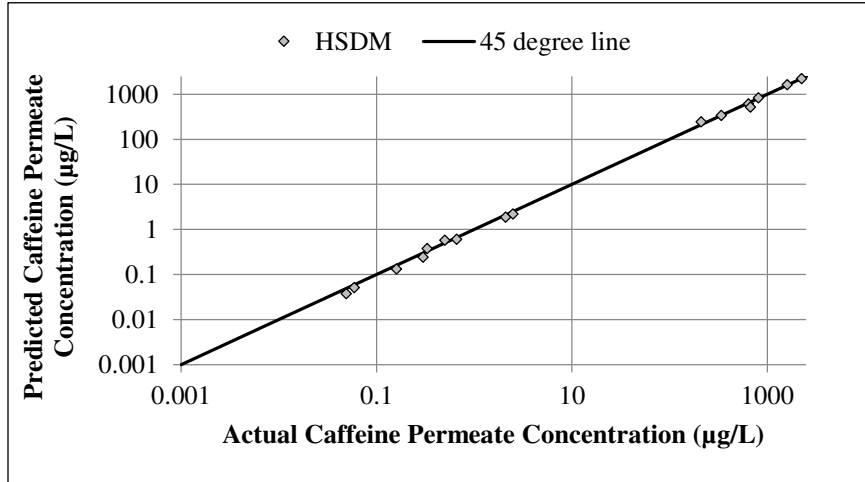


Figure 5-5: Predicted versus actual caffeine concentration from first stage, second stage, and total pilot system permeate using the HSDM at low and high feed concentrations. Results are plotted on a log-scale due to the wide range of concentrations.

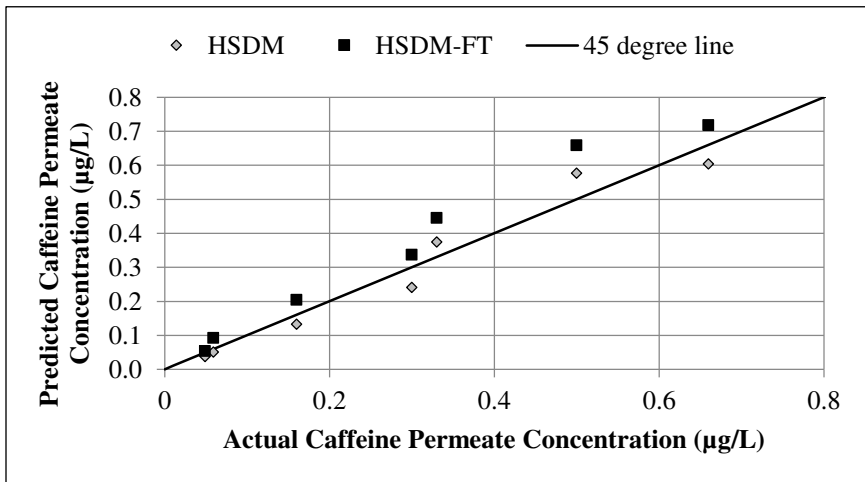


Figure 5-6: Predicted versus actual caffeine concentration from first stage, second stage, and total pilot system permeate using the HSDM and HSDM-FT at low feed concentrations.

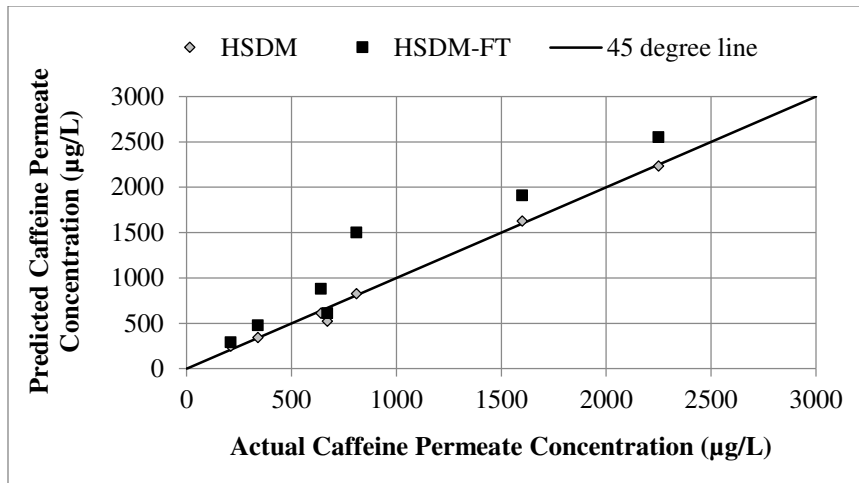


Figure 5-7: Predicted versus actual caffeine concentration from first stage, second stage, and total pilot system permeate using the HSDM and HSDM-FT at high feed concentrations.

When calculated using Sherwood relationships, the mass transfer coefficients appear to over-predict caffeine concentration in the permeate streams, as demonstrated on a log-scale in Figure 5-8. Figure 5-8 presents data from the left and right sides of first and second stages of the pilot system, and the RPD between predicted and actual caffeine concentrations in permeate streams was 104%. Additionally, a paired *t*-test revealed a statistically significant difference between predicted and actual caffeine concentrations. This over-prediction could be due to a variety of reasons that include the possibility of Wilke-Chang coefficients used in Equation 5-12 may be too conservative as well as field conditions. Alternatively, this method could have over-predicted caffeine transport since Sherwood correlations do not strongly consider caffeine or water properties (Duranceau, 1990; Lee et al., 2004). Others have demonstrated similar findings, where models over-predict TDS mass transfer at low TDS concentrations (Zhao et al., 2005) similar to what was experienced in the pilot study.

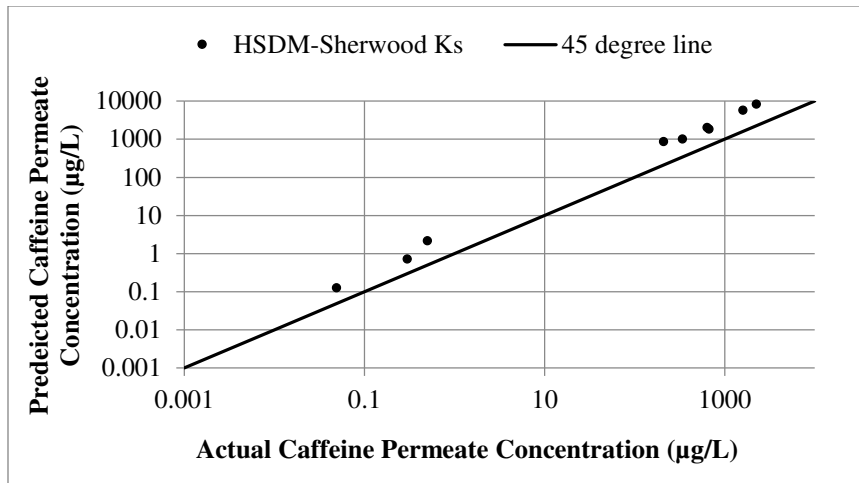


Figure 5-8: Predicted versus actual caffeine concentration in permeate from left and right sides of first and second stages of pilot system using the HSDM with the mass transfer coefficients calculated using Sherwood relationships.

Figure 5-9 was generated using Minitab[®] and illustrates predicted permeate concentrations obtained using the HSDM and mass transfer coefficients presented in Table 5-6, versus actual permeate concentrations using results obtained using data from outside literature sources (Bellona & Drewes, 2007; Comerton et al., 2008; Garcia-Vaquero et al., 2014; Kimura et al., 2004; Shahmansouri & Bellona, 2013; Yangali-Quintanilla et al., 2010). Figure 5-9 is plotted on a log-scale due to the wide range of concentrations. The dashed lines represent 95% confidence bands and the solid line represents the trend line between predicted and actual permeate concentrations. Feed and permeate caffeine concentrations from outside literature data range from 1 to 11,250 µg/L and 0.15 to 8,600 µg/L, respectively. Predicted permeate caffeine concentrations were calculated using operating data from the literature sources. Sources range from loose NF to reverse osmosis membranes, and rejection of caffeine ranges from 24% to 85%. Results indicate that the

HSDM and experimentally-derived caffeine mass transfer coefficients were able to predict the caffeine concentration in the permeate samples from the six outside literature sources.

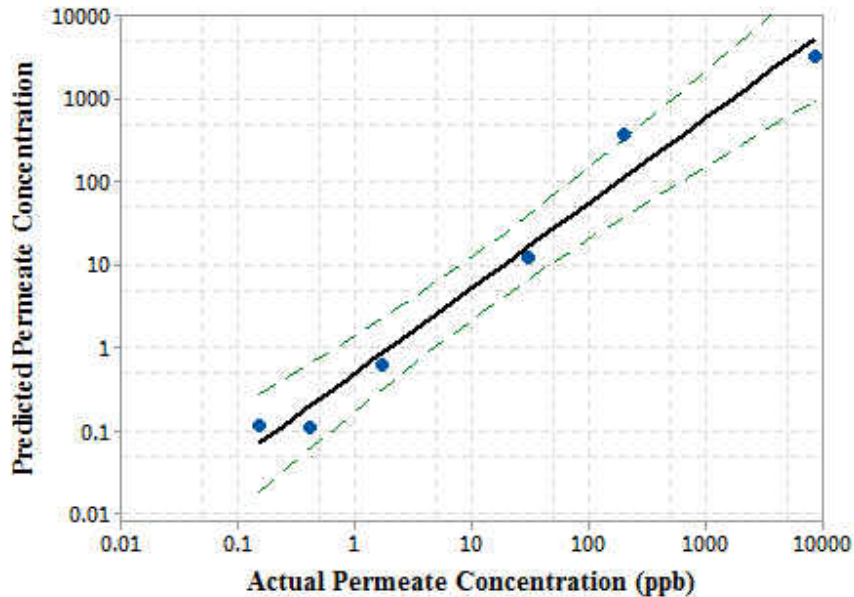


Figure 5-9: Predicted caffeine concentration versus actual caffeine concentration in permeate using results found in the literature.

Conclusions

This work investigated the caffeine removal efficiency of an NF membrane process at the pilot-scale and established mass transfer models for water and caffeine transport using two diffusion-based models: the solution diffusion model and the solution diffusion model with film theory. Experiments were carried out using a 267-gallon per minute, split-feed, center-exit NF pilot operating as a two-stage system that utilizes a surficial groundwater source. Caffeine concentrations ranging from 0.052 to 4,500 $\mu\text{g/L}$ were used in the feed water, and the average caffeine removal efficiency from the total pilot system was 68%, with rejections of 75% and 85% in the first and second stages, respectively. Removal did not

vary by solute concentration for constant flux ($25.6 \text{ L m}^{-2} \text{ h}^{-1}$) and temperature (25°C) operating conditions.

Mass transfer models evaluated in this work include the homogeneous solution diffusion model (HSDM) with and without film theory (FT), in addition to dimensional analysis, using the Sherwood number, and were shown to predict NF solute mass transfer. The models were validated to within a 95 percent confidence interval using a combination of results reported in this research and data obtained from independent literature sources. Predicted versus actual caffeine content was linearly compared, revealing correlation coefficients on the order of 0.99, 0.96, and 0.99 for the HSDM without FT, HSDM-FT, and the Sherwood number, respectively. However, the use of the HSDM-FT and the Sherwood number resulted in the over-prediction of caffeine concentrations in permeate streams by 27 percent and 104 percent, respectively.

Acknowledgments

The work reported herein was funded by UCF project agreement number 16208114. The authors acknowledge the Town of Jupiter Utilities staff, including David Brown, Amanda Barnes, Paul Jurczak, and Rebecca Wilder, for their assistance and support, without whom this work would not have possible. The authors also acknowledge the consultation and advice of Ian Watson (RosTek Associates Inc.) and John Potts (Kimley-Horn & Associates, Inc.). Additional thanks are offered to the UCF graduate and undergraduate students who assisted in this work.

References

- American Water Works Association (AWWA). (2007). *Manual of Water Supply Practices – M46: Reverse Osmosis and Nanofiltration*. Denver, CO: AWWA.
- Barnes, K.K., Kolpin, D.W., Furlong, E.T., Zaugg, S.D., Meyer, M.T., & Barber L.B. (2008). A national reconnaissance of pharmaceuticals and other organic wastewater contaminants in the United States – I) Groundwater. *Science of the Total Environment*, 402, 192-200.
- Bellona, C., & Drewes, J.E. (2007). Viability of a low-pressure nanofilter in treating recycled water for water reuse applications: A pilot-scale study. *Water Research*, 41, 3948-3958.
- Bellona, C., Drewes, J., Xu, P., & Amy, G. (2004). Factors affecting the rejection of organic solutes during NF/RO treatment – a literature review. *Water Research*, 38, 3795-2809.
- Bellona, C., Heil, D., Yu, C., Fu, P., & Drewes, J.E. (2012). The pros and cons of using nanofiltration in lieu of reverse osmosis for indirect potable reuse applications. *Separation and Purification Technology*, 85, 69-76.
- Benotti, M.J., & Snyder, S.A. (2009). Pharmaceuticals and Endocrine Disrupting Compounds: Implications for Groundwater Replenishment with Recycled Water. *Groundwater*, 47, 499-502.
- Boleda, M.R., Majamaa, K., Aerts, P., Gomez, V., Galceran, M.T., & Ventura, F. (2010). Removal of drugs of abuse from municipal wastewater using reverse osmosis membranes. *Desalination and Water Treatment*, 21, 122-130.
- Bodalo, A., Leon, G., Hidalgo, A.M., Gomez, M., Murcia, M.D., Blanco, P. (2010). Atrazine removal from aqueous solutions by nanofiltration. *Desalination and Water Treatment*, 13, 143-148.
- Buerge, I., Poiger, T., Muller, M.D., & Buser, H.R. (2003). Caffeine, an Anthropogenic Marker for Wastewater Contamination of Surface Waters. *Environ. Sci. Technol.*, 37, 691-700.
- Chellam, S., & Taylor, J.S. (2001). Simplified Analysis of Contaminant Rejection during Ground- and Surface Water Nanofiltration Under the Information Collection Rule. *Water Research*, 35, 2460-2474.
- Clara, M., Strenn, B., & Kreuzinger, N. (2004). Carbamazepine as a possible anthropogenic marker in the aquatic environment: investigations on the behavior of Carbamazepine in wastewater treatment and during groundwater infiltration. *Water Research*, 38, 947-954.

- Comerton, A.M., Andrews, R.C., Bagley, D.M., Hao, C. (2008). The rejection of endocrine disrupting and pharmaceutically active compounds by NF and RO membranes as a function of compound and water matrix properties. *Journal of Membrane Science*, 313, 323-335.
- Comerton, A.M., Andrews, R.C., & Bagley, D.M. (2009). The influence of natural organic matter and cations on the rejection of endocrine disrupting and pharmaceutically active compounds by nanofiltration. *Water Research*, 43, 613-622.
- Duranceau, S.J. (1990). *Modeling of Mass Transfer and Synthetic Organic Compound Removal in a Membrane Softening Process*, Ph.D. Dissertation. University of Central Florida.
- Focazio, M.J., Kolpin, D.W., Barnes, K.K., Furlong, E.T., Meyer, M.T., Zaugg, S.D., Barber, L.B., & Thurman, M.E. (2008). A national reconnaissance for pharmaceuticals and other organic wastewater contaminants in the United States – II) Untreated drinking water sources. *Science of the Total Environment*, 402, 201-216.
- Garcia-Vaquero, N., Lee, E., Castaneda, J., Cho, J., & Lopez-Ramirez, J.A. (2014). Comparison of drinking water pollutant removal using a nanofiltration pilot plant powered by renewable energy and a conventional treatment facility. *Desalination*, 347, 94-102.
- Hidalgo, A.M., Leon, G., Gomez, M., Murcia, M.D., Gomez, E., & Gomez, J.L. (2011). Modeling of Aniline Removal by Reverse Osmosis Using Different Membranes. *Chemical Engineering & Technology*, 34, 1753-1759.
- Hidalgo, A.M., Leon, G., Gomez, M., Murcia, M.D., Barbosa, D.S., & Blanco, P. (2012). Application of the solution-diffusion model for the removal of atrazine using a nanofiltration membrane. *Desalination and Water Treatment*, 51, 2244-2252.
- Hillebrand, O., Nodler, K., Licha, T., Sauter, M., & Geyer, T. (2012). Caffeine as an indicator for the quantification of untreated wastewater in karst systems. *Water Research*, 46, 395-402.
- Hung, L.-Y., Lue, S.J., & You, J.-H. (2011). Mass-transfer modeling of reverse-osmosis performance on 0.5-2% salty water. *Desalination*, 265, 67-73.
- Kimura, K., Toshima, S., Amy, G., & Watanabe, Y. (2004). Rejection of neutral endocrine disrupting compounds (EDCs) and pharmaceutical active compounds (PhACs) by RO membranes. *Journal of Membrane Science*, 245, 71-78.
- Kolpin, D.W., Furlong, E.T., Meyer, M.T., Thurman, E.M., Zaugg, S.D., Barber, L.B., & Buxton, H.T. (2002). Pharmaceuticals, Hormones, and Other Organic Wastewater Contaminants in U.S. Streams, 1999 – 2000: A National Reconnaissance. *Environ. Sci. Technol.*, 36, 1202-1211.

- Lee, S., Amy, G., Cho, J. (2004). Applicability of Sherwood correlations for natural organic matter (NOM) transport in nanofiltration (NF) membranes. *Journal of Membrane Science*, 240, 49-65.
- Lin, Y.-L., & Lee, C.-H. (2014). Elucidating the Rejection Mechanisms of PPCPs by Nanofiltration and Reverse Osmosis Membranes. *Ind. Eng. Chem. Res.*, 53, 6798-6806.
- Linton, W.H., & Sherwood, T.K. (1950). Mass transfer from solids shapes to water in streamline and turbulent flow. *Chem. Eng. Progress*, 46, 258.
- Mawhinney, D.B., Young, R.B., Vanderford, B.J., Borch, T., & Snyder, S.A. (2011). Artificial Sweetener Sucralose in U.S. Drinking Water Systems. *Environ. Sci. Technol.*, 45, 8716-8722.
- Miller, G.W. (2006). Integrated concepts in water reuse: managing global water needs. *Desalination*, 187, 65-75.
- Murthy, Z.V.P. & Gupta, S.K. (1997). Estimation of mass transfer coefficient using a combined nonlinear membrane transport and film theory model. *Desalination*, 109, 39-49.
- Nghiem, L.D., Schafer, A.I., & Elimelech, M. (2004). Removal of Natural Hormones by Nanofiltration Membranes: Measurement, Modeling, and Mechanisms. *Environ. Sci. Technol.*, 38, 1888-1896.
- Oppenheimer, J., Eaton, A., Badruzzaman, M., Haghani, A.W., & Jacangelo, J.G. (2011). Occurrence and suitability of sucralose as an indicator compound of wastewater loading to surface waters in urbanized regions. *Water Research*, 45, 4019-4027.
- Radjenovic, J., Petrovic, M., Ventura, F., & Barcelo, D. (2008). Rejection of pharmaceuticals in nanofiltration and reverse osmosis membrane drinking water treatment. *Water Research*, 42, 3601-3610.
- Shahmansouri, A., & Bellona, C. (2013). Application of quantitative structure-property relationships (QSPRs) to predict the rejection of organic solutes by nanofiltration. *Separation and Purification Technology*, 118, 627-638.
- Sherwood, T.K., Brian, P.L.T. & Fisher, R.E. (1967). Desalination by Reverse Osmosis. *Ind. Eng. Chem. Fundamen.*, 6, 2-12.
- Verliefde, A.R.D., Cornelissen, E.R., Heijman, S.J.G., Verberk, J.Q.J.C., Amy, G.L., Van der Bruggen, B., & van Dijk, J.C. (2009). Construction and validation of a full-scale model for rejection of organic micropollutants by NF membranes. *Journal of Membrane Science*, 339, 10-20.

- Wang, J., Dlamini, D.S., Kishra, A.K., Pendergast, M.T.M., Wong, M.C.Y., Mamba, B.B., Freger, V., Verliefde, A.R.D., & Hoek, E.M.V. (2014). A critical review of transport through osmotic membranes. *Journal of Membrane Science*, 454, 516-537.
- Wijmans, J.G., & Baker, R.W. (1995). The solution-diffusion model: a review. *Journal of Membrane Science*, 107, 1-21.
- Wilder, R.J., Duranceau, S.J., Jeffery, S., Brown, D., & Arrington, A. (2016). Contaminants of Emerging Concern: Occurrence in Shallow Groundwater and Removal by Nanofiltration, in: Proceedings from the American Membrane Technology Association Conference, San Antonio, TX.
- Wilke, C.R. & Chang, P. (1955). Correlations of Diffusion Coefficients in Dilute Solutions. *AIChE Journal*, 1, 264-270.
- Xu, P., Drewes, J.E., Bellona, C., Amy, G., Kim, T.-U., Adam, M., & Heberer, T. (2005). Rejection of Emerging Organic Micropollutants in Nanofiltration-Reverse Osmosis Membrane Applications. *Water Environment Research*, 77, 40-48.
- Yangali-Quintanilla, V., Sadmani, A., McConville, M., Kennedy, M., & Amy, G. (2009). Rejection of pharmaceutically active compounds and endocrine disrupting compounds by clean and fouled nanofiltration membranes. *Water Research* 43, 2349-2362.
- Yangali-Quintanilla, V., Maeng, S.K., Fujioka, T., Kennedy, M., & Amy, G. (2010). Proposing nanofiltration as acceptable barrier for organic contaminants in water reuse. *Journal of Membrane Science*, 362, 334-345.
- Yangali-Quintanilla, V., Maeng, S.K., Fujioka, T., Kennedy, M., Li, Z., & Amy, G. (2011). Nanofiltration vs. reverse osmosis for the removal of emerging organic contaminants in water reuse. *Desalination and Water Treatment*, 34, 50-56.
- Zhang, Y., Van der Bruggen, B., Chen, G.X., Braeken, L., & Vandecasteele, C. (2004). Removal of pesticides by nanofiltration: effect of the water matrix. *Separation and Purification Technology*, 38, 163-172.
- Zhao, Y., & Taylor, J.S. (2004). Modeling Membrane Performance over Time. *J. AWWA*, 96, 90-97.
- Zhao, Y., Taylor, J.S., & Chellam, S. (2005). Predicting RO/NF water quality by modified solution diffusion model and artificial neural networks. *Journal of Membrane Science*, 263, 38-46.

CHAPTER 6: GENERAL CONCLUSION

The outcome of this work was fourfold:

1. Various TrOCs were monitored throughout the Town's water supply and full-scale treatment system, starting with reclaimed water used for irrigation to the POE sampling port.
 - Certain TrOCs, including caffeine and DEET, were detected in water samples from irrigation water through the full-scale NF plant, indicating their persistence in not only the aquatic environment, but also the Town's pretreatment and NF processes.
 - However, subsequent dilution with highly-treated RO permeate resulted in TrOCs below detection limits in POE samples.
2. A log-logistic model was developed to explain transport through a uniquely-configured split-feed, center-exit NF process operating at 267 gpm.
 - It was determined that 285 seconds would be needed for changes in the feed water to impact pilot permeate.
3. Two TrOC properties, molecular volume and polarizability, were well-correlated with TrOC rejection from loose NF processes.
 - Polarizability, a TrOC property not significantly studied in the past, may be a useful indicator of whether or not a compound will be rejected by a loose NF membrane.

4. When using the solution diffusion model with experimentally obtained mass transfer coefficients, an anthropogenic solute, caffeine, was successfully modeled through the Town's NF pilot.
- Caffeine was also modeled using the solution diffusion model with film theory, which incorporates a back-transport mass transfer coefficient accounting for the effects of concentration polarization, which describes the build-up of solutes at the feed side of the membrane surface as a result of partial solute rejection. This model over-predicted caffeine in the NF permeate, indicating concentration polarization did not significantly impact caffeine transport through this NF process.
 - Caffeine was also modeled using the solution diffusion model with mass transfer coefficients obtained from Sherwood correlations, which resulted in the over-prediction of caffeine.
 - This could have been the result of limitations associated with using Sherwood correlations:
 1. Wilke-Chang coefficients may be too conservative, or
 2. Water and caffeine properties are not strongly considered, as the Sherwood correlation method places emphasis primarily on membrane properties.

APPENDIX A: QUALITY ASSURANCE AND QUALITY CONTROL

Appendix A presents quality assurance and quality control (QA/QC) results from pilot start up (December 2014) until the completion of the transient response studies (September 2015) for organic content, chloride, and sodium, and QA/QC for additional water quality parameters (not shown) were evaluated in the same manner. To evaluate the precision and accuracy of laboratory instruments and personnel, QA/QC measures were applied every five samples in the form of a replicate and/or duplicate, and spiked sample. The relative standard deviation (RSD) was used to evaluate the closeness of a replicate and/or duplicate to the sample (Equation A-1), and the percent recovery was used to determine the accuracy of the spiked sample (Equation A-2). In general, it is recognized that an $RSD \leq 20\%$ and a percent recovery between 80 and 120% is considered acceptable.

$$RSD (\%) = 100 * \left[\frac{stddev (Sample,Replicate)}{average (Sample,Replicate)} \right] \quad (A-1)$$

$$Recovery (\%) = 100 * \frac{(Sample - Spiked Sample)}{Concentration of Spike} \quad (A-2)$$

Tables A-1 through A-3 present RSD and percent recovery results for various water quality parameters from pilot start up through the time frame in which the transient response studies were conducted. The average and standard deviation of RSD values and percent recoveries are presented as well.

Table A-1: RSD and Percent Recovery for Organic Carbon Analysis

Set	RSD (%)	Recovery (%)
1	17	90
2	2.6	97
3	9.7	93
4	0.49	112
5	6.2	120
6	1.0	107
7	2.9	103
8	12.1	90
9	0.62	92
10	0.56	81
11	1.4	104
12	2.3	N/A
13	0.35	N/A
14	0.070	92
15	0.41	101
16	0.00	96
17	10	94
18	0.46	86
19	7.0	94
20	7.0	92
21	18	99
22	0.12	101
23	3.9	97
24	10	97
Average	4.9	97
Standard Dev.	5.5	8

*N/A = Not Analyzed

Table A-2: RSD and Percent Recovery for Chloride

Set	RSD (%)	Recovery (%)	Set	RSD (%)	Recovery (%)
1	0.10	91	36	0.15	95
2	0.47	96	37	0.76	142
3	0.55	96	38	0.34	102
4	0.14	93	39	0.45	108
5	0.55	92	40	0.92	108
6	0.19	96	41	0.060	N/A
7	0.42	95	42	0.11	N/A
8	0.49	N/A	43	0.080	N/A
9	0.33	N/A	44	0.12	N/A
10	0.42	96	45	0.040	N/A
11	0.53	N/A	46	0.40	N/A
12	0.39	N/A	47	4.4	N/A
13	0.37	89	48	0.020	N/A
14	0.75	N/A	49	0.080	N/A
15	2.1	N/A	50	0.17	N/A
16	0.080	87	51	0.17	N/A
17	0.49	N/A	52	1.2	N/A
18	1.2	N/A	53	0.39	N/A
19	0.77	N/A	54	1.9	106
20	0.090	98	55	0.61	N/A
21	0.14	95	56	0.89	N/A
22	0.060	103	57	0.55	82
23	0.61	90	58	0.16	N/A
24	0.99	80	59	0.18	N/A
25	0.63	86	60	0.53	100
26	1.1	N/A	61	0.18	N/A
27	0.24	104	62	1.1	N/A
28	0.32	99	63	0.060	105
29	0.13	99	64	0.33	106
30	0.60	90	65	0.14	118
31	0.99	80	66	1.2	117
32	0.63	86	67	0.26	116
33	0.060	89	68	0.37	121
34	0.85	121			
35	1.3	115			
			Average	0.55	100
			Standard Dev.	0.64	12.9

*N/A = Not Analyzed

Table A-3: RSD and Percent Recovery for Sodium

Set	RSD (%)	Recovery (%)
1	0.00	113
2	2.3	129
3	1.7	134
4	0.010	111
5	0.14	112
6	1.0	115
7	1.2	96
8	2.1	98
9	1.5	91
10	0.19	100
11	1.7	96
12	1.2	100
13	0.050	102
14	1.4	94
15	2.2	96
16	0.75	104
17	1.8	95
18	0.41	97
19	0.64	100
20	1.5	98
21	0.89	99
22	1.7	98
23	0.20	103
24	1.6	97
25	0.28	99
26	0.61	104
27	0.97	101
28	0.92	101
29	0.61	99
30	1.4	100
31	1.3	97
32	1.7	99
Average	1.1	102
Standard Dev.	0.67	9.3

*N/A = Not Analyzed

APPENDIX B: SHERWOOD CORRELATION CALCULATIONS

Sherwood correlations were calculated according to the following equations:

$$d_h = 4 \left(\frac{xy}{2(x+y)} \right) \cong 2y \quad (\text{B-1})$$

d_h = hydraulic diameter (ft)

x = membrane channel width (ft)

y = feed channel spacer height (ft)

$$S_h = 1.86 \left(R_e S_c \frac{d_h}{L} \right)^{0.33} \quad (\text{B-2})$$

S_h = Sherwood Number (dimensionless)

R_e = Reynolds Number (dimensionless)

S_c = Schmidt Number (dimensionless)

L = Membrane Length (ft)

$$R_e = \frac{d_h V \rho}{\mu} \quad (\text{B-3})$$

V = Feed Channel Velocity $\left(\frac{ft}{s} \right)$

ρ = Density of Water $\left(998 \frac{kg}{m^3} \right)$

μ = Solution Viscosity $\left(9.325 \times \frac{10^{-4} kg}{m \cdot s} \right)$

$$S_c = \frac{\mu}{\rho D_i} \quad (\text{B-4})$$

$S_c = \text{Schmidt Number (dimensionless)}$

$D_i = \text{Diffusivity of Species } \left(\frac{m^2}{s}\right)$

$$D_i = \frac{(117.3 \times 10^{-15})[(\varphi)(MW)]^{0.5}(T)}{\mu V_i^{0.6}} \quad (\text{B-5})$$

$\varphi = \text{Solvent Association Factor (2.26 for Water)}$

$MW = \text{Molecular Weight } \left(\frac{g}{mole}\right)$

$T = \text{Temperature (K)}$

$V_i = \text{Solute Molal Volume at Normal Boiling Point } \left(\frac{m^3}{kmole}\right)$

$$K_s = \frac{S_h D_i}{d_h} \quad (\text{B-6})$$

The following example demonstrates how the mass transfer coefficient was calculated from Sherwood relationships in the first stage of the pilot unit. The solute molal volume at normal boiling point, V_i , was calculated using atomic volumes for caffeine obtained from Wilke & Chang (1955), which has a molecular formula of $C_8H_{10}N_4O_2$.

$$V_i = (8)(0.0148) + (10)(0.0037) + (4)(0.0105) + (2)(0.0074) = 0.2122 \frac{m^3}{kmol}$$

$$D_i = \frac{(1.173 \times 10^{-13}) \left((2.26) \left(194 \frac{g}{mol} \right) \right)^{0.5} (296.15 K)}{\left(0.9325 \frac{mN \cdot s}{m^2} \right) \left(\frac{0.2122 m^3}{kmol} \right)^{0.6}} = 1.98 \times 10^{-9} \frac{m^2}{s}$$

The feed channel spacer height of the NF270 membranes is 28 mils (0.028 inches). Membrane length was provided by DOW Filmtec, and membrane width was calculated using the effective membrane area and number of membrane leaves per element, also provided by DOW Filmtec. Feed velocity was calculated using the average feed flow through the first stage pressure vessels, 14.17 gpm (0.0316 ft³/s)

$$d_h = 4 \left[\frac{[(120 \text{ ft})(0.028 \text{ inches})\left(\frac{1 \text{ ft}}{12 \text{ inches}}\right)]}{2\left((120 \text{ ft})+(0.028 \text{ inches})\left(\frac{1 \text{ ft}}{12 \text{ inches}}\right)\right)} \right] = 0.0047 \text{ ft}$$

$$A = 0.028 \text{ inches} \left(\frac{1 \text{ ft}}{12 \text{ inches}} \right) \times 120 \text{ ft} = 0.28 \text{ ft}^2$$

$$V = \frac{0.0316 \frac{\text{ft}^3}{\text{s}}}{0.28 \text{ ft}^2} = 0.113 \frac{\text{ft}}{\text{s}}$$

$$S_c = \frac{9.325 \times 10^{-4} \frac{\text{kg}}{\text{m} \cdot \text{s}}}{\left(998 \frac{\text{kg}}{\text{m}^3}\right) \left(1.98 \times 10^{-9} \frac{\text{m}^2}{\text{s}}\right)} = 472$$

$$R_e = \frac{(0.0047 \text{ ft}) \left(0.113 \frac{\text{ft}}{\text{s}}\right) \left(998 \frac{\text{kg}}{\text{m}^3}\right) \left(\frac{0.3048 \text{ m}}{\text{ft}}\right)^2}{9.325 \times 10^{-4} \frac{\text{kg}}{\text{m} \cdot \text{s}}} = 52$$

$$Sh = 1.86 \left[(52)(472) \left(\frac{0.0047 \text{ ft}}{3.33 \text{ ft}}\right)^{0.33} \right] = 5.99$$

$$K_s = \frac{\left(\frac{86400 \text{ s}}{\text{day}}\right) (5.99) \left(1.98 \times 10^{-9} \frac{\text{m}^2}{\text{s}}\right)}{\left(\frac{0.3048 \text{ m}}{\text{ft}}\right)^2 (0.0047 \text{ ft})} = 2.36 \text{ ft/d}$$

**APPENDIX C: TRACE ORGANIC COMPOUND
CONCENTRATIONS AND MASS BALANCES**

Concentrations for caffeine, carbamazepine, DEET, naproxen, and sulfamethoxazole in feed, permeate, and concentrates samples are presented in Tables C-1 through C-5. Bisphenol A was below detection in a majority of feed, permeate, and concentrate samples, and gemfibrozil and sucralose were below detection in a majority of permeate samples; consequently, concentrations for these compounds are not presented. During experiments 1 through 5, interstage (first stage concentrate, second stage feed) and final concentrate samples were diluted by a factor of eight prior to shipment to the commercial laboratory for analysis.

Mass balances were calculated during pilot experiments to account for adsorption losses and to verify correct analytical procedures. Mass balance results for caffeine, carbamazepine, DEET, naproxen, and sulfamethoxazole are presented in Tables C-6 through C-10. Mass balances for bisphenol A, gemfibrozil, and sucralose could not be calculated since permeate samples, and sometimes feed samples, were below detection limits. To calculate the percent recovered, mass balance calculations were conducted using Equation C-1. Permeate balances were conducted using Equation C-2.

$$Q_f C_f = Q_p C_p + Q_c C_c \quad (\text{C-1})$$

Where,

$Q_f, Q_p, Q_c = \text{Feed, Permeate, and Concentrate Flow Rate (gpm)}$

$C_f, C_p, C_c = \text{Feed, Permeate, and Concentrate Concentration } \left(\frac{\text{ng}}{\text{L}}\right)$

$$Q_{p_c} C_{p_c} = Q_{p_L} C_{p_L} + Q_{p_R} C_{p_R} \quad (\text{C-2})$$

$Q_{pL}, Q_{pR}, Q_{pC} = \text{Flow Rate in Left, Right, and Combined Permeate (gpm)}$

$C_{pL}, C_{pR}, C_{pC} = \text{Concentration in Left, Right, and Combined Permeate (gpm)}$

In some experiments, the percent recovered from one or more of the stages was greater than 70 – 130%. In these instances, other means of determining sample outliers were used, including conducting a permeate balance. For example, in Table C-6, experiment 2, the percent recovered for first stage and second stage caffeine was 39 and 195%, respectively. The low percent recovery in the first stage would suggest caffeine adsorption to the membrane, pilot pipes or appurtenances; however, since the second stage caffeine recovery was significantly higher than expected, and the first stage, second stage, and total pilot system permeate balances and the percent mass recovered from the total pilot system were within an acceptable range, it was concluded that caffeine did not adsorb and that the interstage sample (first stage concentrate, second stage feed) was incorrect. As a result, the interstage sample was discarded from the data set.

Table C-1: Caffeine Concentrations from Pilot Experiments

Exp. No.	Concentration (ng/L)										
	Target Feed	First Stage Feed	First Stage Permeate			Interstage/ Second Stage Feed	Second Stage Permeate			Final Concentrate	Total Pilot Permeate
			Left	Right	Combined		Left	Right	Combined		
1	150	52	BDL	BDL	BDL	176	44	57	BDL	336	16
2	250	180	54	49	46	1,440	100	130	110	1,200	59
3	250	240	N/C	N/C	57	1,120	N/C	N/C	130	1,520	78
4	500	550	N/C	N/C	160	1,920	N/C	N/C	330	2,240	160
5	2,000	1,000	300	180	290	3,100	500	660	660	5,800	360
6	10	7.7	N/C	N/C	2.1	23	N/C	N/C	1.6	39	2.5
7	100	74	N/C	N/C	20	230	N/C	N/C	45	430	25

Exp. No.	Concentration (µg/L)										
	Target Feed	First Stage Feed	First Stage Permeate			Interstage/ Second Stage Feed	Second Stage Permeate			Final Concentrate	Total Pilot Permeate
			Left	Right	Combined		Left	Right	Combined		
8	1,500	1,020	260	230	220	2,670	450	670	530	4,270	360
9	2,500	1,418	339	290	336	3,930	694	797	748	7,530	401
10	5,000	2,920	750	640	750	8,340	1,450	1,600	1,530	14,460	810
11	7,500	4,500	1,020	960	960	12,010	2,250	2,300	2,220	22,081	1,260

*BDL = Below Detection Limit; N/C = Sample Not Collected

Table C-2: Carbamazepine Concentrations from Pilot Experiments

Exp. No.	Concentration (ng/L)										
	Target Feed	First Stage Feed	First Stage Permeate			Interstage/ Second Stage Feed	Second Stage Permeate			Final Concentrate	Total Pilot Permeate
			Left	Right	Combined		Left	Right	Combined		
1	150	57	5.8	5	5	232	10	11	11	344	5.2
2	250	140	12	9	10	680	23	25	24	880	14
3	250	210	N/C	N/C	20	608	N/C	N/C	35	1,280	24
4	500	420	N/C	N/C	37	880	N/C	N/C	64	1,600	40
5	2,000	470	23	20	23	1,300	39	52	47	2,500	28

*N/C = Sample Not Collected

Table C-3: DEET Concentrations from Pilot Experiments

Exp. No.	Concentration (ng/L)										
	Target Feed	First Stage Feed	First Stage Permeate			Interstage/ Second Stage Feed	Second Stage Permeate			Final Concentrate	Total Pilot Permeate
			Left	Right	Combined		Left	Right	Combined		
1	150	94	14	13	15	704	26	34	27	800	15
2	250	1,200	170	160	160	4,320	360	400	380	7,920	200

Table C-4: Naproxen Concentrations from Pilot Experiments

Exp. No.	Concentration (ng/L)										
	Target Feed	First Stage Feed	First Stage Permeate			Interstage/ Second Stage Feed	Second Stage Permeate			Final Concentrate	Total Pilot Permeate
			Left	Right	Combined		Left	Right	Combined		
1	150	41	BDL	BDL	BDL	BDL	BDL	BDL	BDL	BDL	BDL
2	250	99	BDL	BDL	BDL	336	11	13	13	536	BDL
3	250	110	N/C	N/C	BDL	432	N/C	N/C	19	784	BDL
4	500	230	N/C	N/C	14	960	N/C	N/C	32	1,760	19
5	2,000	230	17	14	15	710	33	40	34	1,400	17

*BDL = Below Detection Limit; N/C = Sample Not Collected

Table C-5: Sulfamethoxazole Concentrations from Pilot Experiments

Exp. No.	Concentration (ng/L)										
	Target Feed	First Stage Feed	First Stage Permeate			Interstage/ Second Stage Feed	Second Stage Permeate			Final Concentrate	Total Pilot Permeate
			Left	Right	Combined		Left	Right	Combined		
1	150	70	7.8	5.7	7.9	232	8.4	14	9.7	464	8.4
2	250	670	100	82	84	21,600	140	330	140	4,400	97
3	250	260	N/C	N/C	37	880	N/C	N/C	63	1,680	42
4	500	550	N/C	N/C	76	1,360	N/C	N/C	110	2,240	78
5	2,000	440	150	180	150	1,300	160	160	160	2,100	120

*N/C = Sample Not Collected

Table C-6: Mass Balance Calculations for Caffeine

Exp. No.	% Recovered			Permeate Balance (%)		
	First Stage	Second Stage	Total Pilot System	First Stage	Second Stage	Total Pilot System
1	N/A	N/A	75	N/A	N/A	N/A
2	39	195	72	90	97	102
3	60	138	79	N/C	N/C	110
4	76	152	113	N/C	N/C	83
5	92	86	81	122	118	100
6	95	101	92	N/C	N/C	125
7	92	87	82	N/C	N/C	101
8	108	101	102	91	94	128
9	103	92	96	109	106	96
10	98	95	96	108	100	90
11	108	90	97	98	97	105

*N/A = Not Applicable, Sample was BDL; N/C = Sample Not Collected

Table C-7: Mass Balance Calculations for Carbamazepine

Exp. No.	% Recovered			Permeate Balance (%)		
	First Stage	Second Stage	Total Pilot System	First Stage	Second Stage	Total Pilot System
1	79	116	93	93	107	87
2	68	134	89	95	102	111
3	101	95	95	N/C	N/C	105
4	137	108	148	N/C	N/C	95
5	120	91	110	108	107	101

*N/C = Sample Not Collected

Table C-8: Mass Balance Calculations for DEET

Exp. No.	% Recovered			Permeate Balance (%)		
	First Stage	Second Stage	Total Pilot System	First Stage	Second Stage	Total Pilot System
1	43	151	65	112	92	75
2	87	93	81	98	108	99

Table C-9: Mass Balance Calculations for Naproxen

Exp. No.	% Recovered			Permeate Balance (%)		
	First Stage	Second Stage	Total Pilot System	First Stage	Second Stage	Total Pilot System
2	N/A	109	N/A	N/A	N/A	N/A
3	N/A	110	N/A	N/C	N/C	N/A
4	73	110	79	N/C	N/C	109
5	107	89	96	98	97	91

*N/A = Not Applicable, Sample was BDL

Table C-10: Mass Balance Calculations for Sulfamethoxazole

Exp. No.	% Recovered			Permeate Balance (%)		
	First Stage	Second Stage	Total Pilot System	First Stage	Second Stage	Total Pilot System
1	95	87	83	112	92	75
2	10	842	82	93	60	103
3	85	103	87	N/C	N/C	100
4	113	118	132	N/C	N/C	95
5	92	103	100	92	104	79

*N/C = Sample Not Collected

**APPENDIX D: DESALINATION AND WATER TREATMENT
COPYRIGHT PERMISSION LETTER**

Desalination and Water Treatment

Miriam Balaban, Editor-in-Chief
36 Walcott Valley Drive
Hopkinton, MA 01748
Tel. +39 348 8848406 (mobile), Fax +1 928 543 3066
E-mail: dwt@deswater.com

June 2nd 2016

TO WHOM IT MAY CONCERN

I hereby grant permission to reproduce material from the following publication

“Mass transfer and transient response time of a split-feed nanofiltration pilot unit”
by *Samantha Jeffery-Black and Steven J. Duranceau*

currently appearing online and identified by doi: 10.1080/19443994.2016.1155498

for inclusion in the 2016 Doctoral Dissertation of Samantha Jeffery.

Please make sure that the relevant reference to *Desalination and Water Treatment* appears.



Miriam Balaban
Editor-in-Chief

**APPENDIX E: DESALINATION AND WATER TREATMENT
ACCEPTANCE LETTER**

Samantha Jeffery

From: onbehalfof+deswaterjournal+gmail.com@manuscriptcentral.com on behalf of deswaterjournal@gmail.com
Sent: Friday, June 03, 2016 8:14 AM
To: Steven.Duranceau@ucf.edu
Cc: Samantha Jeffery
Subject: Desalination and Water Treatment - Decision on Manuscript ID TDWT-2016-0446.R1
Attachments: Attached standard file: * TDWT-Copyright-Form.pdf

03-Jun-2016

Ref.: TDWT-2016-0446.R1
"The Influence of Solute Polarizability and Molecular Volume on the Rejection of Trace Organics in Loose Nanofiltration Membrane Processes"
Desalination and Water Treatment

Dear Dr Duranceau:

We are pleased to accept your revised paper for publication in Desalination and Water Treatment.

You will receive the proofs in due course.

Attached please find the copyright form. Please email the signed form promptly to deswaterjournal@gmail.com.

Thank you for your contribution to Desalination and Water Treatment and we look forward to receiving further submissions from you.

With kind regards,

Miriam Balaban
Editor-in-chief, Desalination and Water Treatment